7-1-2013

# The Role of Snai2/Slug in Diabetes-impaired Wound Healing

Krystle K. Quan

Krystle K. Quan
*Candidate*

Biomedical Sciences
*Department*

This dissertation is approved, and it is acceptable in quality and form for publication:

*Approved by the Dissertation Committee:*

Laurie G. Hudson, Ph.D., Chairperson

Linda Felton, Ph.D.

Michelle Ozbun, Ph.D.

Paul McGuire, Ph.D.

**THE ROLE OF SNAI2/SLUG IN DIABETES-IMPAIRED WOUND HEALING**

**by**

**KRYSTLE K. QUAN**

B.S. Biochemistry, University of Washington, Seattle, 2006

DISSERTATION

Submitted in Partial Fulfillment of the
Requirements for the Degree of

**Doctor of Philosophy**
**Biomedical Sciences**

The University of New Mexico
Albuquerque, New Mexico

**July 2013**

# DEDICATION

This dissertation is dedicated to my loving family for their never-ending support throughout this process. Their continued words of encouragement pulled me through even the darkest of times when I did not believe in myself.

I also dedicate this dissertation to my best friend and love, Michael Yu, who stayed by my side as my number one fan even though it meant we were a thousand miles apart. Thank you for always believing in me.

# ACKNOWLEDGEMENTS

With much appreciation and praise, I acknowledge my advisor and dissertation chair, Dr. Laurie G. Hudson. Her guidance both as a mentor and as a friend has played a vital role in my growth and development both professionally and personally. I thank her for all the advice and help she gave me throughout the years and for supporting me in pursuit of my graduate degree. Everything I have learned from her has been invaluable.

I would also like to thank my committee members, Drs. Linda Felton, Paul McGuire, and Michelle Ozbun, for their guidance throughout graduate school. They constantly challenged me and encouraged me in my research, and this project would not have been as complete without their scientific wisdom.

To the Hudson Lab members past and present, I thank them for their never-ending support. The ideas I received and the help they provided were what made many experiments successful. I will always cherish the memories in the lab and the encouragement and love they gave me.

Lastly, to my best friends in the Biomedical Sciences Graduate Program 2007 Cohort, they are my family, and I love them and all the memories we created together. From our Qualifying Exams to our Dissertation Defenses, we knew how to be each others' support, and I thank them for never letting me quit. Without them all, this journey would never have been as amazing.

# THE ROLE OF SNAI2/SLUG IN DIABETES-IMPAIRED WOUND HEALING

**By**

**Krystle K. Quan**

**B.S. Biochemistry, University of Washington, Seattle**

**Ph.D. Biomedical Sciences, University of New Mexico, Albuquerque**

## ABSTRACT

Impaired wound healing is a common complication of diabetes mellitus. Advanced glycation end products (AGEs) are a consequence of diabetes and are formed from non-enzymatic reactions between glucose and proteins. The accumulation of AGEs is believed to disrupt wound repair and alter protein function. The epidermal growth factor receptor (EGFR) and a downstream effector, Snai2/Slug, are key regulators of reepithelialization, a vital component of wound healing. Reepithelialization requires keratinocyte proliferation and migration. Therefore, we examined the impact of AGEs on these EGF-stimulated responses. In this dissertation, I present evidence for a critical role of Snai2 in diabetes-impaired wound reepithelialization, extending the knowledge of Snai2 past normal wound repair. A well-studied AGE precursor, glyoxal, was used to model a diabetic environment. Glyoxal decreased EGF-stimulated EGFR activation, leading to impaired keratinocyte proliferation and migration in cell culture and in tissue explants. EGF-stimulated and basal Snai2 protein levels decreased following glyoxal treatment, and this decrease was prevented by the glycation inhibitor, aminoguanidine.

Snai2 immunoprecipitated from glyoxal-exposed cells was modified by the AGE product carboxymethyl lysine, identifying Snai2 as an intracellular target of glycation. Furthermore, mice over-expressing Snai2 demonstrated enhanced epithelial outgrowth compared to wild type mice when exposed to glyoxal *ex vivo*. These data represent a significant breakthrough in the field of diabetes and wound healing as it is the first evidence linking Snai2 down-regulation by pathophysiologic stimuli to impairments in reepithelialization. In addition, few intracellular proteins have been identified as targets of glycation, and this work highlights Snai2 as a novel nuclear protein target with demonstrated relevance to diabetic healing. With this knowledge, we may explore methods to pharmacologically induce Snai2 protein to promote healing of diabetic wounds.

# Table of Contents

**Page**

# List of Figures

**Page**

## List of Tables

**Page**

## List of Abbreviations

AG = Aminoguanidine

AGE = Advanced glycation end product

ANOVA = Analysis of variance

$BS^3$ = Bis(sulfosuccinimidyl)suberate

BSA = Bovine serum albumin

CML = Carboxymethyl lysine

DAPI = 4',6-diamidino-2-phenylindole

DCS = Defined calf serum

DMEM = Dulbecco's Modified Eagle's Medium

EDTA = Ethylenediaminetetraacetic acid

EGF = Epidermal growth factor

EGFR = Epidermal growth factor receptor

ECM = Extracellular matrix

EMT = Epithelial to mesenchymal transition

GLUT2 – Glucose transporter type 2

GLUT4 = Glucose transporter type 4

GO = Glyoxal

HB-EGF = Heparin-binding EGF-like growth factor

IB = Immunoblot

ICC = Immunocytochemistry

IP = Immunoprecipitation

IGF-1 = Insulin-like growth factor 1

IRS-1 = Insulin receptor substrate 1

MMP = Matrix metalloproteinase

NHEK = Normal human epidermal keratinocyte

NIDDM = Non-insulin-dependent diabetes mellitus

PARP = Poly (ADP-ribose) polymerase

PBS = Phosphate-buffered saline

PBS-T = Phosphate-buffered saline - Tween 20

PCR = Polymerase chain reaction

PDGF = Platelet-derived growth factor

PVDF = Polyvinylidene fluoride

PY = Phosphotyrosine

qRT-PCR = Quantitative real-time polymerase chain reaction

RIPA = Radio immuno precipitation assay

SCC = Squamous cell carcinoma

SDS = Sodium dodecyl sulfate

SEM = Standard error of the mean

STZ = Streptozotocin

TBS-T = Tris-buffered saline - Tween 20

TGF-α = Transforming growth factor alpha

TGF-β = Transforming growth factor beta

WS = Waardenburg syndrome

# CHAPTER 1

# Introduction

## 1.1 Diabetes: overview

Diabetes mellitus is a metabolic disorder in which people with high blood sugar (hyperglycemia) are unable to regulate and reduce sugar levels (Galtier, 2010; Hotamisligil, 2006). According to the American Diabetes Association and the Centers for Disease Control and Prevention, diabetes was the seventh leading cause of death in the United States in 2011, and it is believed that death caused by diabetes is underreported because of the other associated complications, such as cardiovascular disease. Diabetes is estimated to affect 25.8 million people, or 8.3%, of the U.S. population. Of major concern is that 18.8 million of these people are diagnosed, whereas 7.0 million people remain undiagnosed. Worldwide, diabetes affected 246 million people in 2007, and this figure is predicted to increase to a startling 366 million by 2030 (Setacci et al., 2009). Diabetes is a debilitating disease and is the leading cause of kidney failure, new cases of blindness, heart disease, and stroke. It is also a major cause of non-traumatic lower limb amputation among adults in the United States due to failure of chronic wounds to heal. Therefore, it is vital that a better understanding of the disease, its treatment, and its prevention are explored.

### 1.1.1 Diabetes: insulin and glucose regulation

Throughout the day, an individual's blood glucose levels fluctuate depending on various factors. For example, the time of day, what has been eaten, how much food has been consumed, and the level of physical activity will all affect a glucose measurement.

In general, diabetics are classified as having a fasting glucose level of greater than 126 mg/dL (7 mM) (hyperglycemia). This value was lowered from a higher threshold of 140 mg/dL (7.8 mM) in 1997. In contrast, normal glucose levels are between 70-110 mg/dL (3.9-6.1 mM). In the pre-diabetic state, fasting blood glucose levels range between 110-125 mg/dL (6.1-6.9 mM).

Insulin is a hormone produced by the β-cells of the pancreas and is necessary for converting sugars into energy used by the body. It is crucial for maintaining glucose homeostasis and for regulating carbohydrate, lipid, and protein metabolism (Saltiel and Kahn, 2001). Insulin binding to its receptor regulates a wide variety of biological responses (Goldfine, 1987; White and Kahn, 1994). When glucose increases in the blood, insulin causes the liver to convert glucose into glycogen through a process called glycogenesis. Insulin also stimulates cells to take up glucose from the glucose transporter type 4 (GLUT4) transporter, an insulin-regulated transporter found in adipose tissue and striated muscle (Krook et al., 2004; Leney and Tavare, 2009). GLUT4 is responsible for transporting glucose into the cell, leading to a decrease in blood sugar (Leney and Tavare, 2009; Leto and Saltiel, 2012; Stockli et al., 2011). When insulin levels are low, GLUT4 is contained in vesicles located inside muscle and fat cells (Stockli et al., 2011). Binding of insulin to the insulin receptor leads to activation of the receptor's tyrosine kinase domain (Klip, 2009; Krook et al., 2004). Upon receptor phosphorylation and recruitment of insulin receptor substrate (IRS-1), a signaling cascade is activated, which results in GLUT4 expression on the plasma membrane. This then allows the passive diffusion of glucose down its concentration gradient into the cell. Once inside the cell, glucose becomes phosphorylated to glucose-6-phosphate, which maintains the concentration

gradient necessary for the continued passage of glucose into the cells. Glucose-6-phosphate can undergo glycolysis for energy production or is polymerized into glycogen for energy storage. Mice lacking the insulin receptor die within the first week after birth, and disruptions in the signaling pathway are associated with severe insulin resistance (Accili et al., 1996; Accili et al., 1999; Joshi et al., 1996; Taylor et al., 1992). Therefore, the balance between insulin and glucose signaling is vital to prevent long term pathological complications.

### 1.1.2 Diabetes: clinical effects in humans

Diabetes is classified into several types, and each type is characterized by whether the body is able to produce/use insulin and also who is affected. Over the years, the age at which patients become diabetic has become less of a classification factor, and the symptoms manifested have become the more important determinant.

Type 1 diabetes affects an estimated 5-10% of diagnosed Americans. This form of diabetes was previously called insulin-dependent diabetes mellitus (IDDM) or "juvenile-onset" diabetes. However, an increasing number of cases are demonstrating that type 1 can occur at any age. Symptoms include frequent urination, unusual thirst, extreme hunger, unusual weight loss, extreme fatigue, and irritability. In this form, the body fails to produce insulin due to the destruction of pancreatic β-cells by the immune system. Treatment for this form includes injection of insulin into the body. There is no known way to prevent this form of diabetes, and risk factors may be autoimmune, genetic, or environmental. However, proper treatment and monitoring can lead to a normal, healthy life.

Type 2 diabetes is a heterogenous disorder characterized by decreased production of insulin, resistance to insulin, or failure of the body to use insulin properly. The β-cells are also unable to compensate for insulin resistance (β-cell dysfunction) (DeFronzo, 1997; Flatt, 1997). This form of diabetes was previously called non-insulin-dependent diabetes (NIDDM) or "adult-onset" diabetes. When glucose builds up in the blood due to failure of insulin to move sugar into the cells, it can cause two problems: 1) the cells may be starved for energy immediately and 2) over time, high blood glucose may cause damage to organs such as the eyes, kidneys, nerves, or heart. Most Americans who are diagnosed with diabetes have this form, and symptoms can include those from the type 1 group as well as frequent infections (skin, gums, and bladder), blurred vision, slow-healing cuts or bruises, and tingling or numbness in the hands or feet. Factors that contribute to the development of this form include genetics, obesity, inactivity, and diet (Hotu et al., 2004; Pinhas-Hamiel and Zeitler, 2005). However, not all individuals who have type 2 diabetes display symptoms. In addition, some groups have a higher risk for developing type 2 than others, such as African Americans, Latinos, Native Americans, Asian Americans, Pacific Islanders, and the aged population (Grinstein et al., 2003; Krosnick, 2000).

A third form of diabetes is gestational diabetes, which occurs during pregnancy usually around the 24$^{th}$ week in women who may not have had diabetes previously (Oliveira et al., 2012). 5-10% of pregnant women have this form (~135,000 cases in the United States each year). Often, gestational diabetes does not display symptoms, making it crucial that women get tested during pregnancy. However, risk factors include being overweight prior to pregnancy, a history of gestational diabetes in an earlier pregnancy,

and a family history of diabetes (Oliveira et al., 2012). Gestational diabetes begins when the body is not able to make and use all the insulin it needs for pregnancy (Oliveira et al., 2012), and glucose builds up in the blood to high levels, causing hyperglycemia. The causes are still unknown, but it is believed that hormones from the placenta that help the baby develop are blocking the action of the mother's insulin in her body, causing insulin resistance. Gestational diabetes usually disappears after pregnancy.

The fourth classification of diabetes is the pre-diabetic class and is defined as an individual having blood glucose levels that are higher than normal but are not high enough for a type 2 diagnosis. This form affects about 57 million Americans.

The shocking knowledge that so many forms of diabetes exist and knowing that everyone is susceptible cannot be ignored. Given that many people are already diabetic and therefore vulnerable to the associated health impacts, it is important to both better understand how to prevent and control diabetes and improve strategies to address health issues associated with this debilitating disease.

## 1.2 The skin

As briefly discussed above, a major complication with diabetics is the failure to heal wounds. Often these chronic wounds are found in the extremities such as the feet, and defects in wound repair may ultimately result in amputation of the limb. The skin is the largest organ of the body and acts as the first barrier of protection from the external environment (Fuchs and Raghavan, 2002; McLafferty et al., 2012). It accounts for approximately 16% of a human's body weight, and its thickness varies depending on the region of the body. In addition to protection, the skin has several other important

functions. For example, it contains nerves involved with sensations such as heat, cold, pressure, and pain, assists in body temperature regulation, and acts to prevent loss of fluids from the body. Chronic wounds disrupt the barrier function of the skin, leading to increased risk of infection and other complications.

### 1.2.1 The skin structures

There are two main layers that make up the skin – the epidermis and the dermis (McLafferty et al., 2012). The epidermis prevents fluid loss and protects the body from infection. It lacks blood vessels and relies on the dermis for oxygenation, nutrients, and waste removal (McLafferty et al., 2012). The epidermis consists of four cell types – keratinocytes, melanocytes, Langerhans cells and Merkel cells. Keratinocytes, the predominant cell type in the epidermis, make up about 90% of the cells in the layer and are mainly responsible for protection against the external environment. Melanocytes make up 8% of the cells and produce the pigment melanin. Lastly, Langerhans cells are important in the immune response, and Merkel cells are involved with the touch sensation.

The epidermis is crucial in the reepithelialization phase of wound healing. The epidermis is a stratified squamous epithelium comprised of proliferating basal and differentiated suprabasal keratinocytes (Figure 1.1). In the deepest layer of the epidermis is the stratum basale, also called the stratum germinativum, which sits above the basement membrane (Fuchs and Raghavan, 2002). Above this basale layer are the stratum spinosum (prickle cell layer), the stratum granulosum (granular layer), the stratum lucidum, and the stratum corneum, which is the outermost layer (McLafferty et

al., 2012). The epidermis renews itself through cell division starting in its deepest layer. As cells mature, they move from the stratum basal up to the stratum corneum where the cells are shed.

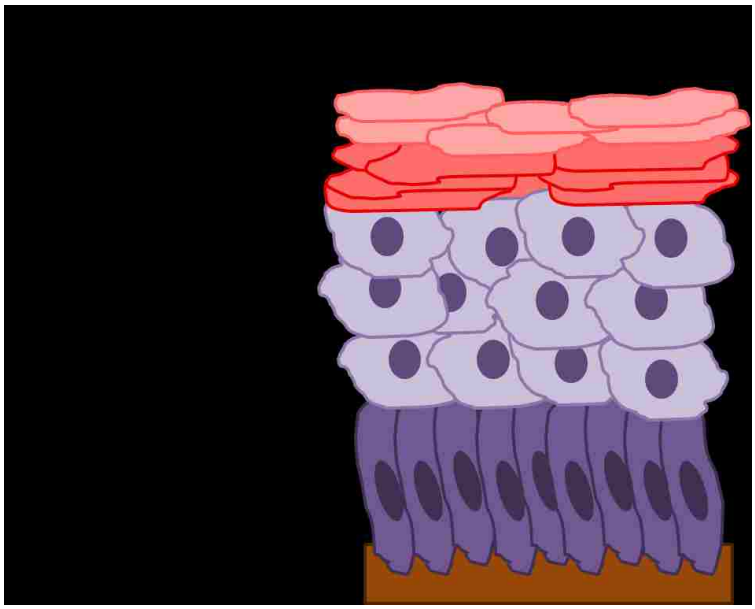

FIGURE 1.1. **The epidermis.** The outermost layer of the epidermis is the stratum corneum. Below this are the stratum lucidum, the stratum granulosum, stratum spinosum, and the stratum basale. The stratum basale layer sits above the basement membrane.

## 1.3 The wound healing process

Wound healing begins immediately after tissue injury and on average, takes seven days for complete repair. However, more extreme injuries such as deep cuts or burns may last for months or even years. The healing process is very carefully orchestrated and involves several overlapping steps, requiring the interactions of many cell types and growth factors (Gurtner et al., 2008; Singer and Clark, 1999). Four main stages occur during the process of wound repair (Figure 1.2) (Singer and Clark, 1999).

### 1.3.1 Phase 1: the fibrin clot

Following tissue injury, the first step consists of formation of the fibrin and fibronectin clot created by platelet aggregation, which leads to a stop in blood loss (hemostasis) (Gurtner et al., 2008; Janis et al., 2010; Rafehi et al., 2011). Platelets make up the greatest number of cells present after injury and release various components into the blood such as extracellular matrix (ECM) proteins and cytokines and growth factors that increase cell division (Santoro and Gaudino, 2005). In addition, proinflammatory elements from nearby blood vessels such as serotonin, prostaglandins, thromboxane, histamine, and others all promote cell proliferation, migration, and blood vessel growth and dilation (Hosgood, 2006; Janis et al., 2010). The fibrin clot closes the wound site to the external environment and prevents further contamination of the wound. It also acts as a structural support for the wound until a provisional matrix is created (Hosgood, 2006).

### 1.3.2 Phase 2: inflammation

The second phase of healing consists of the inflammatory response and includes dilation of blood vessels, which allows entry of elements from the blood stream into the wound site (Rafehi et al., 2011). Factors such as chemokines, cytokines, and inflammatory components such as leukocytes, neutrophils, and macrophages are released into the wound site to remove debris and prevent infection (Eming et al., 2007; Rafehi et al., 2011). Within an hour after tissue injury, neutrophils are the predominant cell for the first two days following injury. Neutrophils phagocytose debris, kill bacteria, and clean the wound by breaking down damaged tissue (Kim et al., 2008; Rafehi et al., 2011).

Monocytes are attracted into the site soon after wounding, and their levels peak 1-1.5 days after wounding. Monocytes then mature into macrophages and remove neutrophils from the wound (Hosgood, 2006). The main role of macrophages is to phagocytose bacteria and damaged tissue and to secrete growth factors and cytokines that promote the proliferation phase, the third stage of wound healing (Rafehi et al., 2011).

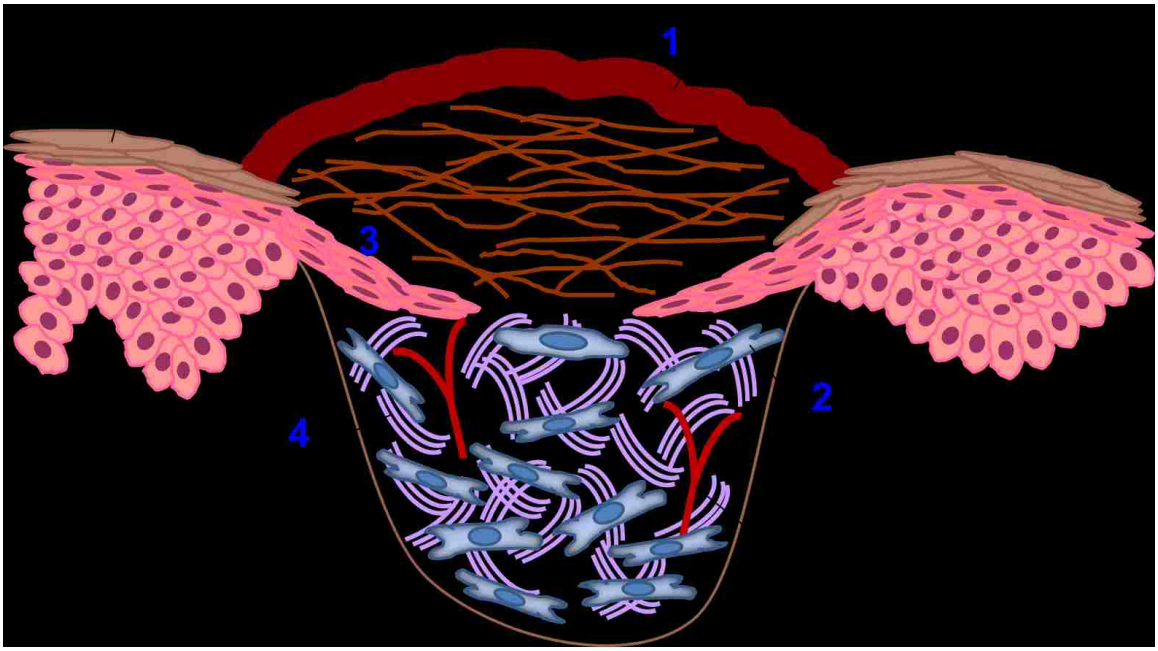


FIGURE 1.2. **The wound healing process.** Healing beings with formation of the fibrin clot (1). The second stage of healing is the inflammatory response (2), which is followed by the proliferative phase (3). The last stage is the remodeling step (4), which lays down a stronger, more permanent extracellular matrix.

### 1.3.3 Phase 3: proliferation

The proliferation phase begins 2-3 days after tissue injury. Fibroblasts enter the wound site even before the inflammatory phase has ended and levels peak 1-2 weeks after wounding, becoming the main cell type in the site. During the first few days after injury, fibroblasts mainly proliferate and migrate, but they then become crucial for

production of a provisional ECM. Granulation tissue forms in the wound 2-5 days post wounding and acts as temporary tissue, taking the place of the fibrin clot (Adamson, 2009). The granulation tissue covers the wound bed and contains new blood vessels, fibroblasts, inflammatory cells, endothelial cells, myofibroblasts, and a provisional ECM. The provisional ECM is comprised of type III collagen, fibronectin, hyaluronan, glycoproteins, and proteoglycans. Though the collagen of the provisional ECM is not as strong as the collagen that makes up normal, healthy tissue, it provides strength to a wound that is otherwise held together by just the fibrin clot.

The provisional ECM also allows for migration of epithelial cells over the wound bed to form a barrier between the wound and the external environment, a process called reepithelialization. Reepithelialization is crucial for repair of damaged tissue and is the focus of the studies described in Chapters 3 and 4.

Reepithelialization is imperative for wound healing because it is required to restore barrier function (Gurtner et al., 2008). Defects would leave the open wound vulnerable to infection and further damage. Growth factors such as platelet-derived growth factor (PDGF), transforming growth factor beta (TGF-β), and fibronectin promote cell proliferation, migration, and ECM production. The basal keratinocytes of the epidermis and the appendages of the dermis, such as hair follicles and sebaceous glands, migrate as a sheet known as the epithelial tongue (Bartkova et al., 2003). Keratinocytes first migrate without proliferation, but eventually, cells are needed to replace the space vacated by the migrated cells, resulting in epithelial cell proliferation at the wound edge (Hosgood, 2006). The cells move through the damaged tissue and the matrix, and together with proliferating epidermal and dermal cells, leads to wound closure. Once

cells from both sides of the wound meet, migration ceases due to contact inhibition. The cells reestablish cell-cell junctions and become anchored to the basement membrane (Santoro and Gaudino, 2005). Basal cells then divide and differentiate to reestablish the strata of normal healthy skin.

In addition to proliferation and reepithelialization in the proliferative phase, the crucial step of angiogenesis, or neovascularization, also occurs. Angiogenesis is triggered by the release of cytokines and growth factors produced by inflammatory cells, keratinocytes, and fibroblasts (Rafehi et al., 2011). Stem cells of endothelial cells from surrounding blood vessels migrate through the ECM to the wound to grow new vessels. These new blood vessels deliver oxygen and nutrients into the wound site (Adams and Alitalo, 2007; Tonnesen et al., 2000), which are required by fibroblasts and epithelial cells. Failures in the proliferative phase can result in a chronic open wound, which may lead to further complications.

### 1.3.4 Phase 4: remodeling

The last phase of healing is the remodeling phase, which begins 2-3 weeks after injury and can last for years (Deonarine et al., 2007; Gurtner et al., 2008). The wound contracts due to activities of growth factors, extracellular matrix proteins, integrin receptors, and myofibroblasts (Darby and Hewitson, 2007; Desmouliere et al., 2005). Earlier events, such as phagocytosis and cell migration, cease, and cells no longer needed, such as endothelial cells and macrophages, undergo apoptosis or leave the wound site. Protease secretion is suppressed, and synthesis and deposition of collagen increases. Fibroblasts, macrophages, and endothelial cells secrete matrix metalloproteinases, which

break down the provisional matrix, and a more permanent matrix made up of the stronger type I collagen is created (Gurtner et al., 2008). This phase can be fragile and lead to scarring or to formation of chronic non-healing wounds.

Chronic wounds differ from acute wounds by their inability to follow the normal healing process. In a chronic wound, there are disturbances in the expression of growth factors, cytokines, and proteins that assist in tissue repair. Multiple forms of chronic cutaneous wounds exist, which include pressure, fungal, and venous wounds and diabetic foot ulcers (Moreo, 2005; Mustoe, 2004). Depending on the severity of a wound and form of treatment, damaged tissues may take weeks to heal. However, in many cases, wounds may take years to fully repair if they are able to heal at all. In addition, even if a wound successfully repairs, the tissues may never fully regain the properties of uninjured skin.

### 1.3.5 Epidermal growth factor receptor and signaling in wound healing

Though there are many factors that contribute to successful wound healing, one vital receptor is the epidermal growth factor receptor (EGFR). The EGFR is a receptor tyrosine kinase that is important for proper development and tissue homeostasis and has been demonstrated to be required for reepithelialization (Brem et al., 2007; Hudson and McCawley, 1998; Stoscheck et al., 1992). In healthy tissue, expression of EGFR and its ligands was found to transiently increase after injury (Stoscheck et al., 1992; Tokumaru et al., 2000). In contrast, EGFR was decreased at wound margins in chronic, non-healing wounds (Brem et al., 2007), further demonstrating an important role of EGFR in wound healing. EGFR signaling leads to rapid and delayed responses necessary for wound

healing, which include cytoskeleton reorganization and modulation of cell-cell contacts necessary for migration. EGFR also affects gene expression. Of particular interest to our studies is transcription factor Snai2/Slug.

One way that EGFR regulates reepithelialization is through the expression of Snai2/Slug. It is a member of the Snail superfamily of transcription factors, which encode zinc-finger proteins and function as transcriptional repressors (Cobaleda et al., 2007; Hemavathy et al., 2000b; Shirley et al., 2010). Snai2 is a vital component of epithelial to mesenchymal transition during embryonic development (Barrallo-Gimeno and Nieto, 2005; Hemavathy et al., 2000a; Nieto, 2002; Sefton et al., 1998; Shook and Keller, 2003) but has also been shown to be highly expressed in adult tissues, such as the skin, heart, placenta, kidney, lung, and uterus (Parent et al., 2004). Snai2 has also been demonstrated to be required for successful reepithelialization (Chandler et al., 2007; Hudson et al., 2009; Savagner et al., 2005). Increased Snai2 expression leads to decreased E-cadherin and β-catenin expression, which are important in adheren junctions, and to enhanced expression of matrix metalloproteinases at wound margins (Chandler et al., 2007). At the wound edges of normally healing canine corneal wounds, Snai2 expression was increased (Chandler et al., 2007). However, Snai2 was decreased at margins of non-healing corneal erosions. In addition, Snai2 expression was found to be elevated in keratinocytes at wound margins in mice as well as in keratinocytes migrating from tissue explants *ex vivo* (Savagner et al., 2005). Lastly, Snai2 null mice display decreased epithelial outgrowth from *ex vivo* skin explants (Kusewitt et al., 2009), and exposure of null mice to ultraviolet radiation resulted in chronic, non-healing wounds (Hudson et al., 2009), further demonstrating a role of Snai2 in wound repair.

It is through the activities of EGFR and Snai2 that we believe contribute to diabetes-impaired wound healing, as Snai2 is an essential mediator of EGFR-mediated reepithelialization.

### 1.3.6 Diabetes-impaired wound healing

The normal process of wound healing requires an intricate orchestration of events. However, with the added complication of diabetes, healing is poorly executed and uncontrolled, resulting in chronic, non-healing wounds (Usui et al., 2008; Velander et al., 2008). Diabetic foot ulcers are the most common cause of non-traumatic lower extremity amputations in the world (Wu and Armstrong, 2005) and occur in up to 15% of diabetics (Rafehi et al., 2011). Impaired wound healing is usually a consequence of macro- and micro-angiopathy and neuropathy, and defects occur in all phases of the wound healing process (Rafehi et al., 2011). Therefore, it is important to better understand the underlying mechanisms of diabetic wound healing and how deficiencies can be remedied.

In diabetes-impaired wound healing, there is dysregulation in the inflammatory response. Macrophages have impaired phagocytic function, leading to failure to remove necrotic tissue (Khanna et al., 2010; Liu et al., 1999). Cytokine and growth factor levels are uncontrolled, which may prolong the inflammatory phase. This then results in delayed progression into the later phases of wound healing (Blakytny and Jude, 2009).

In the proliferation phase, reepithelialization, proliferation, and differentiation are affected. The extracellular matrix is produced in smaller amounts, and cell migration and adhesion to the matrix are disrupted due to covalent modification of collagen, preventing access of a scaffold to almost all cells in the proliferative and migratory phase (Bailey et

al., 1998; Paul et al., 1998; Peppa and Raptis, 2011). Apoptosis of fibroblasts is increased, and migration is decreased, resulting in impaired granulation tissue formation. In addition, keratinocyte proliferation is decreased, and cell morphology and differentiation are altered (Al-Mashat et al., 2006; Peppa and Raptis, 2011; Spravchikov et al., 2001). Therefore, the ability of the wound to restore a barrier against the external environment is no longer achieved, leaving the wound vulnerable to further damage and potential infection. In addition, levels of endothelial progenitor cells, which migrate to the site of injury from the basement membrane, are decreased, leading to impaired angiogenesis (Loomans et al., 2004; Tepper et al., 2002). This then leads to deprivation of nutrients and oxygen required at the wound site, further delaying wound repair.

In addition, the regulation of growth factors, including those that promote keratinocyte migration and angiogenesis, is impaired. Defects in cell migration may result from decreased growth factors such as insulin-like growth factor-1 (IGF-1), which has been demonstrated to increase wound healing in diabetic animal models (Bitar, 1997; Tsuboi et al., 1995). Stimulation of epithelial cells is also impaired due to down-regulation in factors such as EGF, PDGF, IL-8, IL-10, and TGF-β1. Matrix metalloproteinases (MMPs) MMP-2, MMP-8, and MMP-9 are increased, and MMP inhibitors are decreased, resulting in delayed wound healing due to the destruction of proteins and growth factors required for normal healing (Peppa and Raptis, 2011; Yager et al., 1996). Lastly, wound contraction is disrupted in the remodeling phase, and the disorganized deposition of collagen in ECM formation leads to weak tissue repair and avascular scarring (Peppa and Raptis, 2011).

Diabetic wounds continue to be a serious life-changing complication of diabetes, and failure to heal causes substantial morbidity due to deficits in wound repair, including persistent ulcerations, infections, and amputations (Blakytny and Jude, 2009; Rafehi et al., 2011). While treatments are available, they are not completely effective, and current research is focused on developing novel therapeutic strategies for diabetic ulcers (Blakytny and Jude, 2009; Rafehi et al., 2011).

## 1.4 Advanced glycation end products

Among the many issues associated with diabetes, the accumulation of advanced glycation end products (AGEs) contribute to pathology. AGEs are the product of a nonenzymatic reaction between reducing sugars with proteins, lipids, and nucleic acids also called the Maillard reaction (Maillard, 1912; Peppa and Raptis, 2011; Singh et al., 2001). This process was identified in the early 1900's when it was observed that heating amino acids with reducing sugars resulted in a yellow-brown color (John and Lamb, 1993; Maillard, 1912). Following an initial glycation reaction between glucose and proteins, a Schiff base forms, followed by rearrangement to an Amadori product (Lapolla et al., 2003) (Figure 1.3). Through a series of oxidation/reduction reactions and rearrangements, the final products leave proteins damaged and unable to perform their normal functions (Ahmed, 2005). AGEs are constantly formed in the body, but in the presence of conditions such as diabetes, renal failure, Alzheimer's disease, rheumatoid arthritis, and aging, the rate of AGE formation is increased, and removal is decreased (Singh et al., 2001; Takeuchi and Yamagishi, 2008; Vytasek et al., 2010). Histologically, AGEs have been shown to accumulate in various tissues such as the renal cortex

(Bierhaus et al., 1998), the cartilage in rheumatoid arthritis (Takahashi et al., 1994), and cardiac muscle, lung, and liver (Sell and Monnier, 1990). Studies are establishing a causal role of AGEs on processes such as cardiovascular disease and arthritis. For example, AGE accumulation in the vasculature contributes to arterial stiffening in cardiovascular disease and to stiffening of joints in arthritis, demonstrating the broad range in which AGEs can be debilitating.

Exogenously, AGEs are ingested from the diet or through tobacco smoke and account for ~10% of AGEs in the body. They are naturally produced in uncooked foods, and formation is accelerated through processing such as sterilization, pasteurization, and flavor and appearance enhancements (Peppa and Raptis, 2011). Additionally, cooking methods such as grilling and frying also promote AGE formation and levels further increase with higher time and degree of exposure to heat (Goldberg et al., 2004; Luevano-Contreras and Chapman-Novakofski, 2010; Uribarri et al., 2010).

The ability of AGEs to accumulate both endogenously and exogenously in the body makes it a dangerous factor in damaging proteins and preventing normal cell function. These inhibitory actions also extend to impaired diabetic wound healing.

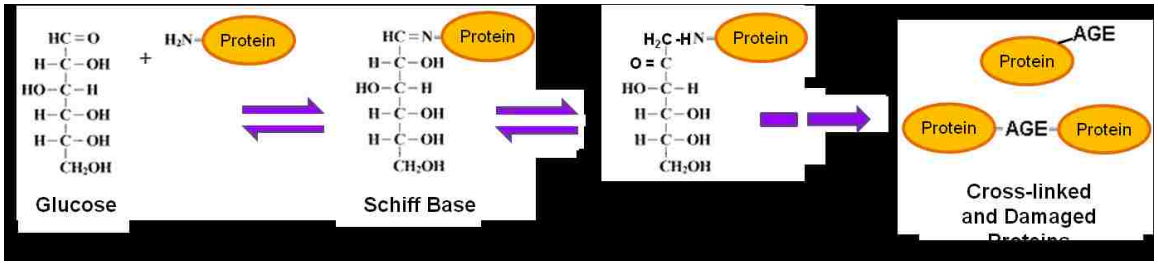


FIGURE 1.3. **The Maillard reaction.** Glucose and proteins react nonenzymatically to form covalently modified proteins, which lead to protein dysfunction and impaired signaling.

### 1.4.1 AGE involvement in diabetic wound repair

Because AGEs form from chemical reactions with glucose, hyperglycemia pushes the forward reaction towards glycation, and an increasing body of evidence suggests that AGEs and associated reactive intermediates disrupt various aspects of the wound healing cascade (Ahmed, 2005; Huijberts et al., 2008; Peppa and Raptis, 2011; Peppa et al., 2009). AGEs have been implicated in defective cell locomotion and survival (Loughlin and Artlett, 2009; Morita et al., 2005; Zhu et al., 2011). In addition, exposure of rats to the AGE precursor methylglyoxal decreased the numbers of cells actively migrating into the wound, decreased angiogenesis, and reduced secretion and accumulation of extracellular matrix components (Berlanga et al., 2005).

High glucose from the diet causes increased AGE levels, and dietary manipulation of AGEs and AGE precursors in mouse models provides evidence that AGEs contribute to the impaired wound healing observed in diabetes (Morita et al., 2005; Peppa et al., 2009; Zhu et al., 2011). Numerous studies have shown that dietary AGEs are absorbed and significantly contribute to the body's AGE level and pathology (Luevano-Contreras and Chapman-Novakofski, 2010). Restricting dietary AGE prevented atherosclerosis (Lin et al., 2003), kidney dysfunction, type 1 and type 2 diabetes, improved insulin sensitivity, and accelerated wound healing in animals (Peppa et al., 2003; Peppa and Raptis, 2011). In addition, restricting dietary AGE in diabetic patients reduced markers of oxidative stress, endothelium dysfunction and inflammation (Luevano-Contreras et al., 2013). In diabetic *db/db* mice fed a high AGE diet, increased levels of the AGE carboxymethyl lysine (CML) was present in wound tissue, and these mice displayed a sustained inflammatory response and incomplete wound closure (Peppa et al., 2003).

Conversely, restricting dietary AGE in diabetic mice improved wound closure compared to those fed a high AGE diet (Peppa et al., 2003). Therefore, studies conducted in both animals and humans demonstrate that dietary AGE significantly contributes to the body's AGE pool and to the complications from diabetes-related pathologies.

**Rationale**

It is vital to better understand the mechanisms involved in defective wound repair in diabetes. Diabetes entails an increase in blood glucose levels, which leads to the accumulation of AGEs. The literature reports that hyperglycemia, AGE precursors, and AGEs lead to impaired EGFR activity. EGFR is a crucial receptor that leads to downstream signaling required for successful wound reepithelialization, suggesting that a defect in EGFR signaling may be a factor in impaired diabetic wound healing.

Our goal is to further explore the impact of AGEs on EGFR signaling and downstream targets in diabetes-impaired wound healing. The work described in this dissertation tested the following hypothesis:

**Hypothesis**

AGE precursors and AGEs, which form because of hyperglycemia in diabetes, cause a decrease in EGFR activation and downstream targets, resulting in impaired reepithelialization (Figure 1.4).

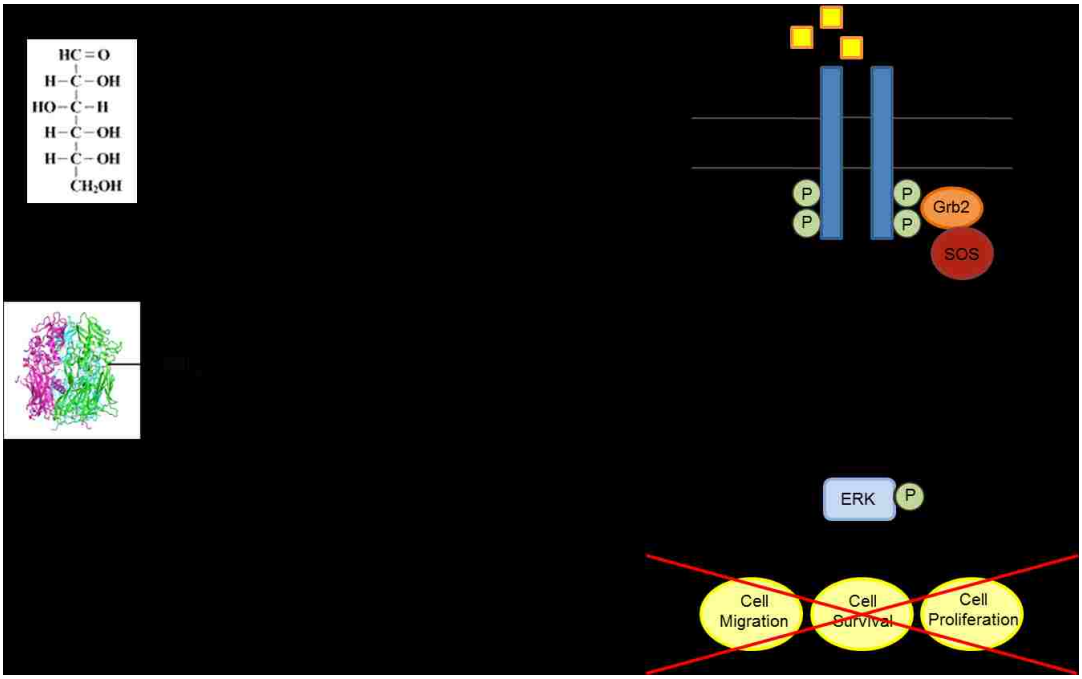


FIGURE 1.4. **Model of AGE involvement in diabetic wound reepithelialization.** Hyperglycemia results from diabetes and reacts with proteins to form AGE precursors and AGEs. AGEs and their precursors lead to impaired EGFR signaling and downstream function, resulting in defective wound repair.

The specific aims to test this hypothesis are as follows:

**Project Aims**

**Aim 1: Investigate the effects of AGE precursors and AGEs on EGFR activity and its downstream functions in a cellular system**

*Hypothesis:* AGE precursors and AGEs will inhibit EGFR signaling and impair migration and proliferation in keratinocytes.

**Results:** Chapter 3 (EGFR in a cellular system)

**Aim 2: Evaluate Snai2 expression and wound healing in diabetic models**

*Hypothesis:* Diabetes will lead to decreased Snai2 expression and impaired wound healing under diabetic conditions.

**Results:** Chapter 4 (Snai2 in a cellular system and in *ex vivo* explants)

**Aim 3: Determine whether modulating Snai2 expression promotes wound repair under diabetic conditions.**

*Hypothesis:* Promoting increased Snai2 expression will allow for recovery of wound healing even under diabetic conditions.

**Results:** Chapter 4 (Snai2 in *ex vivo* explants)

# CHAPTER 2

## Materials and Methods

The following materials and methods were used for the experiments described in this dissertation.

### 2.1 Cell culture studies

The non-tumorigenic human keratinocyte cell line, SCC 12F, was kindly provided by Dr. William A. Toscano, Jr (University of Minnesota, Minneapolis, MN). These cells over-express the EGFR by ~5-fold relative to normal keratinocytes (Hudson and McCawley, 1998), which is similar to what is reported at wound margins during repair (Stoscheck et al., 1992). The SCC 12F cells were maintained in Dulbecco's Modified Eagle's Medium (DMEM) containing physiologically normal glucose levels (6 mM) (Sigma, Saint Louis, MO), supplemented with 5% defined calf serum (DCS) (HyClone, Thermo Scientific, Waltham, MA), 1% L-glutamine (Sigma), and 0.5% antibiotics (penicillin, 100 units/ml, and streptomycin, 50 μg/ml) (Gibco, Grand Island, NY). HaCaT cells were provided by Dr. Mitch Denning (Loyola University Medical Center, Maywood, IL). These cells are a spontaneously transformed, non-tumorigenic human keratinocyte cell line (Boukamp et al., 1988). HaCaTs were maintained in medium containing DMEM:F12 (Sigma) supplemented with 10% newborn calf serum (Gibco/Invitrogen, Grand Island, NY), 4x MEM amino acids (Sigma), 1% L-glutamine, and 0.5% antibiotics (penicillin, 100 units/ml, and streptomycin, 50 μg/ml) as previously described (Cooper et al., 2007). Normal human epidermal keratinocytes (NHEK) (Life Line Cell Technology, Frederick, MD) were maintained in DermaLife K Medium

Complete Kit (Life Line Cell Technology), a serum-free medium. SCC 12F and HaCaT keratinocytes were cultured at 37°C in 5% $CO_2$/95% air humidified incubators. The cells were grown to 50-60% confluency and changed into serum-free media [6 mM glucose DMEM containing 0.1% bovine serum albumin (BSA), 1% L-glutamine, and 0.5% antibiotics (penicillin, 100 units/ml, and streptomycin, 50 μg/ml) for SCC 12F experiments and DMEM:F12 containing 0.1% BSA, 1% L-glutamine, and 0.5% antibiotics (penicillin, 100 units/ml, and streptomycin, 50 μg/ml) for HaCaT experiments] overnight prior to treatments. Because NHEK medium is provided serum-free, experiments were started as soon as ideal confluency was reached.

### 2.1.1 Cell culture drug treatments

To mimic a diabetic environment, either high glucose medium [25 mM glucose DMEM (Sigma) with supplements (0.1% BSA, 1% L-glutamine, and 0.5% antibiotics (penicillin, 100 units/ml, and streptomycin, 50 μg/ml))] or the AGE precursor, glyoxal, in low glucose media [6 mM glucose DMEM (Sigma) with supplements (0.1% BSA, 1% L-glutamine, and 0.5% antibiotics (penicillin, 100 units/ml, and streptomycin, 50 μg/ml))] was used. The reactive intermediate, glyoxal, has been demonstrated to be formed from all stages of the glycation process (Bucala, 1997). Glyoxal leads to the AGE, carboxymethyl lysine (CML), which was the first AGE discovered forming *in vivo* (Ahmed et al., 1986; Tessier, 2010) and is used as one of the major biomarkers of the Maillard reaction in human tissues (Thorpe and Baynes, 2002).

The stock of glyoxal (GO, Sigma) is provided at 40% in $H_2O$ (~8.8 M). The working concentration of glyoxal was prepared by diluting the 8.8 M stock in the serum-

free medium corresponding to each cell line (Section 2.1) or in explant medium (Section 2.2.2). Cells were stimulated with 10 nM epidermal growth factor (EGF) (Biomedical Technologies, Stoughton, MA) reconstituted in Minimum Essential Medium Eagle (Sigma) with supplements [0.1% BSA, 1% L-glutamine 0.5% antibiotics (penicillin, 100 units/ml, and streptomycin, 50 μg/ml), and 1% sodium pyruvate (Sigma)] for the times indicated in the figure legends prior to protein collection. For experiments involving the glycation inhibitor, aminoguanidine hydrochloride (AG, Sigma, > 98% crystalline), cells were pre-treated with 5 mM AG made up in 0.1% BSA/6 mM glucose DMEM for 6 h before the addition of glyoxal, and AG was present for the duration of the experiment. To pharmacologically induce Snai2 protein, tetracycline hydrochloride (Sigma) dissolved in sterile water was added to the cells with a final concentration of 10 μM, and transforming growth factor beta (TGF-β) (Millipore, Billerica, MA) reconstituted in sterile water was given to the samples at a final concentration of 10 ng/ml. Keratinocytes and explants were exposed to the chemicals for a maximum of 5 d.

### 2.1.2 MTS proliferation assay

$8x10^3$ cells of SCC 12F cells were plated into a 96-well plate. The next day, the keratinocytes were serum-starved in 0.1% BSA/6 mM glucose DMEM overnight. The cells were then treated with 0.5 mM glyoxal made up with serum-free medium for 24 h and stimulated with 1 nM EGF for 2 or 24 h to promote cell proliferation. At the end of the treatment period, the medium in the wells was removed and replaced with fresh medium to remove cellular debris. 20 μl of the solution (3-(4,5-dimethylthiazol-2-yl)-5-(3-carboxymethoxyphenyl)-2-(4-sulfophenyl)-2H-tetrazolium; MTS) / (phenazine

methosulfate; PMS) [PMS (Pierce) - 0.92 mg/ml in Dulbecco's PBS; MTS (Promega, Madison, WI) - 2 mg/ml in Dulbecco's PBS; MTS/PMS solution – 100 µl PMS in 2 ml MTS] was added to each well and incubated for 1.5 h at 37ºC while shaking. Results were then read at 490 nm with the SpectraMax 340 (Molecular Devices, Sunnyvale, CA).

### 2.1.3 Boyden chamber migration assay

$2x10^4$ cells of SCC 12F cells were plated into inserts of a 24-well companion plate (Becton Dickinson, Franklin Lakes, NJ). Keratinocytes were allowed to adhere for 2 h and then treated with 0.5 mM glyoxal diluted in 0.1% BSA/6 mM glucose DMEM and to 1 nM or 10 nM EGF for 24 h to promote cell migration. At the end of the 24 h incubation period, the insides of the inserts were wiped clean with a cotton swab. They were then fixed in ice-cold 100% methanol and stained with 0.2% crystal violet (Sigma) in water for 5 min. The membranes of the inserts were removed and mounted onto glass slides using VectaShield with 2 µg/mL DAPI (Vector Labs Inc., Burlingame, CA). Treatment groups were performed in triplicate, and images were obtained using the Olympus IX70 inverted fluorescence microscope (Olympus, Center Valley, PA) and a 10x objective with 4 fields per membrane. DAPI-stained cells were counted to determine the number of migrated cells.

### 2.1.4 Immunoblot analysis

Cells were rinsed in ice-cold phosphate-buffered saline (PBS) (137 mM sodium chloride, 2.7 mM potassium chloride, 4.3 mM sodium phosphate dibasic heptahydrate, and 1.5 mM potassium phosphate monobasic, pH 7.2) and harvested in Radio Immuno

Precipitation Assay (RIPA) buffer (50 mM Tris pH 7.4, 1% NP40, 0.25% sodium deoxycholate, 150 mM sodium chloride, 1 mM ethylenediaminetetraacetic acid (EDTA), 1 mM phenylmethylsulfonyl fluoride, 1 mM sodium orthovanadate, 10 mM sodium fluoride, 1 µg/mL pepstatin, 1 µg/mL aprotinin, 1 µg/mL leupeptin, 10 mM sodium pyrophosphate, and 10 mM β-glycerophosphate). Cell lysates were sonicated using the Sonifier Cell Disruptor 200 (Branson Ultrasonics Corporation, Danbury, CT) with an output control of 5 and duty cycle 30%. Extracts were clarified by centrifugation (14,000 RPM, 4 min, 4ºC) in the Centrifuge 5417R (Eppendorf, Hauppauge, NY), and the supernatant was collected for protein analysis. Protein quantification was performed using the BCA protein assay (Pierce, Rockford, IL). 20 µg of protein was separated by electrophoresis through a 7.5% SDS-polyacrylamide gel for detection of carboxymethyl lysine (CML) or phosphotyrosine, and 50 µg of protein was separated in a 12% gel for Snai2. Proteins were transferred overnight to polyvinylidene difluoride membrane for CML and phosphotyrosine and to nitrocellulose for Snai2. Membranes were blocked in either 3% BSA/Tris-buffered saline-Tween 20 (TBS-T) or 5% milk/TBS-T for 1 h and were probed overnight with antibodies for CML (Abcam, Cambridge, MA) 1:2,500 diluted in 3% BSA, phosphotyrosine (Millipore) 1:2,000 diluted in 3% BSA/TBS-T, Snai2 (Cell Signaling, Danvers, MA) 1:500 diluted in 3% BSA/TBS-T, and β-Tubulin (Santa Cruz Biotechnology, Inc., Santa Cruz, CA) 1:500 diluted in 5% milk/TBS-T (Table 2.1). Membranes were washed with 1x TBS-T and incubated with an anti-rabbit secondary antibody (Promega) 1:5,000 for CML and β-Tubulin and 1:10,000 for Snai2, and with an anti-mouse secondary antibody (Promega) 1:2,500 for phosphotyrosine in the respective blocking agents for 1 h at room temperature. Membranes were washed in 1x

TBS-T and developed using the SuperSignal chemiluminescent detection system (Pierce). Immunoblot results were imaged using a Digital Science Image Station on a Kodak 440CF Imager (Kodak, New Haven, CT). A region of interest was selected around the largest band on the membrane, and the box was replicated over the remaining bands. The intensity of the perimeter of the box was identified as the background, and the value of this intensity was subtracted from the total intensity measured in each of the regions of interest. This yielded the densitometry measures of the immunobands.

TABLE 2.1. Summary of specific western blot conditions

| Primary Antibody | Dilution | Block | Membrane | Secondary Antibody | Dilution |
|---|---|---|---|---|---|
| β-Tubulin Santa Cruz #sc-9104 | 1:500 | 5% milk/TBS-T | Nitrocellulose/ PVDF | Anti-Rabbit Promega #W401B | 1:5,000 |
| CML Abcam #ab27684 | 1:2,500 | 3% BSA/TBS-T | Nitrocellulose | Anti-Rabbit | 1:5,000 |
| EGFR Santa Cruz #sc-03 | 1:1,000 | 5% milk | PVDF | Anti-Rabbit | 1:10,000 |
| GAPDH Chemicon #MAB374 | 1:300 | 5% milk | Nitrocellulose | Anti-Mouse Promega #W402B | 1:5,000 |
| PARP Cell Signaling #9542 | 1:1,000 | 5% milk | Nitrocellulose | Anti-Rabbit | 1:2,000 |
| Phosphotyrosine Millipore #05-1050 | 1:2,000 | 3% BSA | PVDF | Anti-Mouse | 1:2,500 |
| Sp1 Cell Signaling #5931 | 1:1,000 | 3% BSA | Nitrocellulose | Anti-Rabbit | 1:1,000 |
| Snai1/Snail Abcam #17732 | 1:1,000 | 3% BSA | Nitrocellulose | Anti-Rabbit | 1:20,000 |
| Snai2/Slug Cell Signaling #9585s | 1:500 | 3% BSA | Nitrocellulose | Anti-Rabbit | 1:10,000 |

### 2.1.5 RNA isolation and quantitative real-time PCR (qRT-PCR)

RNA was isolated from SCC 12F cells by first washing cells with PBS and then incubating the cells with TRIzol reagent (Invitrogen) for 10 min at room temperature. Using a cell scraper, the samples were collected into a microcentrifuge tube and vortexed. RNase-free chloroform was added to each sample, vortexed, and allowed to sit for 3 min. The samples were then clarified by centrifugation (14,000 RPM, 10 min, 4°C) in the Centrifuge 5417R (Eppendorf). The aqueous phase was collected into a new microfuge tube, and the samples were incubated with RNase-free isopropanol for 10 min at room temperature to precipitate RNA. The samples were then centrifuged (14,000 RPM, 10 min, 4°C), and then the supernatant was collected. RNase-free 70% ethanol was used to wash the pellet, and then the samples were centrifuged once more (14,000 RPM, 5 min, 4°C). The supernatant was discarded, and the remaining pellet was air-dried for 5 min, followed by resuspension in RNase-free water.

The RNA was quantified using the NanoDrop ND-1000 Spectrophotometer (NanoDrop Technologies, Inc., Wilmington, DE). The High Capacity cDNA reverse transcription kit (Applied Biosystems, Life Technologies, Carlsbad, CA) was used to make cDNA from 2 µg RNA, and Mastermix made according to manufacturer's protocol (10x RT buffer, 100 mM dNTP Mix, 10x random primers, Multiscribe RT, and RNase-free water) was added to each tube. The samples were run in the PTC-200 Peltier Thermal Cycler (MJ Research, Ramsey, MN) with the following conditions: 25°C for 10 min, 37°C for 2 h, hold at 4°.

The cDNA was diluted 1:5, and 2 µl was used for quantitative real-time PCR. PCR reactions were run in a 384-well plate with a total volume of 10 µl containing

cDNA product, Syber Green PCR mastermix (Applied Biosystems), and primers (final concentration 0.2 µM). Primers were purchased from Qiagen (Germantown, MD) and consisted of the following:

QuantiTect primer QT00044128 (Snai2 119 bp)

QuantiTect primer QT01192646 (GAPDH 119 bp)

The samples were run in the real time machine 7900HT Fast Real Time (Applied Biosystems) with the following conditions (Xiong et al., 2005): 95°C for 10 min, 40 cycles of 95°C for 30 s, 56°C for 40 s, and 72°C for 30 s. The relative quantification of the target gene was determined using the $2^{-\Delta\Delta Ct}$ method described by (Livak and Schmittgen, 2001).

### 2.1.6 Immunoprecipitation

Immunoprecipitation was carried out according to the immunoprecipitation and crosslinking protocols as described by Invitrogen. Briefly, Snai2 antibody (Cell Signaling) diluted in PBS/0.02% Tween 20 pH 7.4 was incubated with 50 µl Dynabeads Protein G (Invitrogen) for 30 min at room temperature while rotating. The Dynabead-antibody complex was washed and crosslinked with 5 mM Bis(sulfosuccinimidyl)suberate ($BS^3$) (Thermo Fisher Scientific Inc., Waltham, MA) diluted in Conjugation Buffer [20 mM sodium phosphate, 0.15 M sodium chloride (pH 7-9)] for 30 min while rotating at room temperature. The crosslinking reaction was quenched by addition of $BS^3$ Quenching Buffer (1 M Tris-HCl, pH 7.5) for 15 min. The Dynabeads were then washed 3x in phosphate-buffered saline - Tween 20 (PBS-T), and the beads were retained in the tube by a magnet. 1250 µg protein was brought up to 600

µl with RIPA collection buffer (Section 2.1.4) and added to the Dynabeads-antibody complex. The mixture was incubated for 3 h at 4°C while shaking. The Dynabeads-antibody-antigen complex was washed 3x in PBS and resuspended in 20 µl loading buffer (3x, 187.5 mM Tris-HCl, pH 6.8, 6% (w/v) sodium dodecyl sulfate (SDS), 30% glycerol, 150 mM dithiothreitol, and 0.03% (w/v) bromophenol blue). The samples were heated at 100°C for 5 min to remove the protein from the Dynabeads, and using the magnet to retain the beads in the tube, the supernatant was loaded into wells of a 12% gel. Immunoblotting for CML and Snai2 was performed as described above (Section 2.1.4) (Figure 2.1).

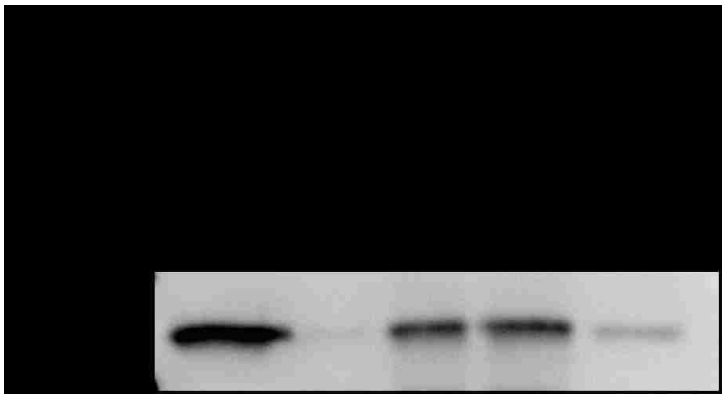

FIGURE 2.1. **Immunoprecipitation of Snai2 protein.** SCC 12F keratinocytes were treated with 10 nM EGF for 24 h to stimulate Snai2 protein. Snai2 was immunoprecipitated and detected by immunoblotting.

## 2.2 Animal studies

Studies involving animals were conducted according to the guidelines for the use and care of laboratory animals of the Institutional Animal Care and Use Committee under the University of New Mexico protocol #10-100483-HSC. FVB mice (Taconic, Hudson, NY) were used for all studies.

### 2.2.1 Transgenic mice

Snai2/Slug transgenic mice were created in the lab of Dr. Donna F. Kusewitt. Snai2 cDNA was cloned into a keratin 5 expression vector kindly provided by Dr. Jose Jorcano and injected into pronuclei of FVB mice. DNA was isolated from tail tips by overnight incubation of the tails with genomic lysis solution (20 mM Tris-Cl, pH 8.0, 50 mM NaCl, 100 mM EDTA, pH 8.0, and 1% SDS) and with 0.133 mg/ml Proteinase K (Invitrogen) in a 55°C incubator while shaking. The next day, the samples were cooled to room temperature. Protein Precipitation Solution (Qiagen) was added to each sample. The samples were cooled on ice for 5 min and then clarified by centrifugation (14,000 RPM, 5 min, 4°C) in the Centrifuge 5417R (Eppendorf). The supernatant containing the DNA was removed to a new microfuge tube, and 100% isopropanol was added to the sample and inverted until DNA precipitated out of solution. The samples were then centrifuged (14,000 RPM, 2 min, 4°C), and the supernatant was discarded. 70% ethanol was added to the DNA to wash the pellet, and then the samples were centrifuged (14,000 RPM, 1 min, 4°C). The ethanol was discarded, and the DNA pellet was air-dried over ice for 15 min. The DNA was resuspended in TE buffer (10 mM Tris-HCl and 1 mM EDTA, pH 8.0) and allowed to hydrate overnight at 4°C.

The following day, the amount of DNA in each sample was ascertained using the NanoDrop ND-1000 Spectrophotometer (NanoDrop Technologies, Inc.), and 20 ng DNA was calculated for use in the PCR reaction. The GoTaq® Flexi DNA Polymerase kit (Promega) was used according to manufacturer's instructions for PCR. PCR

amplification was performed using primers that produce amplicons specific for the K5-Snai2 transgene. Primer sets were as follows:

β glob F: 5'-TGCTGTCTCATCATTTTGGC-3'

Snai2 R: 5'-GCATTCTGTTTGAGTAAACACTGG-3'.

Amplifications were carried out on a PTC-200 Peltier Thermal Cycler (MJ Research) with the following conditions: 95°C for 4 min, 40x (95°C for 30 sec, 60°C for 30 sec, 72°C for 60 sec), 72°C for 10 min, hold at 4°C. The PCR products were run through a 2% agarose gel containing SYBR Safe DNA Gel Stain (Invitrogen) at 1:10,000. A band located at ~920 bp indicated a Snai2 over-expressing mouse (Figure 2.2A).

The K5 Snai2 transgenic mice are smaller in size compared to wild type mice, and differences in the skin include hyperkeratosis, increased follicular density, and more active hair growth (Figure 2.2B) in the over-expressing mice.

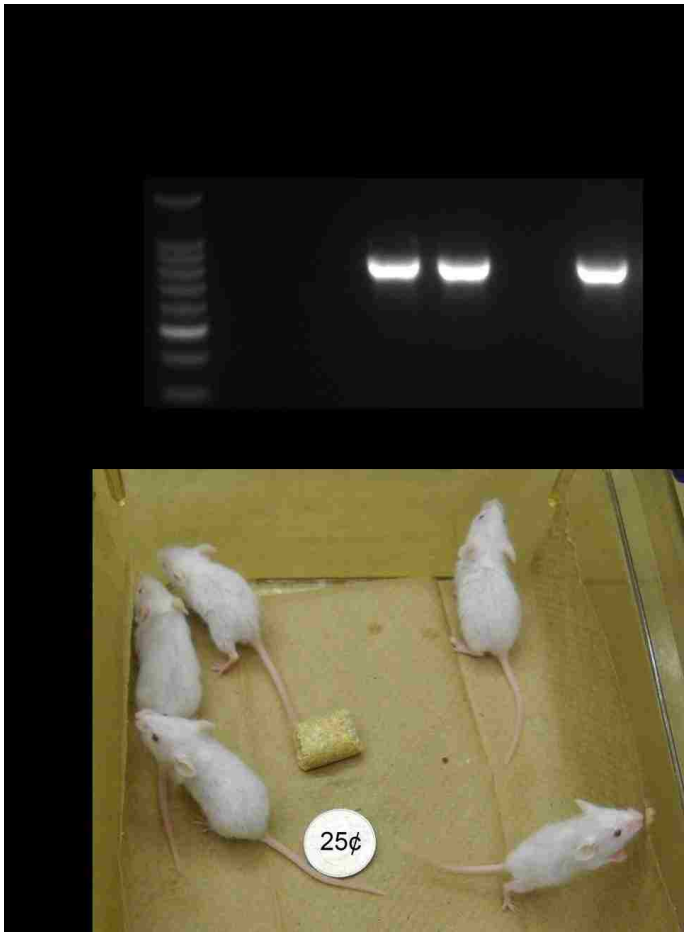


FIGURE 2.2. **K5 Snai2 transgenic mice. (A)** The presence of a band at ~920 bp indicates a Snai2 over-expressing animal. **(B)** FVB Snai2 over-expressing mice are smaller in size compared to wild type littermates, have hyperkeratosis, increased follicular density, and more active hair growth. Mice shown above are ~21 days old. The coin was provided for sense of scale.

### 2.2.2 Epithelial outgrowth

FVB mice aged 7 weeks were euthanized by first $CO_2$ inhalation followed by cervical dislocation. The hair from the dorsal side was shaved, and Nair (Church & Dwight Co., Inc. Princeton, NJ) was used to remove the stubble (Figure 2.3A). The Nair was rinsed off with water, and the skin was cleaned with iodine and 70% ethanol. The skin was then dissected out and placed dermal side down onto a glass plate. Using a 3.5 mm disposable biopsy punch (Miltex, Inc., York, PA), four circular skin explants were

isolated per animal and plated into wells of a 4-well chamber slide (Nalge Nunc International, Rochester, NY). Following a 1 h incubation at room temperature, the explants were submerged in 75 µl of explant medium (Mazzalupo et al., 2002). The medium composition was as follows: DMEM (Invitrogen) and DMEM:F12 (Sigma) powder were dissolved according to manufacturer's instructions, and pH'ed to 7.0. DMEM and DMEM:F12 were combined in a 1:1 (v/v) mixture and supplements were added [10% fetal bovine serum (Invitrogen), 0.1 mM cholera toxin (Sigma), 10 ng/ml EGF (Biomedical Technologies), 2 nM Triiodothyronine (Sigma), 2.5 µg/ml transferrin / 5 µg/ml insulin (Invitrogen), 0.4 µg/ml hydrocortisone (Sigma), 60 µg/ml penicillin/streptomycin (Sigma), 25 µg/ml gentamicin (Sigma)]. Explants were cultured overnight in 95% air/5% $CO_2$ humidified incubators at 37°C. The following day, an additional 425 µl of medium was added to each explant and incubated for another 24 h. Explants were exposed to 0.1, 0.3, or 0.5 mM glyoxal or to 10 ng/ml TGF-β (Millipore) diluted in explant medium for up to 5 d. Images of explants were taken on days 0, 1, 3, and 5 from the start of glyoxal/TGF-β treatment using 4x (quantitative analysis) and 10x (qualitative analysis) objectives and phase contrast microscopy on the Olympus IX70 inverted microscope (Olympus) (Figure 2.3B). Epithelial outgrowth was measured by selecting the area of keratinocyte outgrowth around the explant and using the Olympus software DP2-BSW-E-V2.2 to determine the area ($\mu m^2$).

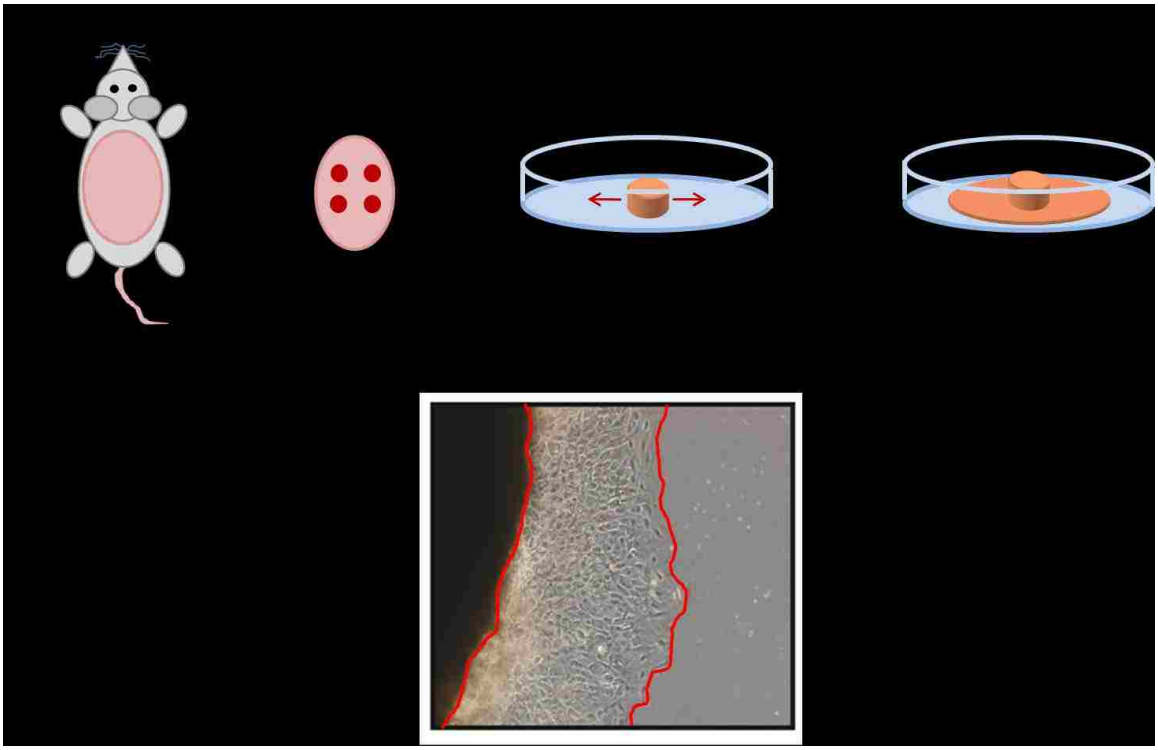

FIGURE 2.3. ***Ex vivo* explant collection. (A)** Mice were euthanized, and the skin was cleared of hair and removed from the dorsal side. Biopsy punches were used to isolate 3.5 mm-sized explants, and the tissues were plated into 4-well chamber slides. Treatments were given for as long as 5 d, and epithelial outgrowth was measured by selecting the region of cells around the tissue (red lines) and using computer software analysis to determine outgrowth area ($\mu m^2$) **(B)**.

### 2.2.3 Immunocytochemistry

At the end of the incubation period, media from explants were removed by aspiration, and explants were washed briefly in ice cold PBS. The PBS was removed and explants were fixed in 3.7% paraformaldehyde for 15 min at room temperature while gently shaking. The paraformaldehyde was then removed, and the explants were briefly rinsed in PBS followed by three more washes in PBS for 10 min each while shaking. After the second PBS wash, the explants were carefully dissected away from the cells using a straight teasing surgical needle and fine forceps, leaving the ring of epithelial cells in the wells. The cells were then permeabilized with 0.2% Triton-X-100 in PBS for

10 min. Non-specific binding was blocked by incubating keratinocytes with 0.2% fish skin gelatin (Sigma)/PBS for 1 h at room temperature. Primary Snai2 antibody (Cell Signaling) was prepared in blocking solution at a dilution of 1:100. The blocking solution was replaced with the primary antibody, and the samples were incubated overnight at 4°C while shaking. The following day, the outgrowths were washed with TBS-T 3x 10 min each. Secondary goat antibody to rabbit IgG (FITC) (Abcam) was added to the samples 1:1,000 in blocking solution and wrapped in foil to protect from light. The explants were incubated for 1 h at room temperature while shaking and then washed with 0.1% Triton-X-100/5 mg/ml BSA/ PBS 3x for 5 min each. A fourth wash was performed in TBS-T for 10 min, and a fifth containing 0.75 µg/ml DAPI (Calbiochem, Billerica, MA) in TBS-T was performed for 15 min. The samples were then mounted with VectaShield without DAPI (Vector Labs, Inc.) and sealed with nail polish for storage.

The explant outgrowths were imaged using a DSU Olympus IX81 inverted microscope (Olympus) and Stereo Investigator software (MBF Bioscience, Williston, VT). 2D confocal montages of the outgrowths were created using a 20x objective and saved as "mbf.jpg2000" images. The files were then converted to ".tiff" format using Fiji imaging software (Schindelin et al., 2012). The images were opened with SlideBook imaging software (Intelligent Imaging Innovations, Denver, CO), and a DAPI mask was set at a low threshold of 7500. Using the DAPI image, objects (nuclei) were identified as having a minimum of 25 pixels in a cluster. Snai2 staining (FITC) was evaluated by measuring the mean intensity of the green within each of the objects (nuclei) identified.

The sum of the mean FITC intensities in all the objects (nuclei) was evaluated and normalized to the total number of objects to determine the mean intensity per cell.

### 2.2.4 TUNEL staining

TUNEL staining was performed using the DeadEnd Fluorometric TUNEL System (Promega). Tissue explants from wild type mice were isolated and cultured as described in Section 2.2.2 and exposed to 0.5 mM glyoxal made up in explant medium for 5 d or to 100 µM Etoposide (Trevigen Inc., Gaithersburg, MD) as the positive control for 6 h prior to the end of the experiment. At the end of the test period, explants were fixed in 3.7% paraformaldehyde/PBS, pH 7.4 for 25 min at 4°C. The skin tissues were then dissected away, and the remaining cells were washed 2x in PBS for 5 min each at room temperature. The cells were permeabilized with 0.2% Triton X-100/PBS for 5 min and then washed again in PBS for 5 min at room temperature. Equilibration Buffer provided by the kit was then added to each sample and incubated at room temperature for 10 min. rTdT Incubation Buffer (Equilibration Buffer, Nucleotide Mix, and rTdT Enzyme) was prepared as described by manufacturer's instructions and added to each sample. Cells were covered with Plastic Coverslips provided in the kit to ensure even distribution of the reagent and to prevent the cells from drying and were then incubated at 37°C for 1 h to allow the tailing reaction to occur. Plastic Coverslips were removed, and the reaction was terminated by the addition of 2X SSC solution provided by the kit for 15 min at room temperature. The samples were washed with PBS 3x for 5 min each to remove unincorporated fluorescein-12-dUTP and then mounted with VectaShield with DAPI (Vector Labs, Inc.) to stain nuclei. The cells were then imaged at 4x using the Olympus

IX70 inverted fluorescence microscope (Olympus) and the Olympus software DP2-BSW-E-V2.2. Fluorescein-12-dUTP incorporation resulted in green fluorescence within the nuclei of apoptotic cells.

### 2.2.5 Epidermal protein isolation

Wild type and Snai2 overexpressing mice were euthanized as discussed above (Section 2.2.2). Skin from the dorsal side of mice was removed and placed in PBS over ice until all samples were collected. The skin was draped dermal-side down over 500 µl of 0.25% trypsin-EDTA (Gibco) and incubated at 37°C for 30 min. The tissue was then placed dermal-side up. With forceps, the dermal tissue was removed by scraping and peeling it away from the epidermal layer, leaving the semi-transparent epidermal layer. A 1 $cm^2$ piece of tissue was placed into RIPA collection buffer as discussed above (Section 2.1.4), and the remaining skin was placed back into PBS and stored at -80°C. The 1 $cm^2$ samples were homogenized with the Power Gen 125 tissue homogenizer with a #5 setting (Thermo Fisher Scientific Inc.) and then clarified by centrifugation (14,000 RPM, 4 min, 4ºC) in the Centrifuge 5417R (Eppendorf). The supernatant was collected, and the protein was analyzed via BCA protein assay and immunoblot as discussed above (Section 2.1.4). 75 µg protein was calculated for analysis in the immunoblot detection for Snai2.

## 2.3 Statistical analysis

Densitometry readings from the immunoblots were analyzed using one-way Analysis of Variance (ANOVA) followed by Tukey's post-test. Student's t-test was used

to compare densitometry of wild type and over-expressing mice protein levels. Cell proliferation and migration assays and explant outgrowths were analyzed using a two-way ANOVA followed by Bonferroni's post-test. Statistical analyses and data plotting were performed using GraphPad Prism version 5 for Windows (GraphPad Software, San Diego, CA). Error bars are defined as the mean +/- standard error of the mean (SEM). Values of $p<0.05$ were considered statistically significant.

# CHAPTER 3

## Epidermal growth factor receptor signaling and downstream function are impaired under diabetic conditions

### 3.1 Introduction

Wound repair is a complex process that involves the coordination of many elements including the release and action of growth factors and cytokines. A crucial component of healing is the epidermal growth factor receptor (EGFR) also known as ErbB1. This receptor is part of the ErbB family of receptor tyrosine kinases, which in addition to EGFR, include ErbB2, ErbB3, and ErbB4 (Danielsen and Maihle, 2002). EGFR, ErbB2, and ErbB3 are expressed in human skin with EGFR being demonstrated as the dominant receptor (Schneider et al., 2008; Stoll et al., 2001). Once activated, these receptors homo- and heterodimerize to induce cell signaling and function (Bazley and Gullick, 2005; Werner and Grose, 2003).

The EGFR is a receptor tyrosine kinase located on the plasma membrane and is important for proper development and tissue homeostasis (Bazley and Gullick, 2005; Schneider et al., 2008). Several ligands activate the EGFR, including epidermal growth factor (EGF), transforming growth factor alpha (TGF-α), heparin-binding EGF-like growth factor (HB-EGF), amphiregulin, and epiregulin (Pastore et al., 2008). Activation of the EGFR leads to several signaling pathways, which include the ERK pathway (cell migration, proliferation, and survival), PI3K/AKT pathway (protein synthesis and cell survival), and the JAK/STAT pathway (cell survival) (Figure 3.1) in addition to others. In the following studies, we focused on the binding of EGF ligand and subsequent activation of ERK, which is required for cell migration and proliferation.

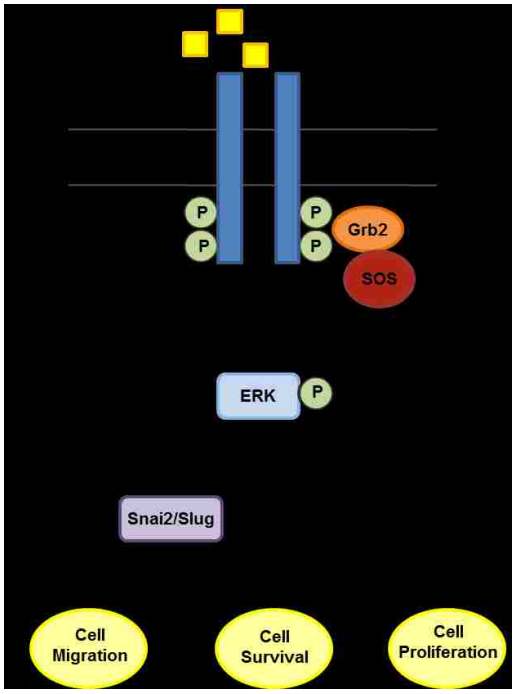


FIGURE 3.1. **EGFR signaling in wound healing.** Binding of a ligand such as EGF leads to dimerization and autophosphorylation of the receptors. This leads to activation of signaling cascades required for proper cell migration, proliferation, and overall cell survival.

There is much evidence demonstrating the importance of EGFR in reepithelialization (Hudson and McCawley, 1998). For example, expression of EGFR transiently increases after wounding in mice and humans (Schaffer and Nanney, 1996; Stoscheck et al., 1992; Wenczak et al., 1992) and decreases at the wound margins in chronic, non-healing wounds (Brem et al., 2007). Abnormal EGFR function leads to tumorigenesis (Casanova et al., 2002; Karashima et al., 2002), and down-regulation of the receptor rapidly results in cellular proliferation and differentiation defects, impaired wound healing, lesion development, and hair follicle defects (Hansen et al., 1997; Maklad et al., 2009; Repertinger et al., 2004). In addition to increased edema, erythema, and eschar, EGFR null mice demonstrated contractile function impairments during healing and overall delayed wound closure compared to wild type mice (Repertinger et al., 2004). EGFR promotes epithelial proliferation early in wounding (Nakamura et al., 2001; Repertinger et al., 2004) as well as regulates acute inflammation by suppressing

neutrophil and enhancing mast cell populations after wounding (Repertinger et al., 2004). Lastly, though the EGFR was shown to be required for wound-induced angiogenesis, and healing was delayed in null mice, complete tissue repair was eventually observed even in the absence of the receptor (Repertinger et al., 2004), suggesting that the EGFR is a main contributor but not the only mechanism for successful wound healing. In addition, there is evidence that hyperglycemia impairs EGFR activity. When cells are exposed to high glucose, EGFR signaling is blunted in corneal epithelial cells and in fibroblasts (Obata et al., 1998; Xu et al., 2009). Taken together, these studies demonstrate that the EGFR is an important part of successful wound repair, and that inhibition or abnormal receptor activity, such as that caused by hyperglycemia, may lead to defective healing.

Though much research supports the crucial role of the EGFR in wound healing, it is also important to recognize the contribution of EGFR ligands in tissue repair (Werner and Grose, 2003). The earliest of these reports came from analysis of wound fluid when EGF-like elements were found to act as chemoattractants for endothelial cells in rats (Grotendorst et al., 1989). In addition to EGF, it has been shown that TGF-α and HB-EGF stimulate the EGFR and promote keratinocyte migration and proliferation (Repertinger et al., 2004; Tokumaru et al., 2000). Furthermore, when chronic diabetic foot ulcers were topically treated with EGF, they achieved 76% complete healing of the wounds (Hong et al., 2006), further demonstrating the significance of both EGFR and its ligands in wound healing and diabetes.

Hyperglycemia caused by diabetes leads to the formation of advanced glycation end products (AGEs), and there is evidence that identify AGEs as culprits in diabetes-impaired wound healing (Morita et al., 2005; Peppa et al., 2009; Zhu et al., 2011) as

discussed in Chapter 1. There is also evidence demonstrating the inhibitory effect of AGE precursors, glyoxal and methylglyoxal, on EGFR activation in umbilical vein endothelial cells (Portero-Otin et al., 2002). However, other than the few studies investigating the relationship between AGEs and EGFR (Cai et al., 2006; Chen et al., 2010; Portero-Otin et al., 2002), little is known about the functional outcome of EGFR glycation on wound healing with keratinocytes. Therefore, we explored activation of the receptor and subsequent cell function in human keratinocytes following exposures to AGE precursor glyoxal.

## 3.2 Materials and Methods

Squamous cell carcinoma cells (SCC 12F) cells, HaCaT cells, and normal keratinocytes were used in the following experiments. These keratinocytes were exposed to glyoxal and stimulated with EGF. Assays used to assess cell signaling and function include the following:

Section 2.1 – Cell culture

Section 2.1.1 – Cell culture drug treatments

Section 2.1.2 – MTS proliferation assay

Section 2.1.3 – Boyden chamber migration assay

Section 2.1.4 – Immunoblot analysis

Section 2.2 – Animal studies

Section 2.2.2 – Epithelial outgrowth

Section 2.2.4 – TUNEL staining

Section 2.3 – Statistical analysis

## 3.3 Results

*High glucose impairs EGF-stimulated keratinocyte migration*

Because studies have reported defective cell migration in the presence of high glucose (Obata et al., 1998; Xu et al., 2009), the ability of keratinocytes to migrate in the presence of high glucose was tested with the squamous cell carcinoma cells (SCC 12F), a human keratinocyte cell line. Cells maintained in either 6 mM glucose or 25 mM glucose were plated into inserts of a 24-well companion plate (Section 2.1.1 and 2.1.3). After stimulation with EGF, cell migration was measured by counting cells that crossed the membrane inserts and that were stained with DAPI (Section 2.1.3). Exposure of high glucose to SCC 12F cells resulted in impaired cell migration even with EGF stimulation (Figure 3.2), demonstrating the inhibitory effect of high glucose on EGFR activity.

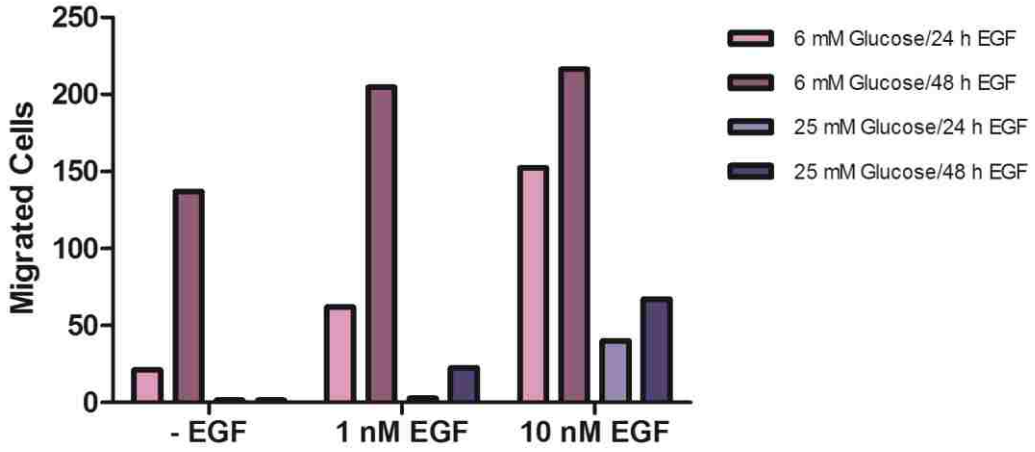


FIGURE 3.2. **Keratinocyte migration is impaired when exposed to high glucose.** The Boyden chamber migration assay demonstrated that exposure of keratinocytes to chronic high glucose impaired 24 h EGF-stimulated cell migration. Purple bars = low glucose (6 mM). Blue bars = high glucose (25 mM). Results are representative of one experiment.

*Glyoxal impairs EGF-dependent keratinocyte proliferation and migration*

In the presence of glyoxal and other reactive AGE intermediates, levels of covalently modified proteins increase, leading to potential disruption of cell function (Ahmed, 2005; Peppa et al., 2009; Thomas, 2011). To observe the effects of glyoxal on cells, we measured EGF-stimulated cell proliferation and migration. SCC 12F cells treated with 10 nM EGF resulted in the breakdown of cell-cell junctions and induction of cell migration as indicative of epithelial to mesenchymal transition (EMT) (Figure 3.3).

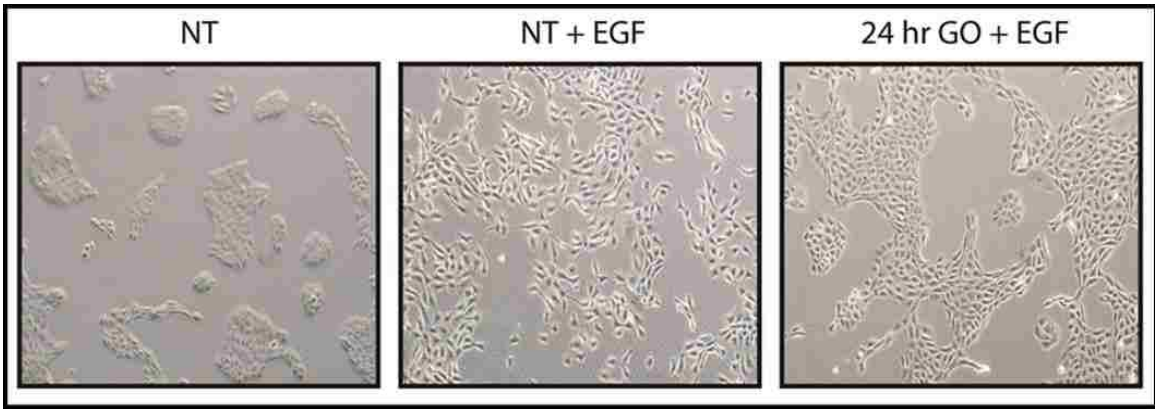


FIGURE 3.3. **Cell scattering.** Exposure of SCC 12F keratinocytes to 24 h EGF induces cell scattering. In contrast, glyoxal inhibits EGF-stimulated keratinocyte scattering.

In contrast, cells exposed to a high dose of glyoxal (0.5 mM) and stimulated with EGF did not display cell scattering, but rather they maintained their cell-cell junctions and remained inert. This is in agreement with studies demonstrating the impact of diabetic elements in impaired wound healing in diabetic patients (Lan et al., 2008; Lan et al., 2009; Spravchikov et al., 2001). EGF-dependent proliferation was inhibited by exposure to 0.5 mM glyoxal (Figure 3.4A) as assessed by the MTS assay. As discussed above, our data and others have reported that keratinocyte migration is decreased by high glucose (Lan et al., 2009). Because glyoxal formation is increased under high glucose conditions,

we tested the impact of glyoxal on EGF-stimulated migration using a modified Boyden chamber (Brown and Bicknell, 2001; Falasca et al., 2011). EGF treatment (1 or 10 nM) for 24 h effectively stimulated migration, whereas migration was severely impaired upon concurrent exposure to EGF and glyoxal (Figure 3.4B). In addition, epithelial outgrowth was measured in skin explants obtained from 7 wk old FVB mice. Over the 5 d period, outgrowth was detected from untreated explants and a dose dependent inhibition of outgrowth was evident in all explants exposed to varying glyoxal doses (0.1–0.5 mM GO) (Figure 3.4C and 3.4D).

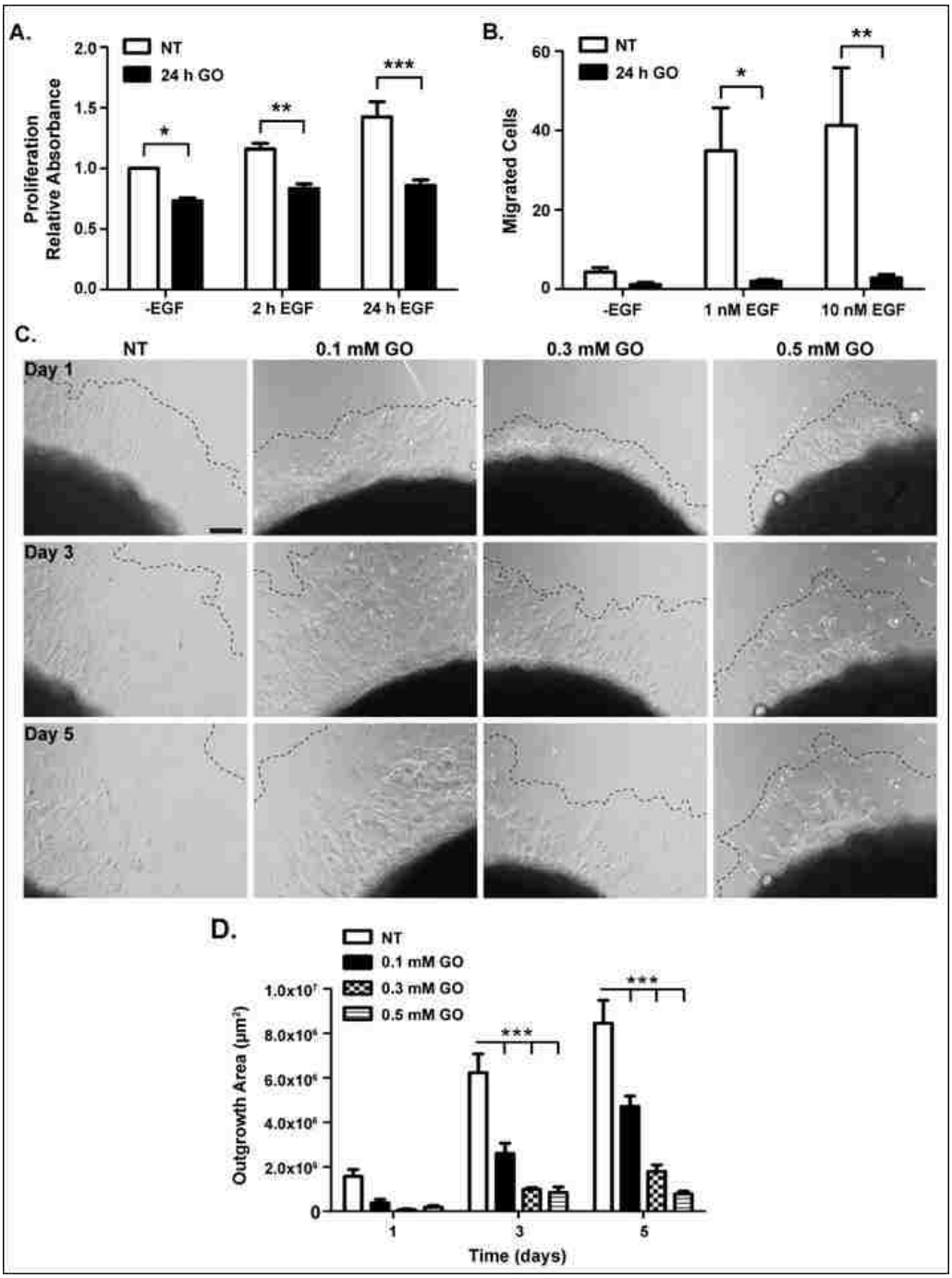


FIGURE 3.4. **Glyoxal impairs cell proliferation and migration. (A)** Proliferation of SCC 12F keratinocytes measured following 24 h 0.5 mM glyoxal (GO) and stimulation with 2 or 24 h 1 nM EGF. **(B)** Keratinocytes were exposed to 0.5 mM GO and to 1 or 10 nM EGF for 24 h. Cell migration determined by counting DAPI-stained nuclei. **(C)** Mouse skin explants exposed to GO over 5 d. Epithelial outgrowths observed using phase contrast microscopy. Dashed line indicates migrating front. Scale bar equals 200 µm. **(D)** Outgrowths evaluated by measuring areas around explants. Results represent minimum three independent experiments for proliferation and migration and at least eight mice per group for explants. Error bars defined as mean +/- SEM. Two-way ANOVA and Bonferroni's post-test demonstrate significance *$p<0.05$, **$p<0.01$, and ***$p<0.001$.

Analysis of apoptosis by TUNEL staining was performed to determine if the differences observed between untreated and glyoxal-treated explants was due to cell death caused by glyoxal toxicity (Figure 3.5). Incorporation of fluorescein-12-dUTP indicates fragmented DNA of apoptotic cells. Etoposide was used as a positive control and is an anti-cancer agent that functions as a topoisomerase inhibitor (Hande, 1998). It forms ternary complexes with DNA and the topoisomerase II enzyme and prevents re-ligation of the DNA strands, leading to DNA strand breaks. This results in DNA synthesis errors and leads to apoptosis. Little difference between the non-treated and glyoxal-treated explants was observed (Figure 3.5). In contrast, the etoposide-treated explants led to greater numbers of apoptotic cells. The data suggest that the impaired outgrowth is not due to glyoxal-induced cell death.

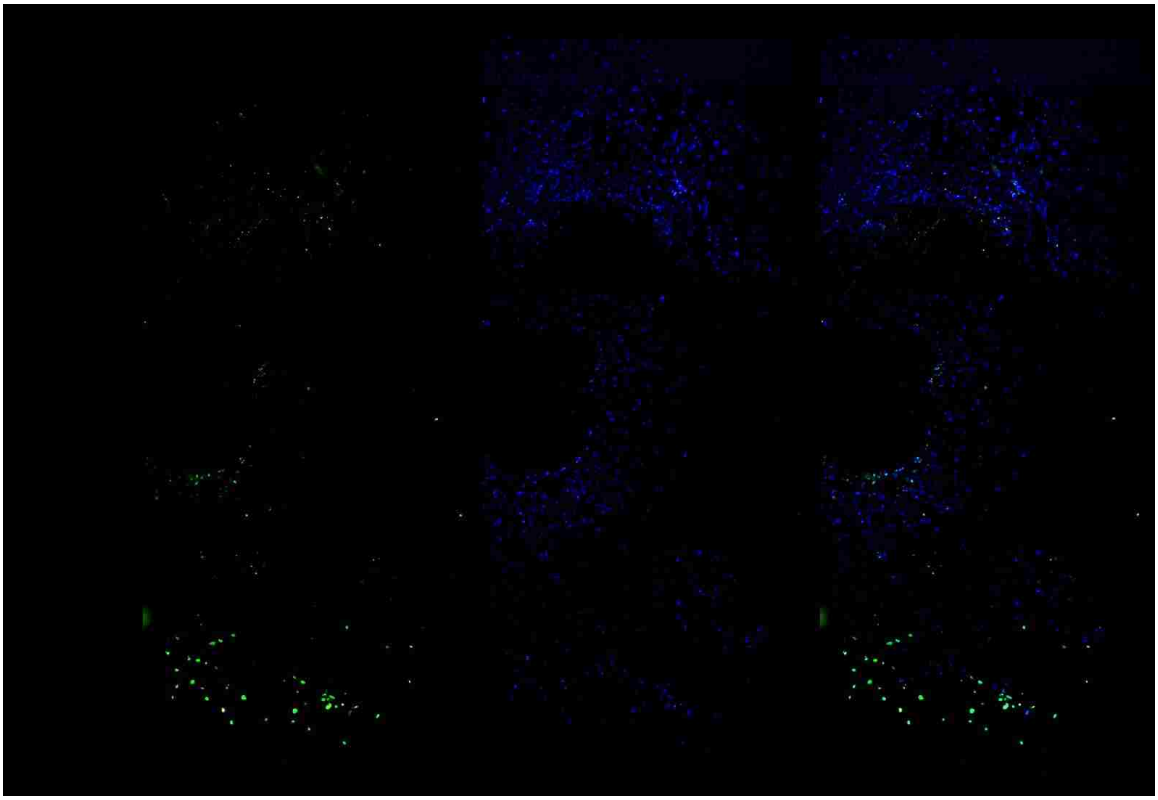

FIGURE 3.5. **Effect of high glyoxal on apoptosis.** *Ex vivo* skin explants from wild type mice were exposed to 0.5 mM glyoxal for 5 d. Outgrowth areas were analyzed for apoptosis as indicated by detection of fluorescein-12-dUTP incorporation (green). Glyoxal induces very little cell death compared to non-treated cells (NT). Etoposide represents positive control of apoptosis. DAPI (blue) represent cell nuclei. Results are representative of one experiment.

These observations in an *ex vivo* system further demonstrate the inhibitory effect of glyoxal on the reepithelialization component of wound healing.

*Glyoxal increases modification of proteins in keratinocytes*

In the presence of glyoxal and other reactive AGE intermediates, levels of covalently modified proteins increase. Glyoxal leads to formation of carboxymethyl lysine (CML), the first AGE discovered *in vivo* (Ahmed et al., 1986; Tessier, 2010) and a major biomarker of the Maillard reaction in human tissues (Thorpe and Baynes, 2002).

When SCC 12F keratinocytes and HaCaT cells were exposed to varying glyoxal doses (0 to 0.5 mM) for 24 h, the CML levels increased as a function of dose as assessed by immunoblotting (Figure 3.6A and 3.6C). CML levels also increased with time; modified proteins were evident within 2 h of exposure to 0.5 mM glyoxal (Figure 3.6B and 3.6D). When normal human keratinocytes were exposed to 0.5 mM glyoxal for 24 h, CML was also detected (Figure 3.6E lane 3). To confirm that increased CML was due to glyoxal exposure, keratinocytes were pretreated with aminoguanidine (AG), a potent inhibitor of glycation (Brownlee et al., 1986). Preincubation with 5 mM AG for 6 h prevented CML formation in response to glyoxal in both normal keratinocytes and in SCC 12F cells (Figure 3.6E and 3.6F). These findings demonstrate that the AGE precursor glyoxal promotes CML formation and protein modification in keratinocytes as indicated by the increased number of anti-CML immunoreactive bands across the immunoblot.

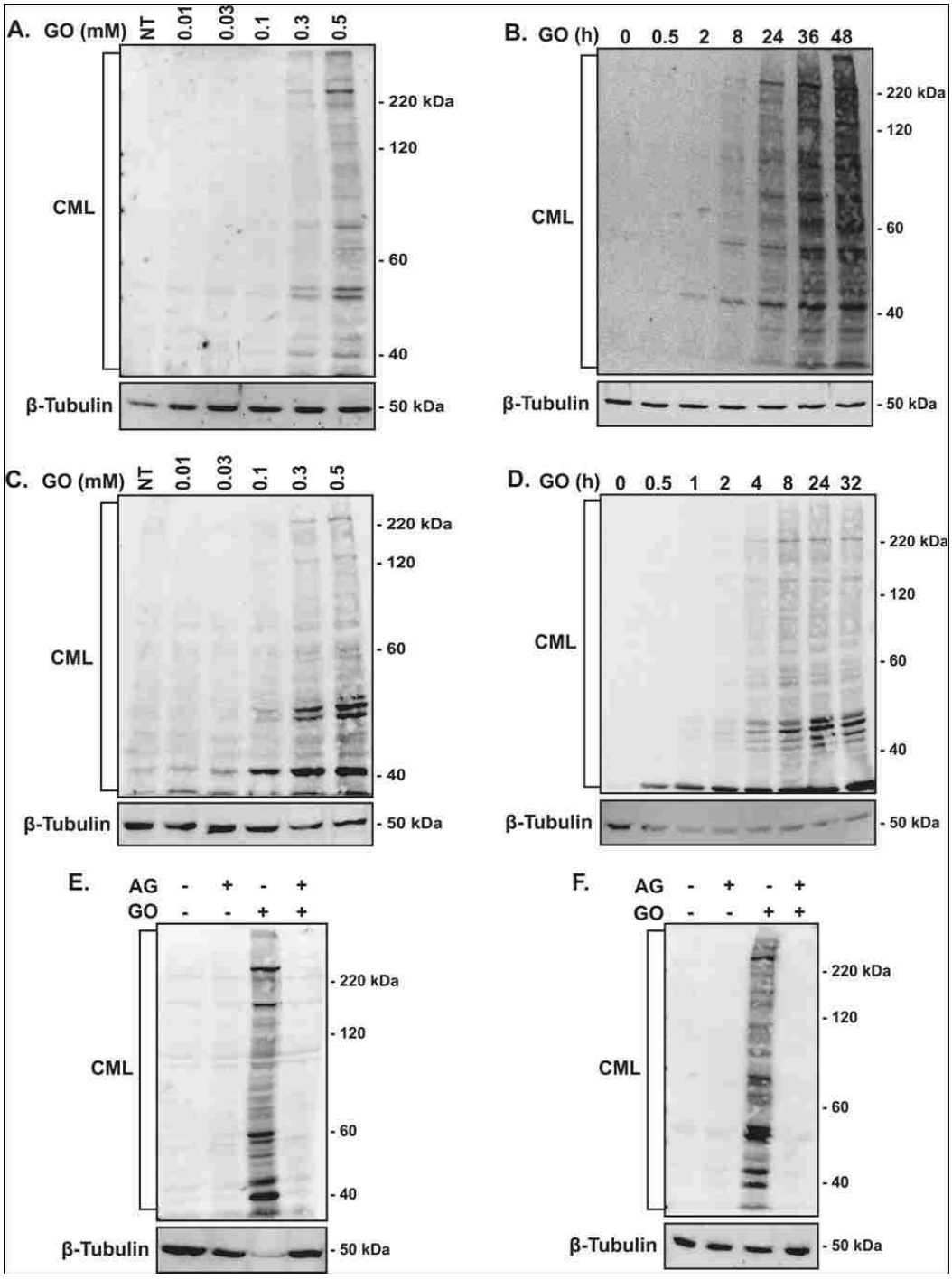


FIGURE 3.6. **Glyoxal increases modified protein levels.** Exposing keratinocytes to glyoxal (GO) dose-dependently and time-dependently leads to increased AGE carboxymethyl lysine (CML) in **(A)&(B)** SCC 12F keratinocytes **(C)&(D)** HaCaT cells **(E)** normal keratinocytes. Glycation inhibitor, aminoguanidine (AG), prevents protein modification in normal keratinocytes **(E)** and in SCC 12F cells **(F)**. β-Tubulin is used as loading control. Results are representative of at least three independent experiments.

*Glyoxal impairs EGF-stimulated tyrosine phosphorylation*

Because AGE modification can disrupt protein function (Ahmed, 2005; Peppa et al., 2009; Thomas, 2011), we next tested the effect of glyoxal on EGFR autophosphorylation. Cells were exposed to 0.5 mM glyoxal for varying times then stimulated with 10 nM EGF for 10 min. EGFR activation, as detected by phosphotyrosine at 170 kDa, decreased with glyoxal incubation time (Figure 3.7A and 3.7B). A significant decrease in EGF-stimulated tyrosine phosphorylation was evident within 4 h of glyoxal treatment, and maximal inhibition was achieved by 8 h. EGF-stimulated EGFR activation was also tested in HaCaT cells exposed to 0.5 mM glyoxal, and a trend in impaired receptor activation was observed over the 32 h time period tested (Figure 3.7C and 3.7D). Similar impairments in EGF-stimulated phosphotyrosine were observed when cells were acutely exposed to high glucose (25 mM) in our studies (Figure 3.7E and 3.7F) as well as in what has been previously shown (Obata et al., 1998; Xu et al., 2009). The glyoxal-induced decrease in phosphotyrosine is not due to a reduction of total EGFR protein levels (Figure 3.7G). The impairment of EGFR kinase activity was due to CML formation under these conditions as EGF-stimulated tyrosine phosphorylation was preserved in the presence of AG as demonstrated in both SCC 12F cells (Figure 3.7H and 3.7I) and normal keratinocytes (Figure 3.7J and 3.7K). EGFR was previously demonstrated to be covalently modified by glyoxal in endothelial cells (Portero-Otin et al., 2002), and a similar modification may be occurring in the keratinocytes.

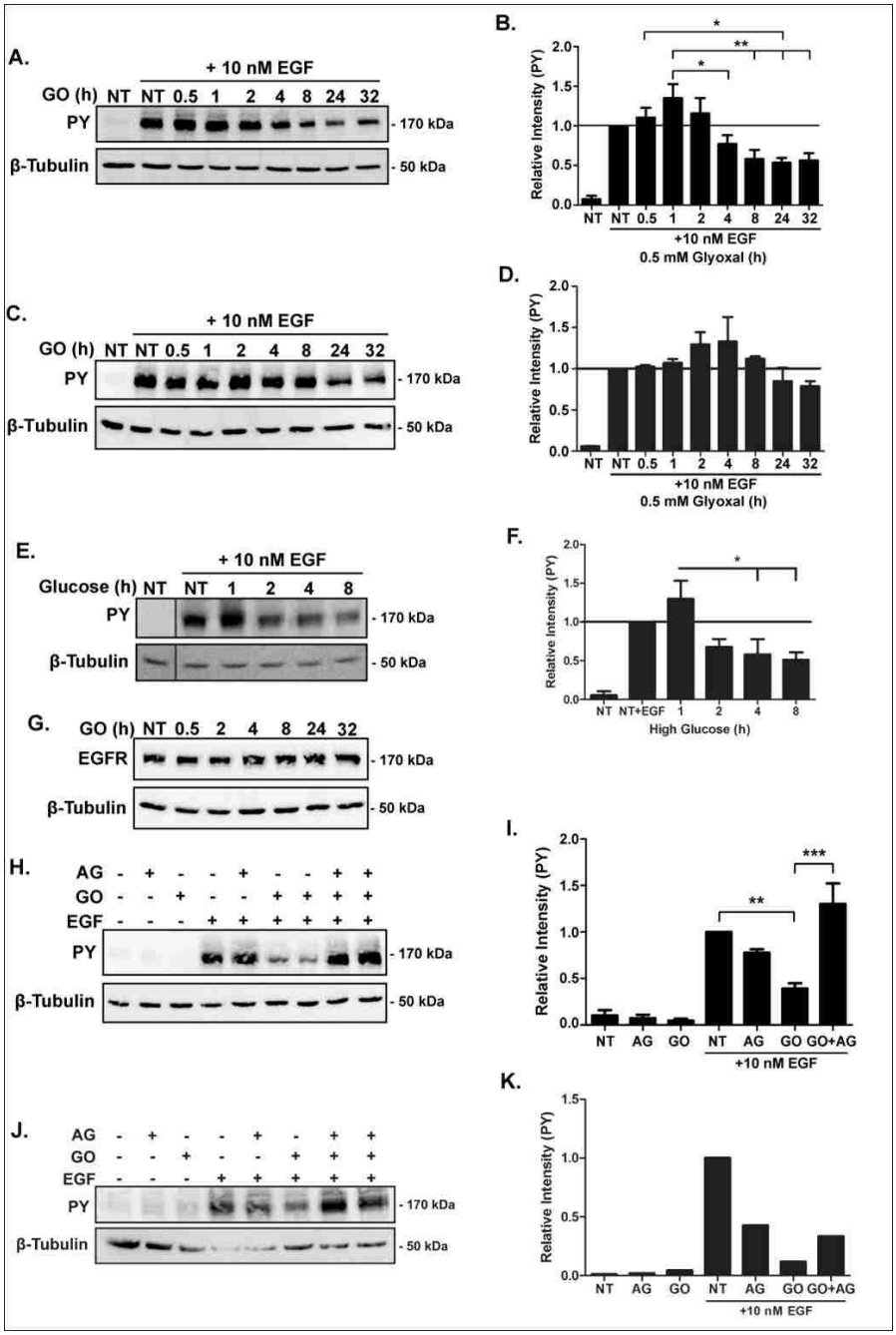


FIGURE 3.7. **Glyoxal decreases EGF-stimulated EGFR activation.** Keratinocytes were treated with 0.5 mM glyoxal (GO) at the indicated times, then stimulated with 10 nM EGF for 10 min. The immunoblots and densitometries represent activation of EGFR as indicated by phosphotyrosine (PY) at 170 kDa in SCC 12F cells **(A)&(B)** and in HaCaT cells **(C)&(D)**. **(E)&(F)** SCC 12F keratinocytes were exposed to 25 mM glucose over 8 h and stimulated with 10 nM EGF for 10 min. PY levels were evaluated. **(G)** Total EGFR protein is not affected in SCC 12F cells following GO exposures. SCC 12F cells **(H)&(I)** and normal keratinocytes **(J)&(K)** were pretreated with 5 mM aminoguanidine (AG), exposed to 0.5 mM GO for 24 h, then stimulated with 10 nM EGF. Lanes 6&7 and 8&9 **(H)** and Lanes 7&8 **(J)** were collected from duplicate plates as indicated. β-Tubulin was used as a loading control. Results are representative of at least three independent experiments but two for (C)&(D) and one for (J)&(K). Error bars are defined as mean +/- SEM. One-way ANOVA and Tukey's post-test revealed significance *$p<0.05$, **$p<0.01$, and ***$p<0.001$.

However, it is possible that the affect observed in activated EGFR was due to a modified EGF ligand by glyoxal. Therefore, we tested this theory by pre-incubating EGF ligand with glyoxal for either 10 min (the length of time for EGF stimulation of EGFR) or for 24 h (the length of time glyoxal is incubated with cells). The keratinocytes were then exposed to these solutions and observed for effects on EGFR activation. We observed no effects of glyoxal on the activity of EGF itself (Figure 3.8) further demonstrating glyoxal inhibition on the EGF receptor.

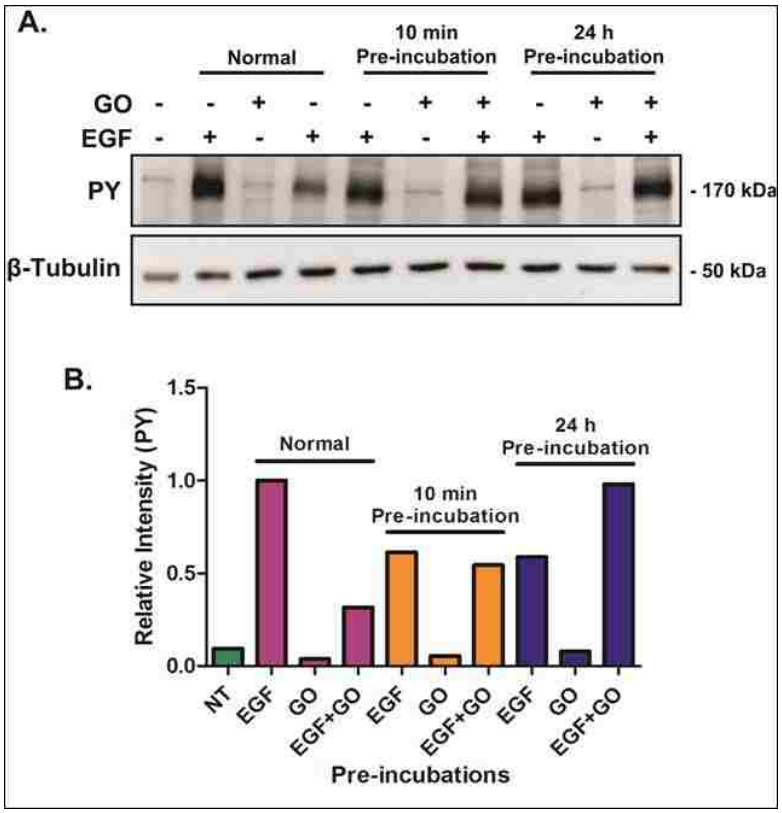


FIGURE 3.8. **Glyoxal does not affect EGF ligand.** Pre-incubations with EGF ligand and glyoxal (GO) were done in fresh media prior to addition to keratinocytes. EGF was still able to stimulate EGFR regardless of the pre-incubations with GO. **(A)** Western blot demonstrating changes in activated EGFR as demonstrated by phosphotyrosine (PY) detection. **(B)** densitometry of western in (A) quantifying changes in protein levels. Results are representative of one experiment.

A lower dose of glyoxal (0.2 mM) was tested and assessed for EGF-stimulated EGFR activation. This dose was chosen based on the observation that very low levels of modified proteins are detected following exposure to keratinocytes for 24 h (Figure 3.6). There was no significant effect of the low dose glyoxal on receptor activation during the 24 h time period tested (Figure 3.9). Altogether, these findings suggest that glyoxal-induced defects in EGF-stimulated EGFR activation may lead to further disruption in downstream signaling and cellular function.

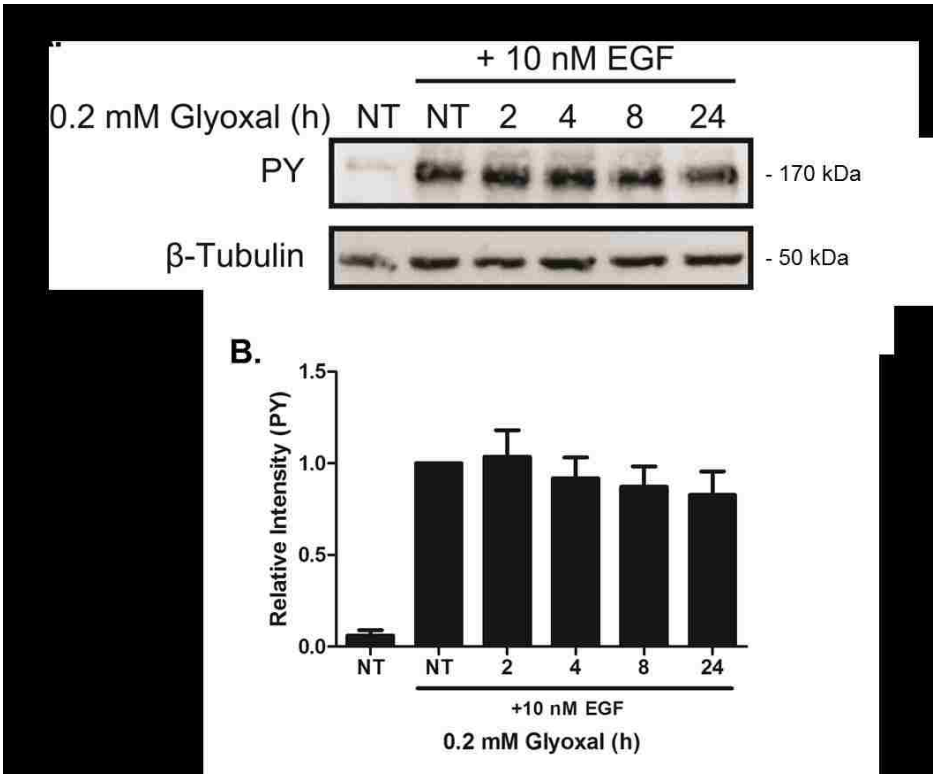


FIGURE 3.9. **Low dose glyoxal has no effect on EGF-stimulated EGFR activation.** SCC 12F keratinocytes were treated with 0.2 mM glyoxal for the indicated times then stimulated with 10 nM EGF for 10 min. The immunoblot **(A)** and densitometry **(B)** represent activation of EGFR as indicated by phosphotyrosine (PY) at 170 kDa. β-Tubulin was used as a loading control. Results are representative of three independent experiments. Error bars are defined as mean +/- SEM. One-way ANOVA and Tukey's post-test did not show statistical significance.

## 3.4 Discussion

The EGFR is a receptor that has been implicated in many signaling pathways required for proper cell function and survival (Danielsen and Maihle, 2002; Maklad et al., 2009; Pastore et al., 2008; Repertinger et al., 2004; Schneider et al., 2008; Werner and Grose, 2003). However, dysfunctional regulation of the EGFR leads to damaging results such as delayed cell migration and proliferation as in the case of wound healing (Repertinger et al., 2004; Werner and Grose, 2003).

In patients suffering from chronic wounds, EGFR levels were decreased at the wound margins and increased in areas adjacent to the wound site (Brem et al., 2007). In addition, the availability of EGF is also decreased in chronic diabetic foot ulcers. Current studies are being performed to evaluate the success of using topical and intralesional routes of EGF administration on wounds (Tiaka et al., 2012). So far, results demonstrate successful wound closure following EGF treatment (Fernandez-Montequin et al., 2007; Fernandez-Montequin et al., 2009; Tuyet et al., 2009) and even greater healing when given in combination with other therapies (Hong et al., 2006; Tsang et al., 2003). Investigations into optimal dosing, methods of administration, and characteristics of ulcers most likely to heal are yet to be performed to evaluate the effectiveness of exogenous EGF on diabetic wounds (Tiaka et al., 2012).

Our early studies examined the effects of high glucose on EGFR activation and cell migration and proliferation. We found that high glucose blunted the ability of EGF to stimulate the EGFR in keratinocytes. Similar findings were observed in other studies demonstrating the inhibitory effect of glucose on EGFR and its function. For example, high glucose was shown to attenuate EGF-stimulated EGFR activation in Rat 1

fibroblasts (Obata et al., 1998) and to impair EGFR signaling in human corneal epithelial cells (Xu et al., 2009). In contrast, there is also evidence suggesting high glucose promotes pancreatic cancer cell and proximal tubule cell proliferation through induction of EGF expression and transactivation of the EGFR (Han et al., 2011; Saad et al., 2005), demonstrating the difference in roles that glucose has on EGFR in various cells and environments.

Because high glucose ultimately leads to formation of the AGE precursor, glyoxal, we examined the effect of glyoxal on EGFR activation, which we expected would disrupt effective wound healing. Though the highest dose of glyoxal tested (0.5 mM) is greater than what is found in diabetic patients (Lapolla et al., 2003), the concentrations and times of exposure are comparable to what has been used in other studies (Berge et al., 2007; Nass et al., 2010; Rattan et al., 2007; Sliman et al., 2010). Inhibitory effects due to glyoxal were also still observable in lower doses and exposures tested. Our studies demonstrated that high doses of glyoxal impair EGFR activation in keratinocytes. EGFR has also been shown to be covalently modified by both of the AGE precursors glyoxal and methylglyoxal (Portero-Otin et al., 2002). However, to the best of our knowledge, there have been no further studies examining the specific residues that are modified on the EGFR. The EGFR is located on the plasma membrane, exposing it to potential glycation. Based off the known amino acid sequence of the EGFR, it is possible to identify regions of the receptor that may be more susceptible to modification. Cysteine residues have been implicated in protein glycation (Mostafa et al., 2007; Schwarzenbolz et al., 2008). Therefore, due to the presence of the cysteine-rich regions in the ligand-

binding domain of the EGFR (Garrett et al., 2002; Ward et al., 2007), it is possible there is modification at these sites, leading to impairments in EGF binding to the receptor.

The EGFR regulates numerous signaling pathways including the ERK, PI3K/AKT, and the JAK/STAT pathways, and high glucose affects receptor activation. Because high glucose results in AGE formation, it is likely that impairments in EGFR activation as a consequence of glycation (Portero-Otin et al., 2002) will lead to further downstream defects in signaling and function. A possible avenue to explore is the transcription factor Snai2/Slug. This protein down-regulates factors such as E-cadherin and β-catenin, which are important in adheren junctions (Chandler et al., 2007). Snai2 is also a key element in successful reepithelialization (Chandler et al., 2007; Hudson et al., 2009; Savagner et al., 2005). Therefore, we further investigated this effector protein of EGFR and its involvement in diabetes-impaired wound healing.

# CHAPTER 4

## Glyoxal leads to defective keratinocyte migration and down-regulation of Snai2

### 4.1 Introduction

Snai2/Slug is an important downstream effector of the EGFR (Chapter 3, Figure 3.1) (Velander et al., 2008). It is a member of the Snail superfamily of transcription factors, which encode zinc-finger proteins and function as transcriptional repressors (Cobaleda et al., 2007; Hemavathy et al., 2000b; Shirley et al., 2010) (Figure 4.1). The Snail superfamily is characterized by a highly conserved region at the carboxy terminus that contains four to six $C_2H_2$-type zinc fingers (Cobaleda et al., 2007; Hemavathy et al., 2000a; Nieto, 2002). Snail family genes consist of six common bases, CAGGTG (Cobaleda et al., 2007), and this motif makes up a subset of the E-box (CANNTG), the conserved binding site of basic helix-loop-helix transcription factors (Hemavathy et al., 2000a). The amino termini are less conserved, but most vertebrates contain the conserved SNAG domain (Hemavathy et al., 2000a; Nieto, 2002). Snai2 consists of 268 amino acids in length with five zinc fingers at the carboxy terminus (Cohen et al., 1998). Its repressive activity is thought to arise from the SNAG domain as well as through recruitment of a corepressor, such as carboxy-terminal binding protein (CtBP-1) (Cobaleda et al., 2007).

Snai2 is an essential zinc finger protein required for development, EMT, cell adhesion, and cell migration (Barrallo-Gimeno and Nieto, 2005; Cobaleda et al., 2007; Hemavathy et al., 2000a; Katafiasz et al., 2011; Nieto, 2002; Nieto et al., 1994; Sefton et al., 1998; Shook and Keller, 2003). It was first discovered in the neural crest and

developing mesoderm of the chick embryo (Nieto et al., 1994). However, it was also shown to be required for successful reepithelialization (Chandler et al., 2007; Hudson et al., 2009; Savagner et al., 2005). In the chick embryo, Snai2 is expressed in cells undergoing EMT and is crucial to primitive streak formation, endocardial cushions, decondensing somites, and palate closure (Cobaleda et al., 2007). It is also highly expressed in adult tissues such as the skin, stomach, kidney, lung, and uterus (Cohen et al., 1998; Parent et al., 2004; Parent et al., 2010). Much of what is known about Snai2 was derived from loss-of-function mutations (Jiang et al., 1998; Sanchez-Martin et al., 2003; Sanchez-Martin et al., 2002). Mice deficient in Snai2 are viable but have a white forehead blaze, patchy depigmentation, macrocytic anemia, and are infertile (Perez-Losada et al., 2002). These studies suggest that Snai2 may play an important role in melanocyte stem cells, hematopoietic stem cells, and germ cells.

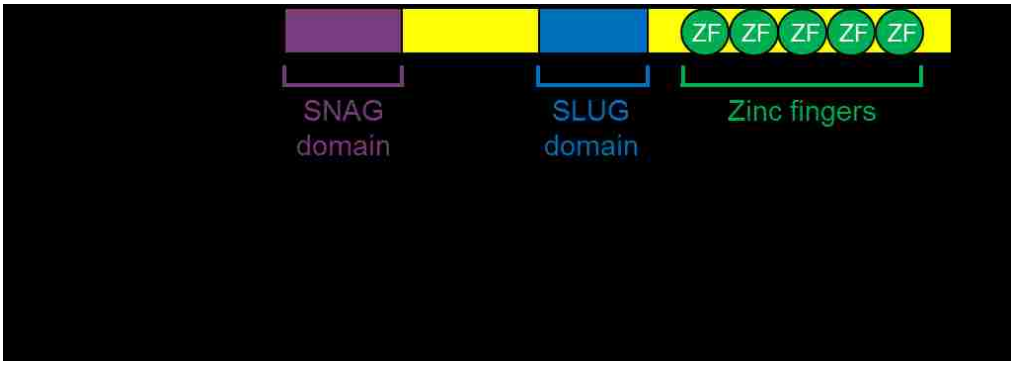


FIGURE 4.1. **Transcription factor Snai2.** Snai2 is a member of the Snail superfamily of transcriptional repressors. It is 268 amino acids in length and contains five zinc fingers.

In addition, SNAI2 deletions have been implicated in two melanocyte development disorders characterized by white-spotting – Waardenburg syndrome and piebaldism. Waardenburg syndrome (WS) is a congenital disorder caused by defective

embryonic neural crest function, and there are four variants (WS1, WS2, WS3, and WS4). WS1, WS3, and WS4 relate to failures of neural crest derivatives, and WS2 is a failure in the melanocytes (Cobaleda et al., 2007; Sanchez-Martin et al., 2002). In some patients with WS, homozygous deletions of SNAI2 have been the only detected abnormality (Sanchez-Martin et al., 2002). In piebaldism, this disorder results from mutations in the KIT proto-oncogene (Giebel and Spritz, 1991), which contains Snai2 as a downstream target in the kit signaling pathway. Individuals with piebaldism have white finger tips, long nails, and patchy hypopigmentation. In patients with piebaldism, though there were observable differences in the SNAI2 gene, there was no detectable defect in the KIT gene, implicating Snai2 as a cause for piebaldism (Sanchez-Martin et al., 2003).

Snai2 was also shown to be required for reepithelialization (Chandler et al., 2007; Hudson et al., 2009; Savagner et al., 2005). As mentioned above, Snai2 is an important downstream effector of the EGFR (Arnoux et al., 2008; Kusewitt et al., 2009). Activation of the EGFR induces Snai2, and reepithelialization is compromised in Snai2 null mice (Kusewitt et al., 2009; Savagner et al., 2005). Furthermore, Snai2 null mice display decreased epithelial outgrowth from *ex vivo* skin explants (Kusewitt et al., 2009), and exposure of the null mice to ultraviolet radiation resulted in chronic, non-healing wounds (Hudson et al., 2009). In contrast, wild type mice achieved complete wound closure, further demonstrating the importance of Snai2 in reepithelialization.

While Snai2 is known to be required for successful reepithelialization, its role in diabetes has not been elucidated. The literature on EGFR and diabetes and the lack of literature involving Snai2 and diabetes emphasizes the need for further research on reepithelialization in the diabetic environment. The goal of the following study was to

investigate the role of transcription factor Snai2/Slug in reepithelialization, more specifically, its involvement in impaired diabetic wound healing.

In the present study, we modeled a diabetic environment by exposing human keratinocytes to the AGE precursor glyoxal, one of the best-studied reactive AGE intermediates. We hypothesized that EGF-stimulated, as well as basal, Snai2 protein decreases as a consequence of glyoxal exposure. In addition, glyoxal will impair epithelial outgrowth of skin explants from mice. Lastly, transgenic mice over-expressing Snai2 protein may be sufficient to overcome impairments in epithelial outgrowth as assessed using explants. The results of this study may suggest that critical intracellular proteins may be targets of glycation and contribute to impaired wound reepithelialization in diabetes. In addition, we may then be able to implicate Snai2 in diabetes-impaired wound healing and identify it as a potential therapeutic target for reepithelialization.

## 4.2 Materials and Methods

Squamous cell carcinoma cells (SCC 12F) cells and normal keratinocytes were used in the following experiments. These keratinocytes were exposed to glyoxal and stimulated with EGF. Assays used to assess cell signaling and function include the following:

Section 2.1 – Cell culture

Section 2.1.1 – Cell culture drug treatments

Section 2.1.4 – Immunoblot analysis

Section 2.1.5 – qRT PCR

Section 2.1.6 – Immunoprecipitation

Section 2.2 – Animal studies

Section 2.2.1 – Transgenic mice

Section 2.2.2 – Epithelial outgrowth

Section 2.2.3 – Immunocytochemistry

Section 2.2.5 – Epidermal protein isolation

Section 2.3 – Statistical analysis

## 4.3 Results

*Glyoxal decreases Snai2 protein levels*

In Chapter 3, we demonstrated the inhibitory effect of glyoxal on the reepithelialization component of wound healing. Because the impact of glyoxal on cell migration was more pronounced than that observed for proliferation, we tested the effects of glyoxal on Snai2, a critical mediator of epithelial outgrowth downstream of EGFR activation. The transcription factor Snai2 is an effector of EGF-stimulated reepithelialization and is required for effective epithelial outgrowth (Hudson et al., 2009; Savagner et al., 2005). When SCC 12F cells were treated with EGF, Snai2 protein increased compared to non-treated cells (Figure 4.2A and 4.2B). However, glyoxal significantly inhibited EGF-stimulated Snai2 protein expression (**$p<0.01$). Interestingly, a time-dependent decrease of basal Snai2 protein was detected in response to glyoxal (>8 h, *$p<0.05$) (Figure 4.2C and 4.2D). Similar results were observed in normal human keratinocytes (Figure 4.2E and 4.2F).

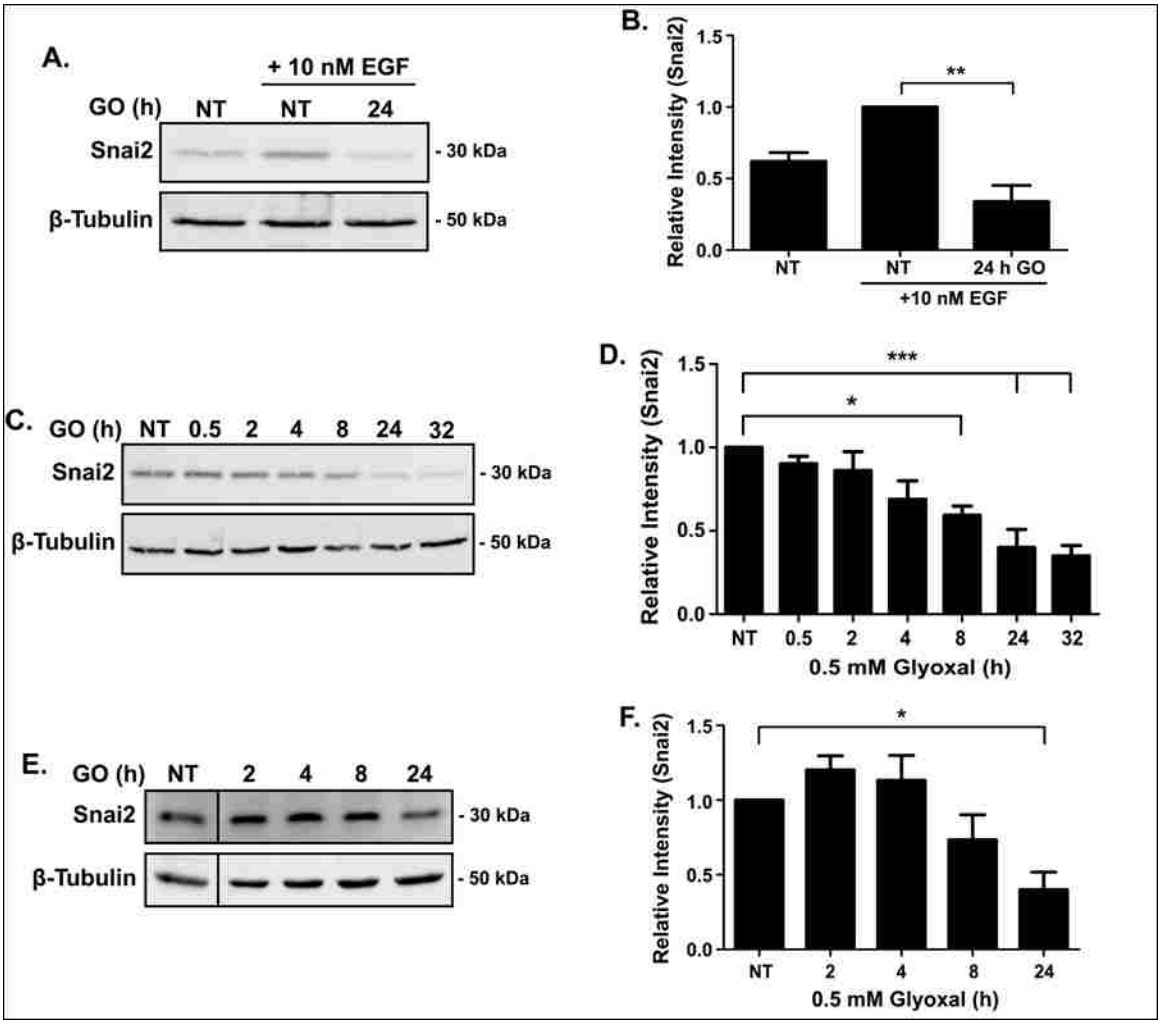


FIGURE 4.2. **Glyoxal down-regulates EGF-stimulated and basal Snai2 protein. (A)&(B)** SCC 12F cells were treated with 0.5 mM glyoxal (GO) and 10 nM EGF for 24 h. Protein was analyzed for EGF-stimulated Snai2 protein. **(C)&(D)** SCC 12F keratinocytes were exposed to 0.5 mM GO for 32 h. Basal Snai2 protein levels were evaluated. **(E)&(F)** Normal keratinocytes were exposed to 0.5 mM GO over 24 h. Basal Snai2 was evaluated by immunoblotting. Densitometries were normalized to β-Tubulin and to either "NT+EGF" (B) or to "NT" (D, F). Results are representative of at least three independent experiments. Error bars are defined as mean +/- SEM. One-way ANOVA and Tukey's post-test revealed statistical significance *$p<0.05$, **$p<0.01$, and ***$p<0.001$.

We then measured Snai2 protein levels in *ex vivo* skin explants. Tissues were isolated from FVB mice and exposed to 0.5 mM glyoxal for 24 h. Immunocytochemistry was performed to analyze changes in Snai2 protein between glyoxal-treated and untreated tissues. In agreement with what was observed in the immunoblots (Figure 4.2), exposure of glyoxal to explants resulted in decreased Snai2 protein (Figure 4.3).

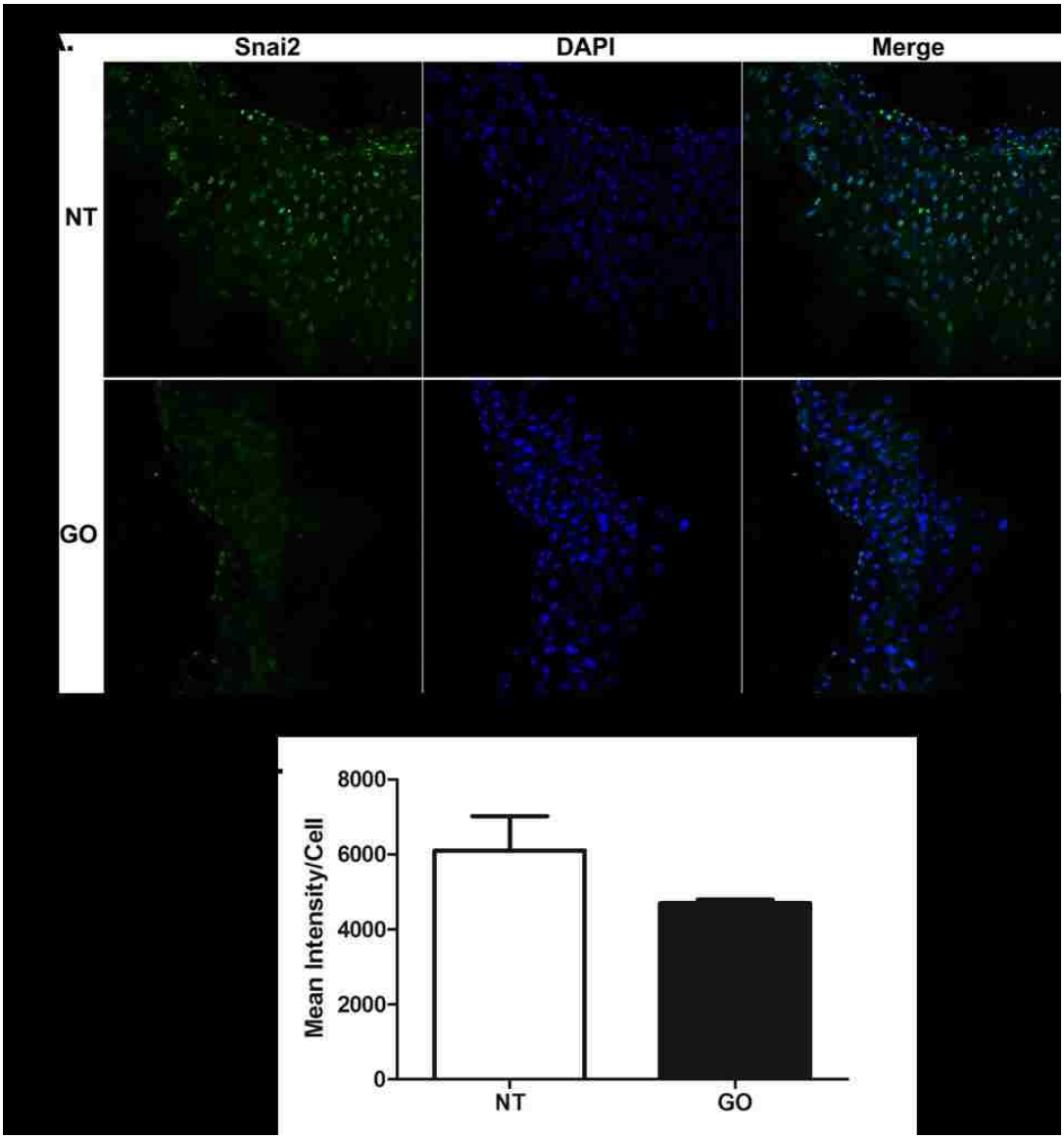


FIGURE 4.3. **Snai2 protein is decreased in tissue explants.** *Ex vivo* skin explants were isolated from mice and exposed to 0.5 mM glyoxal (GO) for 24 h. Snai2 was evaluated by immunocytochemistry **(A)**, and results are expressed as "Mean Intensity/Cell" **(B)**. Results are representative of two animals per group.

A lower dose of glyoxal (0.2 mM) was also tested and assessed for effects on Snai2 protein. This dose was chosen based on the observation that very low levels of modified proteins are detected following exposure to keratinocytes for 24 h (Chapter 3, Figure 3.6). There was no significant effect of the low dose glyoxal on Snai2 during the 24 h time period tested (Figure 4.4).

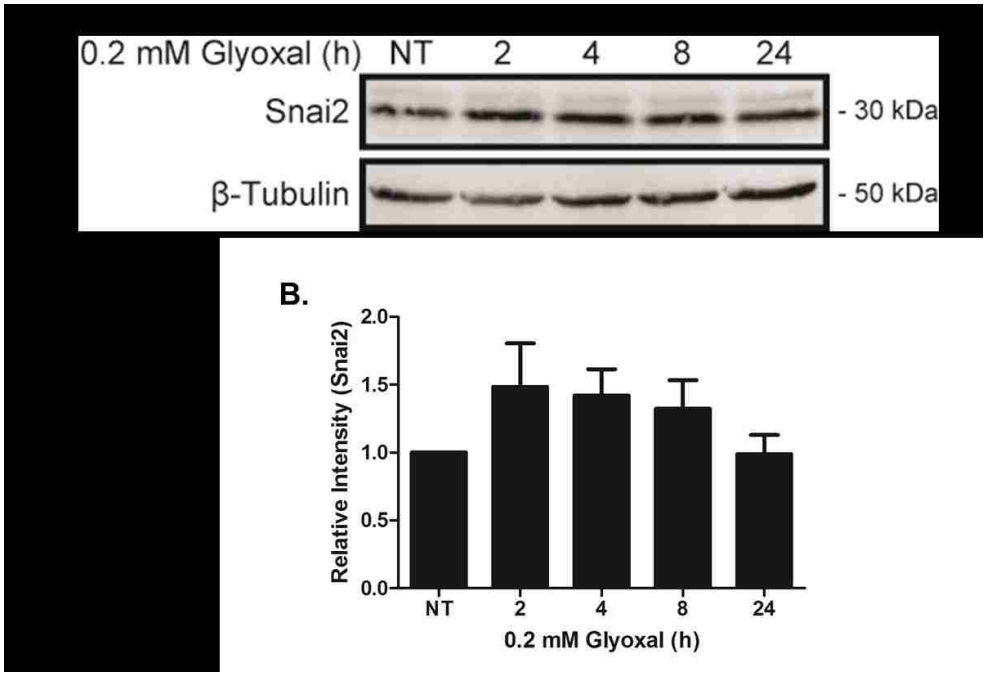


FIGURE 4.4. **Low dose glyoxal does not decrease Snai2 protein.** SCC 12F keratinocytes were treated with 0.2 mM glyoxal for the indicated times. The immunoblot **(A)** and densitometry **(B)** represent basal Snai2 protein levels. β-Tubulin was used as a loading control. Results are representative of four independent experiments. Error bars are defined as mean +/- SEM. One-way ANOVA and Tukey's post-test did not show statistical significance.

In addition, while it was demonstrated that a closely related family member, Snai1 (Snail), was enhanced by the AGE precursor, methylglyoxal (Hirahara et al., 2009), we observed no effect on Snai1 following exposures to glyoxal (Figure 4.5) suggesting glyoxal may be specifically targeting certain proteins rather than acting ubiquitously.

Furthermore, the decrease of Snai2 protein was not due to decreased mRNA expression as measured by qRT-PCR (Figure 4.6).

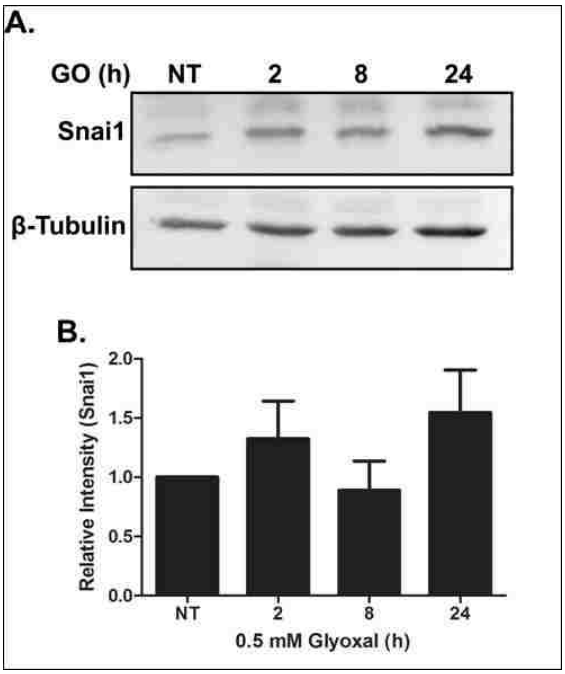


FIGURE 4.5. **Glyoxal has no effect on Snai1 protein. (A)** SCC 12F keratinocytes were exposed to 0.5 mM glyoxal (GO) for 24 h. Basal Snai1 protein levels were evaluated by immunoblotting. **(B)** Densitometries of immunoblots measuring Snai1 protein levels. Densitometries were normalized to β-Tubulin and to "NT" controls. Results are representative of three independent experiments. Error bars are defined as mean +/- SEM. One-way ANOVA and Tukey's post-test revealed no statistical effect.

FIGURE 4.6. **Glyoxal does not affect Snai2 at the transcriptional level.** RNA was isolated from SCC 12F keratinocytes exposed to 0.5 mM glyoxal over a 24 h period. One-way ANOVA and Tukey's post-test revealed statistical significance (*$p<0.05$) at the 8 h treatment but no overall inhibitory effect of glyoxal on Snai2 mRNA levels. Results are representative of three independent experiments. Error bars are defined as mean +/- SEM.

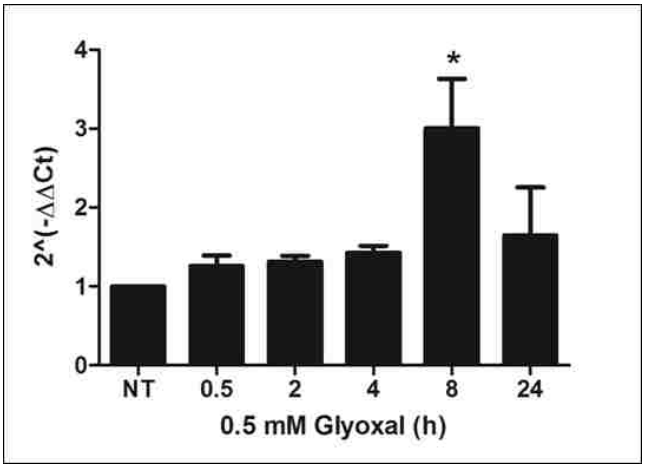

*Snai2 is covalently modified by glyoxal*

Because we observed an increase in covalently modified proteins with increasing glyoxal dose and exposure time (Chapter 3, Figure 3.6), we tested the hypothesis that Snai2 is a target for glyoxal-induced glycation. To determine whether Snai2 was modified, we immune-precipitated Snai2 from glyoxal-treated cells and found that Snai2 was modified by CML as detected by immunoblot analysis (Figure 4.7A). When the keratinocytes were pre-treated with 5 mM aminoguanidine (AG), a potent glycation inhibitor (Brownlee et al., 1986), and then exposed to glyoxal, Snai2 protein was preserved (Figure 4.7B and 4.7C), further indicating that the decrease in protein level is due to glycation and that Snai2 is a target for CML modification.

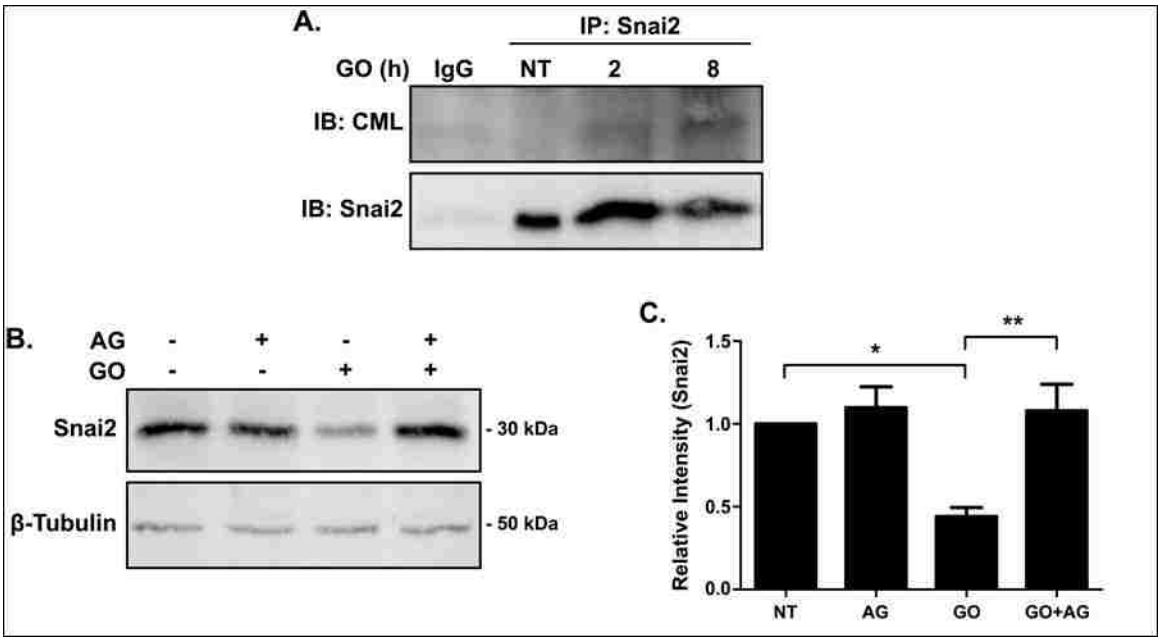


FIGURE 4.7. **Glyoxal leads to covalently modified Snai2. (A)** Keratinocytes were exposed to 0.5 mM Glyoxal (GO) over 24 h. Snai2 was immunoprecipitated and immunoblotted for CML. **(B)&(C)** Cells were pre-treated with 5 mM aminoguanidine (AG) and exposed to 24 h 0.5 mM GO. Protein was immunoblotted for Snai2. Densitometries in (B) were normalized to β-Tubulin. Results are representative of at least three independent experiments. Error bars are defined as mean +/- SEM. One-way ANOVA and Tukey's post-test demonstrate significance *$p<0.05$ and **$p<0.01$.

*Enhancing Snai2 protein promotes epithelial outgrowth in the presence of glyoxal*

Because Snai2 was decreased and modified by glyoxal, we explored the possibility of enhancing Snai2 to promote epithelial outgrowth. Protein from the epidermis of wild type and Snai2 transgenic FVB mice was collected. The epidermal layer was separated from the dermal layer, and protein from the epidermal layer was extracted and analyzed via immunoblot. The transgenic mice displayed approximately three-fold higher levels of Snai2 in the epidermis compared to wild type mice (Figure 4.8A and 4.8B). Skin explants isolated from both wild type and Snai2 over-expressing mice were grown in culture over 5 d. The over-expressing mice showed a significant increase in outgrowth compared to wild type mice after 5 d in culture (Figure 4.8C and 4.8D), demonstrating the ability of Snai2 to enhance epithelial outgrowth.

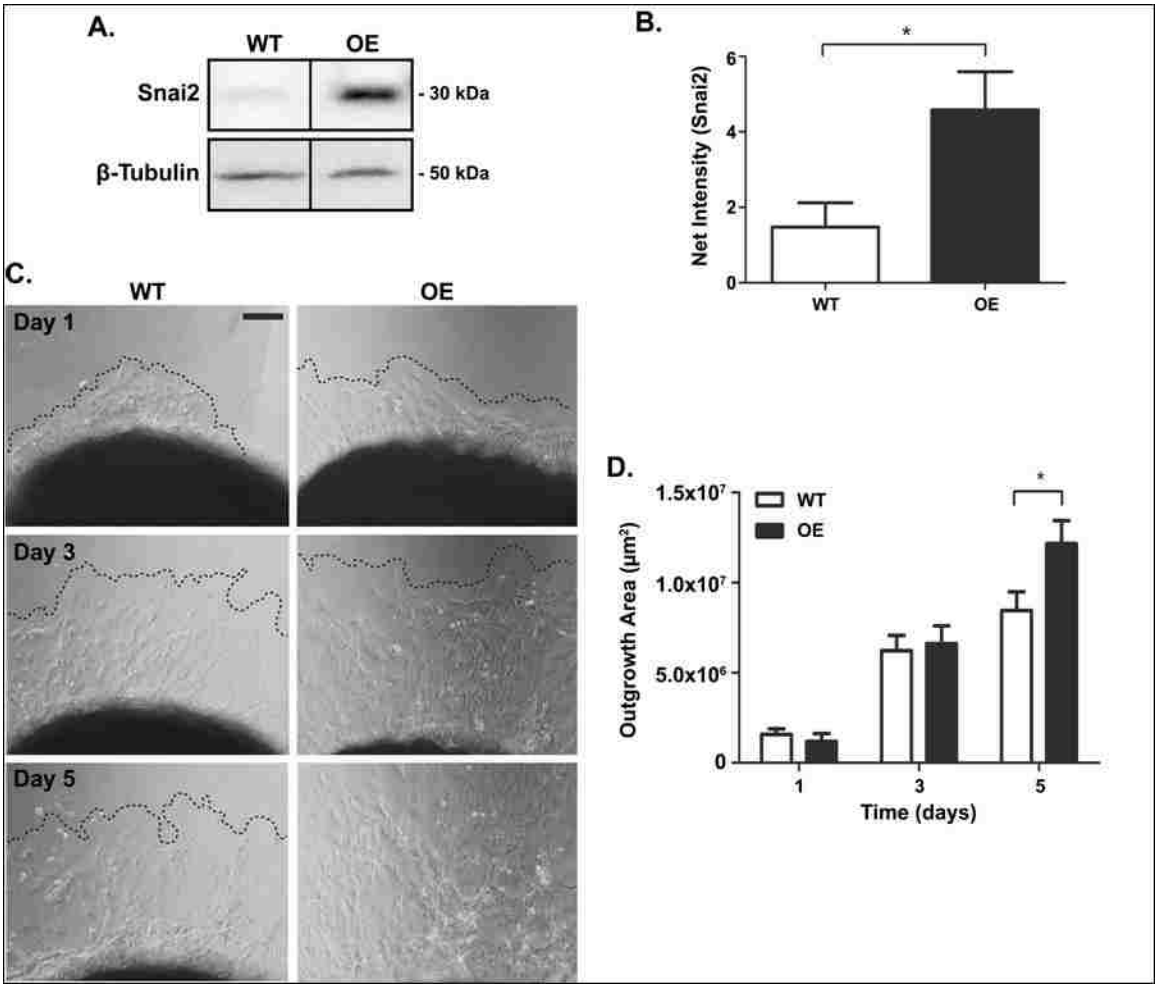


FIGURE 4.8. **Snai2 protein over-expression in mice promotes epithelial outgrowth. (A)&(B)** Protein was isolated from mouse epidermis. Differences in Snai2 between wildtype (WT) and Snai2 over-expressing (OE) mice measured by immunoblot. **(C)** Skin explants were isolated from mice and cultured for 5 d. Epithelial outgrowth of keratinocytes was observed by taking phase contrast microscopy images. Dashed line indicates migrating front. Scale bar equals 200 μm. **(D)** Outgrowth of epithelial cells was evaluated by measuring the area around explants. Results are representative of five mice per group for (A)&(B) and at least seven mice per group for (C)&(D). Error bars are defined as mean +/- SEM. Student's t-test for the immunoblots and two-way ANOVA with Bonferroni's post-test for the explants demonstrate significance *$p<0.05$.

Explants were then isolated from wild type and Snai2 over-expressing mice. The tissues were exposed to 0.5 mM glyoxal over a 5 d period (Figure 4.9A). Image analysis and outgrowth area measurements over the incubation period demonstrate improved epithelial outgrowth in the over-expressing mice compared to wild type, and this was significant as early as 3 d after the addition of glyoxal (Figure 4.9B). These data suggest

the potential of Snai2 over-expression to promote epithelial outgrowth under diabetic conditions.

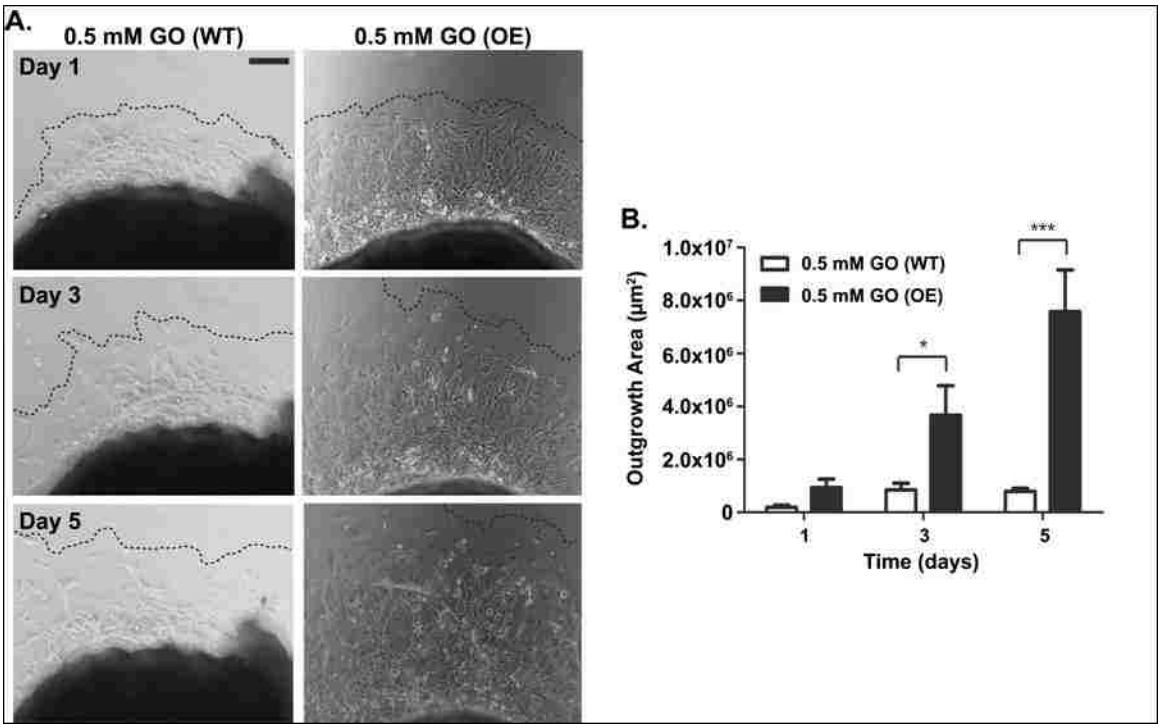


FIGURE 4.9. **Snai2 protein over-expression in mice promotes epithelial outgrowth in the presence of glyoxal. (A)** Skin explants isolated from the dorsal side of wild type (WT) and Snai2 over-expressing (OE) mice were cultured for 5 d. Explants were exposed to 0.5 mM glyoxal (GO), and epithelial outgrowth of keratinocytes was observed by phase contrast microscopy. Dashed line indicates migrating front. Scale bar equals 200 µm. **(B)** Outgrowth of epithelial cells was evaluated by measuring the area around explants. Results are representative of at least seven mice per group. Error bars are defined as mean +/- SEM. Two-way ANOVA with Bonferroni's post-test demonstrates significance *$p<0.05$ and ***$p<0.001$.

## 4.4 Discussion

Elevated AGEs are present in numerous pathologies including Alzheimer's disease, arthritis, and diabetes (Singh et al., 2001; Takeuchi and Yamagishi, 2008; Vytasek et al., 2010) and are believed to impair protein function (Ahmed, 2005). An increasing body of evidence suggests that glycation disrupts various aspects of the wound

healing cascade (Ahmed, 2005; Huijberts et al., 2008; Peppa and Raptis, 2011). Exposure of rats to the AGE precursor methylglyoxal decreased the numbers of cells actively migrating into the wound, decreased angiogenesis, and reduced secretion and accumulation of extracellular matrix components (Berlanga et al., 2005). In diabetic *db/db* mice fed a high AGE diet, increased CML was present in wound tissue, and these mice displayed a sustained inflammatory response and incomplete wound closure (Peppa et al., 2003). Conversely, restricting dietary AGE in diabetic mice improved wound repair compared to those fed a high AGE diet (Peppa et al., 2003). In addition, our studies demonstrate the AGE precursor glyoxal decreases keratinocyte migration and epithelial outgrowth from skin explants *ex vivo*. There is mounting evidence implicating AGEs in defective cell locomotion and survival (Loughlin and Artlett, 2009; Morita et al., 2005; Zhu et al., 2011), further connecting AGEs to impaired diabetic wound healing.

In the present study, Snai2 was identified as a novel target for down-regulation by the AGE precursor glyoxal. Reduction of Snai2 protein is predicted to impair reepithelialization based on its demonstrated role in keratinocyte migration and wound repair (Chandler et al., 2007; Hudson et al., 2009; Savagner et al., 2005; Shirley et al., 2010). Snai2 was up-regulated at the margins of healing wounds (Savagner et al., 2005), and wound sections obtained from non-healing canine corneas were deficient in Snai2 (Chandler et al., 2007). Furthermore, epithelial outgrowth was impaired in both canine corneas and Snai2 null mice skin explants (Chandler et al., 2007; Kusewitt et al., 2009; Savagner et al., 2005), suggesting that Snai2 deficiency may be associated with failure to heal. Because Snai2 has been shown to be an essential mediator of EGFR-mediated keratinocyte outgrowth (Arnoux et al., 2008; Kusewitt et al., 2009), the impact of glyoxal

and CML on both EGF-stimulated and basal Snai2 levels could contribute to deficits in reepithelialization.

Determinants of lysine glycation include the number and the density of lysine residues in a peptide, residue position, and availability of the residues on the protein surface (Kueper et al., 2007; Venkatraman et al., 2001). Snai1 and Snai2 are highly related proteins, but Snai1 was not down-regulated in response to glyoxal, demonstrating selectivity in protein glycation. Interestingly, Snai2 and Snai1 differ in lysine content (8.2% versus 5.3%, respectively), and Snai2 contains 3 lysine pairs compared to a single pair in Snai1, another factor thought to contribute to the likelihood of glycation. The immediate impact of glyoxal-induced modification of Snai2 is unclear. It is possible that covalent modification of Snai2 may be promoting protein degradation (Bulteau et al., 2001; Cervantes-Laurean et al., 2005) as our immunoblots demonstrated decreased levels of Snai2 following glyoxal exposure. However, additional studies need to be done to further explore the glyoxal-Snai2 relationship.

Furthermore, we demonstrated that Snai2 over-expression in skin could promote epithelial outgrowth under diabetic conditions *ex vivo*. Though enhancing Snai2 may increase reepithelialization, Snai2 modulation may also affect inflammation, angiogenesis, the extracellular matrix, differentiation, and apoptosis (Shirley et al., 2010). To the best of our knowledge, the effect of other reactive AGE intermediates, such as methylglyoxal and 3-deoxyglucosone, on Snai2 has not been explored, so it is possible that other AGE precursors may also have an effect on Snai2-dependent wound reepithelialization. Together, the findings suggest a link between increased glycation that occurs in diabetes and impaired wound closure through down-regulation of Snai2.

Moreover, enhancing Snai2 is an attractive mode of promoting reepithelialization in diabetes.

# CHAPTER 5

## Future Directions and Perspectives

Diabetes mellitus is a debilitating metabolic disease that can ultimately result in death (Galtier, 2010; Setacci et al., 2009). One troubling complication is non-healing skin wounds, and we investigated the effect of the advanced glycation end product precursor, glyoxal, on proteins known to be required for successful reepithelialization (Usui et al., 2008; Velander et al., 2008). The data presented in this dissertation presents for the first time a role of transcription factor Snai2 in diabetes-impaired wound reepithelialization.

## 5.1 AGEs as culprits in diabetes-impaired wound repair

An important consequence of diabetes is the elevation of advanced glycation end products (AGE), which are present in numerous pathologies and have been implicated in impaired diabetic wound healing (Ahmed, 2005; Huijberts et al., 2008; Peppa and Raptis, 2011; Singh et al., 2001; Takeuchi and Yamagishi, 2008; Vytasek et al., 2010). There is mounting evidence implicating AGEs in defective cell locomotion and survival (Loughlin and Artlett, 2009; Morita et al., 2005; Zhu et al., 2011), and our studies further demonstrate keratinocyte migration and epithelial outgrowth impairments as a consequence of glyoxal exposures (Chapter 3). In addition, exposing glyoxal led to increased levels of covalently modified proteins and demonstrates the broad range of potential glycation targets (Chapter 3). A limitation of the studies discussed in this dissertation is that the highest dose of glyoxal tested (0.5 mM) is greater than what is found in diabetic patients (Lapolla et al., 2003), but the concentrations and times of

exposure are comparable to what has been used in other studies (Berge et al., 2007; Nass et al., 2010; Rattan et al., 2007; Sliman et al., 2010). In addition, AGE formation and accumulation may take years to occur. Therefore, for the purposes of scientific studies, the dose is increased, and the exposure times are decreased to mimic a diabetic environment. More studies will be needed in order to ascertain which proteins are targets of glycation and whether or not they play important roles in the healing process. Identifying the specific proteins being AGE-modified may allow us to target these proteins to promote healing over the observed deficiencies in diabetic wound healing.

### 5.1.1 Selectivity in protein glycation

There is evidence for selectivity of protein glycation; sites of glycation include thiols, lysine, and arginine residues, and the N-terminus of proteins (Miller et al., 2003; Mostafa et al., 2007; Schwarzenbolz et al., 2008; Venkatraman et al., 2001). Other factors that influence glycation are protein turnover, intracellular localization, and structure (Kueper et al., 2007). The traditional belief is that collagen and other extracellular matrix components and proteins such as myelin, plasminogen activator 1, and fibrinogen, are recognized targets of glycation because they are long-lived and easily accessible to AGE modification (Goh and Cooper, 2008; Kragstrup et al., 2011; Zieman and Kass, 2004). However, there is evidence for modification of intracellular proteins as well (Kueper et al., 2007). Lysine glycation is dependent on the number and density of lysine residues in a peptide, residue position, and availability of the residues on the protein surface (Kueper et al., 2007; Venkatraman et al., 2001). Though Snai2 was shown to be modified by CML following glyoxal exposure, the closely related family

member Snai1 was not, suggesting selectivity in glycation. In addition to Snai1, we also examined the effect of glyoxal on other intracellular proteins such as Specificity Protein 1 (SP1), poly (ADP-ribose) polymerase (PARP) (Figure 5.1), β-Tubulin, glyceraldehyde 3-phosphate dehydrogenase (GAPDH), and EGFR (Chapter 3, Figure 3.7). We found that out of all proteins tested, Snai2 was the only protein affected. Evidence of CML-modification of Snai2 supports the conclusion that Snai2 is a target of glycation. Furthermore, we demonstrated the ability of Snai2 protein over-expression to overcome the inhibition of epithelial outgrowth caused by glyoxal.

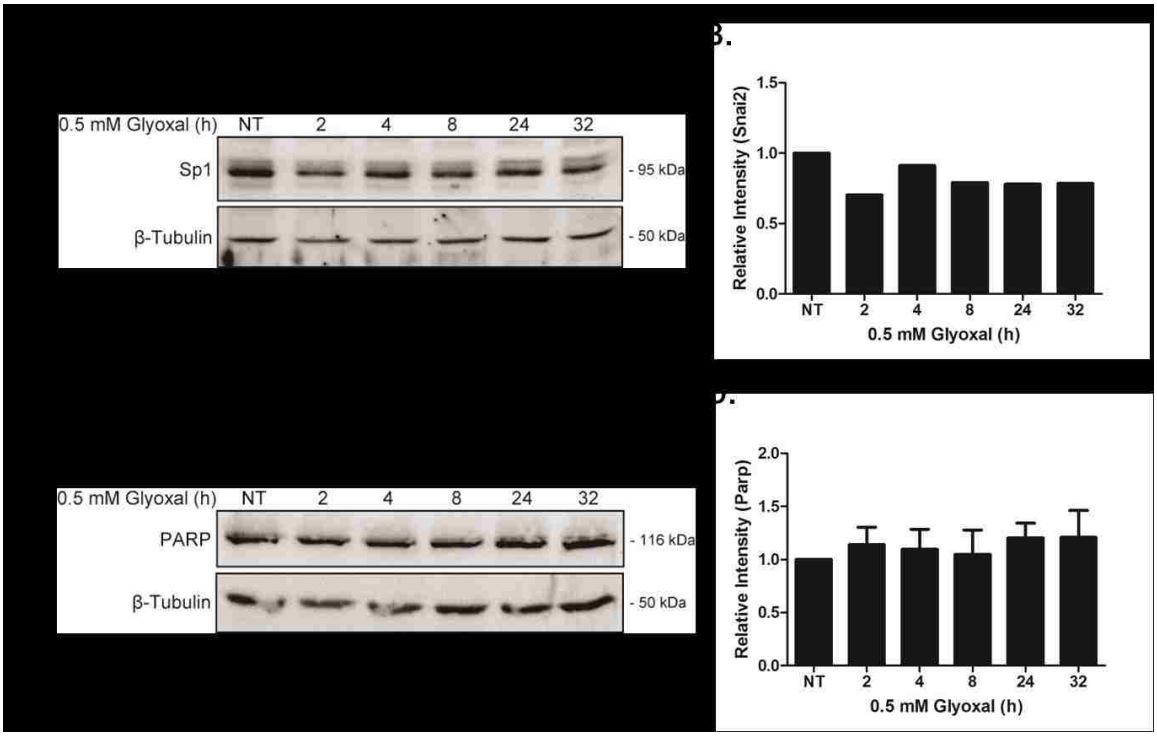


FIGURE 5.1. **Glyoxal has no effect on Sp1 and PARP protein.** SCC 12F keratinocytes were treated with 0.5 mM glyoxal for the indicated times. **(A)&(B)** Protein was analyzed for changes in transcription factor Sp1. **(C)&(D)** Protein was analyzed for changes in PARP. β-Tubulin was used as a loading control. Results are representative of one independent experiment for Sp1detection and three independent experiments for PARP assessment. Error bars are defined as mean +/- SEM. One-way ANOVA and Tukey's post-test did not show statistical significance.

This work provides more evidence of an emerging idea that glycation occurs not just to proteins with long half-lives such as with collagen and other easily available extracellular matrix proteins. It demonstrates that glycation may be a specific event and can even affect nuclear proteins. Therefore, it is crucial to begin identifying which proteins are targets of glycation to rectify impairments in cell function.

## 5.2 Current therapies in diabetic ulcer treatment

Diabetic foot complications are the most common cause of non-traumatic lower extremity amputations in the world (Wu and Armstrong, 2005). Diabetic wound care begins by assessing the state of the wound and asking questions such as what is the etiology and the diagnosis of the wound? Why has the wound become chronic? Why has the healing rate slowed or stopped? Many factors contribute to the state of a chronic diabetic wound (Figure 5.2), making successful healing difficult.

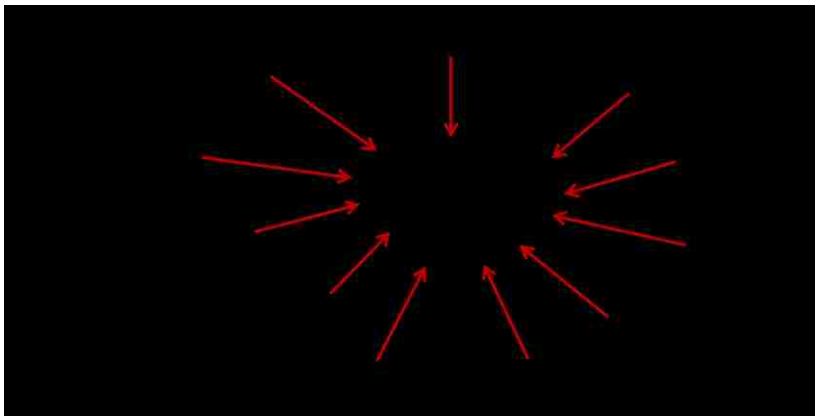

FIGURE 5.2. **Factors that contribute to a chronic wound state in diabetes.** Many different factors play roles in wound healing, making repair a complicated process.

The International Working Group of the Diabetic Foot has issued guidelines on the management of the diabetic foot since 1999, but even today, effective treatment remains a major problem (Game et al., 2012). Diabetic wound treatments range anywhere from improving patient nutrition to full limb amputations.

### 5.2.1 Pharmacological treatment of diabetic ulcers

Wound care also includes maintenance of a moist environment through hydrogels, hydrocolloids, foams, and alginates (Janis et al., 2010). These products may contain silver to provide anti-microbial activity (Janis et al., 2010). As measured by the migration of new epithelium into the wound bed, moist wounds healed two to three times faster than dry wounds, demonstrating the importance of keeping wounds wet (Winter, 1962). In contrast, a dry environment impairs fibroblast proliferation and prevents cell migration (Chang et al., 1996). A moist environment also promotes granulation tissue formation and epithelial cell migration, accelerates angiogenesis, increases the breakdown of necrotic tissues and fibrin, and potentiates interactions between growth factors and target cells.

### 5.2.2 Skin substitutes promote wound healing

The use of bioengineered skin has also been explored to heal wounds that have not closed by at least 50% after four weeks. For example, Dermagrafts and Apligrafts act as scaffolds and skin substitutes. Dermagrafts are produced by culturing human dermal fibroblasts from newborn foreskin onto a mesh scaffold. As the fibroblasts proliferate, they secrete collagen, matrix proteins, growth factors, and cytokines to help promote

reepithelialization. It was shown that patients using the fibroblast-derived dermis healed faster and had lower rates of infection than those who did not use the dermagraft (Hanft and Surprenant, 2002; Marston et al., 2003). An alternative substitute, the Apligraft, is bi-layered and contains an epidermis and a dermis cultured from neonatal foreskin. The Apligrafts produce all cytokines and growth factors expressed in normal healing skin. Apligrafts have been shown to heal chronic ulcers faster than conventional debridement and saline dressing therapy (Veves et al., 2001). Therefore, the use of skin substitutes does provide further assistance in promoting wound repair. However, these treatments are costly.

### 5.2.3 Tissue debridement and amputation

If necessary, necrotic and devitalized tissues are removed by debridement, which converts a chronic wound into an acute wound and removes all the damaged or dead tissues that harbored harmful bacteria. Decisions to amputate are performed only if absolutely necessary and begin with removal of small tissues, such as the toes. However, this can escalate into full removal of the limb. If an amputation is needed, wounds are sutured closed, and wound vacs are used to promote the granulation process of healing (Janis et al., 2010; Nather, 2011).

Though many factors play roles in successful diabetic wound closure, treatment can also be expensive or ineffective. Much is left to be discovered regarding specific factors that prevent diabetic tissue repair. The work in this dissertation has identified a novel protein known to be crucial for successful reepithelialization that is decreased in a

diabetic state. Thus, further examination of the effect of diabetes on Snai2 protein must be explored.

## 5.3 Exploring pharmacological therapies to enhance reepithelialization

It is clear that the current methods used to treat chronic wounds are ineffective in stopping infection, in promoting wound closure, and in preventing amputations. Therefore, there is a continued need to explore alternative therapies.

### 5.3.1 Targeting EGFR to promote healing

As discussed in Chapter 3, many studies have demonstrated the crucial contribution of the epidermal growth factor receptor (EGFR) in wound healing. Furthermore, there is evidence of EGFR involvement in diabetic tissue repair. Currently, investigations into using recombinant EGF to promote tissue repair in diabetic rats (Dogan et al., 2009; Lao et al., 2012) and prevent amputation of diabetic foot ulcers are being conducted (Tiaka et al., 2012). EGF treatment alone has demonstrated successful wound closure in a significant number of diabetic patients (Fernandez-Montequin et al., 2007; Fernandez-Montequin et al., 2009; Tuyet et al., 2009). When given in combination with other therapies, EGF treatments resulted in even greater healing compared to EGF alone (Hong et al., 2006; Tsang et al., 2003). More importantly, reduced amputations were observed with EGF applications (Acosta et al., 2006; Tsang et al., 2003). Optimizations on concentrations and method of administration, such as through dressings, intra-lesional injections, and EGF-conjugated nanofibers (Berlanga-Acosta, 2011; Choi et al., 2008; Fernandez-Montequin et al., 2009; Lao et al., 2012), are yet to be

determined but offer attractive possibilities into promoting tissue repair. However, though these studies and treatments show potential in improving reepithelialization, they may still be met with limited success. It has been demonstrated that the EGFR itself is a target of glycation (Portero-Otin et al., 2002), yet we found no glycation of the EGF ligand, suggesting AGEs target the receptor. It is possible the covalent modification can be occurring in the cysteine-rich regions of the binding site required for proper receptor activation (Garrett et al., 2002; Ward et al., 2007). Because the EGFR may be modified in some diabetic wound cases, it is important to continue exploring other protein targets to promote healing.

### 5.3.2 Snai2/Slug is a novel therapeutic target in diabetic wound healing

The data presented in this dissertation demonstrate impairments in EGFR activation and its function following glyoxal exposure. However, enhancing Snai2 protein by bypassing the EGFR may be sufficient to overcome the reepithelialization impairments observed in diabetes (Figure 5.3). In data recently obtained from our collaborator Dr. Donna F. Kusewitt (University of Texas MD Anderson Cancer Center, Smithville, Texas), wounded diabetic mice sustained a larger wound bed length compared to wounded control mice. In addition, basal Snai2 protein was detected at lower levels in wounded diabetic mice compared to controls. Therefore, further exploration of the potential of enhancing Snai2 levels to overcome impaired reepithelialization is of interest.

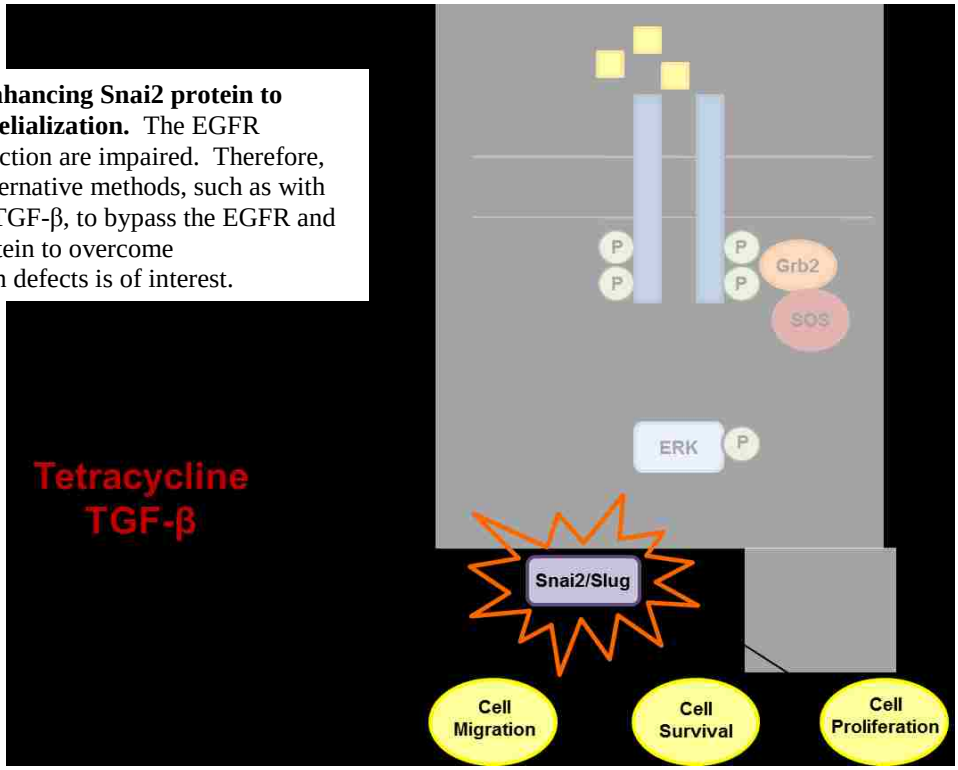


FIGURE 5.3. **Enhancing Snai2 protein to promote reepithelialization.** The EGFR signaling and function are impaired. Therefore, exploration of alternative methods, such as with tetracycline and TGF-β, to bypass the EGFR and induce Snai2 protein to overcome reepithelialization defects is of interest.

In addition to the EGFR signaling pathway to induce Snai2, tetracyclines are known to enhance expression of TGF-β, a growth factor important in both corneal wound healing and Snai2 induction (Aomatsu et al., 2011; Chandler et al., 2007; Shlopov et al., 2001). Crosstalk between the EGFR-ERK and TGF-β-SMAD signaling pathways is known to enhance TGF-β-dependent responses (Aomatsu et al., 2011; Hayashida et al., 2003; Uttamsingh et al., 2008). It was recently shown in dogs with refractory corneal ulcers that topical tetracycline ophthalmic ointment resulted in a significantly shorter healing time than dogs who received a control treatment (Chandler et al., 2010). In future studies, we can then move to *in vivo* studies involving diabetic mice. These mice will be wounded, and we can test the ability of a topical tetracycline ointment to enhance wound healing.

We first examined the ability of tetracycline hydrochloride to induce Snai2 protein in SCC 12F keratinocytes as described in Section 2.1.1. The preliminary data shows that with increasing exposure to tetracycline hydrochloride, enhanced levels of Snai2 protein are observed (Figure 5.4A and 5.4B). This suggests that it may be possible to induce Snai2 protein in an EGF-independent mechanism, and therefore it may be considered in promoting healing in diabetes.

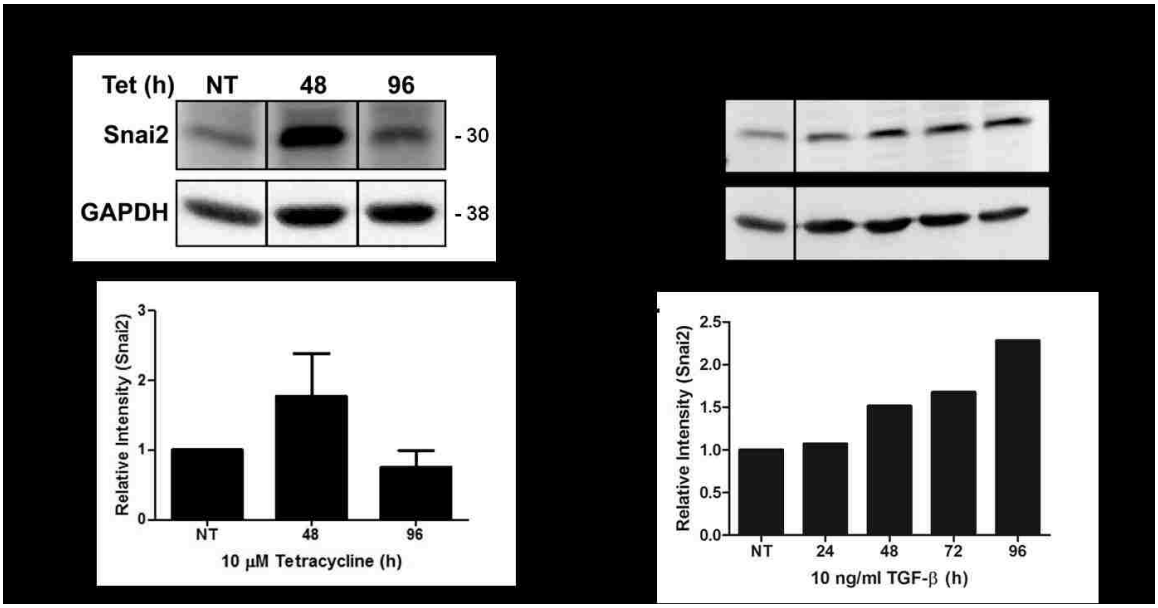


FIGURE 5.4. **Tetracycline hydrochloride and TGF-β induce Snai2 protein in keratinocytes.** SCC 12F cells were exposed to 10 µM tetracycline hydrochloride (Tet) **(A)&(B)** or to 10 ng/ml TGF-β **(C)&(D)** for 96 h. Snai2 protein levels were evaluated via immunoblot, and densitometries revealed increased Snai2 following Tet and TGF-β exposures. Results are representative of two experiments for (A)&(B) and one experiment for (C)&(D). Error bars are defined as mean +/- SEM.

Tetracycline is a drug of choice to use in these studies because it is already commercially available in various forms, and it induces Snai2 by up-regulating TGF-β (Chandler et al., 2007). However tetracycline hydrochloride has a short-acting half-life of 6-8 hrs. Therefore, we may need to use a different form of tetracycline, such as doxycycline, which has been used in other studies (Chandler et al., 2007) and has a long-

acting half-life of 18-22 hrs. In addition, if the observed increases in Snai2 are too mild for the short duration of our experiments (~1 wk), direct treatment with TGF-β may be an alternative approach to enhance Snai2 (Figure 5.4C and 5.4D). In initial studies, we exposed tissue explants obtained from mice (Section 2.2.2) to 10 ng/ml TGF-β and to 0.5 mM glyoxal. We observed that TGF-β induced explant outgrowth (Figure 5.5). In contrast, glyoxal impaired epithelial outgrowth, which was similar to what was observed in Chapter 3, Figure 3.4. However, the combination of TGF-β and glyoxal was sufficient to induce keratinocyte outgrowth. This further demonstrates that though Snai2 protein is impaired under diabetic conditions, it is possible to boost Snai2 levels with pharmacological inducers. Therefore, we may have a novel alternative method to promote wound healing in diabetes.

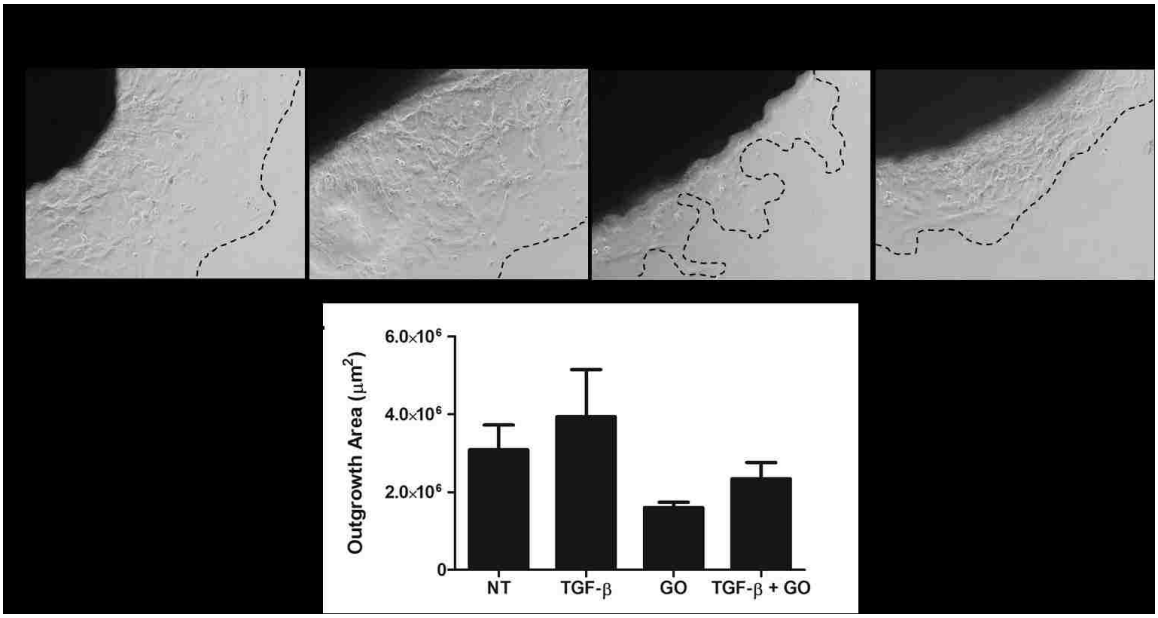


FIGURE 5.5. **TGF-β induces epithelial outgrowth in the presence of glyoxal. (A)** Skin explants isolated from the dorsal side of wild type were cultured for 3 d with 10 ng/ml TGF-β and 0.5 mM glyoxal (GO). Epithelial outgrowth of keratinocytes was observed by phase contrast microscopy. Dashed line indicates migrating front. **(B)** Outgrowth of epithelial cells was evaluated by measuring the area around explants. Results are representative of three mice per group. Error bars are defined as mean +/- SEM.

## 5.4 Future directions

The work discussed in this dissertation demonstrates signaling pathways known to be required for successful wound closure are defective in a diabetic environment. In addition, glycation is targeting Snai2 protein, a transcription factor required for reepithelialization. However, Snai2 enhancement via a different signaling pathway, TGF-β, is sufficient to promote cell migration. Thus, further studies are needed to determine if targeting Snai2 *in vivo* can enhance wound healing.

It will be informative to investigate repair of full thickness wounds in the backs of diabetic mice (Figure 5.6). Wounds will be created using 6 mm biopsy punches, and healing and rates of closure will be evaluated between wild type and diabetic mice. Parameters measured from a wound include the wound margin length (the distance the cells have migrated into the wound) and the wound bed length (the diameter of the wound not yet healed). In addition, the wounds can be isolated from the mice and analyzed using immunohistochemistry. Snai2 protein can be analyzed using immunofluorescence to determine if there is a correlation between wound healing rate and Snai2 protein levels, location, and modification.

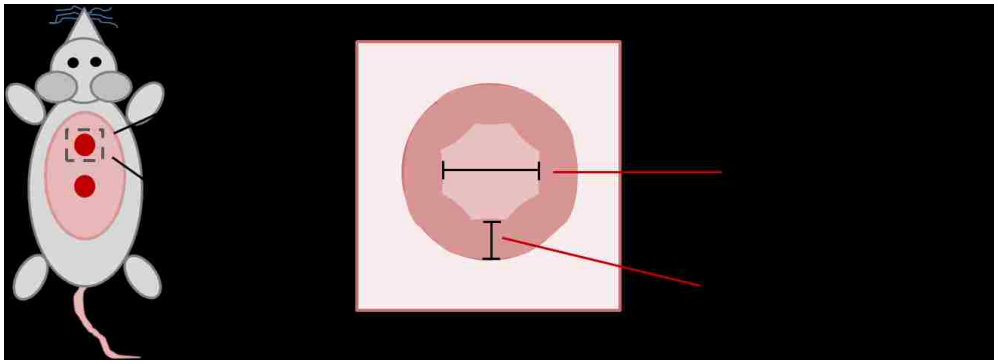

FIGURE 5.6. **Live animal wounding studies.** Full thickness wounds will be introduced into the backs of mice. Rates of wound closure as well as wound bed and margin lengths can be examined comparing wild type and diabetic mice. Wounds can also be harvested from mice and analyzed for changes in Snai2 protein using immunohistochemistry.

Following exploration of protein differences between wild type and diabetic mice, we will wound diabetic mice and treat the damaged tissue with tetracycline. As discussed above, tetracycline has been demonstrated to induce Snai2 protein and promote wound healing in canine corneas (Chandler et al., 2007; Chandler et al., 2010). By treating diabetic wounds with tetracycline, we hope to observe significant improvements in closure compared to untreated diabetic wounds. This data will contribute to possibilities of cheaper, more manageable, wound care. In addition, it will be a more targeted approach, as current therapies aim to promote an environment suitable for overall healing and do not address the underlying causes of diabetic repair deficiencies.

### 5.4.1 Applications of animal models in diabetes research

Our future studies will include the use of diabetic animals. Most often, rodents are used due to their size, cost, and the ability to provide a controllable diabetic environment *in vivo*. The models can be divided into two categories – genetically-induced spontaneous diabetes models and chemically-induced non-spontaneous diabetes models (Islam and Loots du, 2009). Three examples of popular animal models of diabetes include the *ob/ob*, the *db/db*, and the Streptozotocin (STZ) mice, where the *ob/ob* and the *db/db* mice are genetically-induced models of diabetes, and the STZ mouse is a chemically-induced model.

### 5.4.2 Genetically-induced models of diabetes

The genetically-induced models develop diabetes spontaneously, may have insulin resistance, and reduced β-cell mass (Kim et al., 1998). However, though the

genetic animal models have advantages, they are difficult to maintain, are expensive, and do not fully express the pathology of diabetes (Peters and Schmitt, 2012).

The o*b/ob* mouse is a model of type 2 diabetes and obesity and was created by Jackson Laboratories in Bar Harbor, Maine (Ingalls et al., 1950) (Lindstrom, 2007). The affected gene is a recessive mutation in the *obese* (*ob*) gene (Zhang et al., 1994), resulting in an inability to produce the hormone leptin. This hormone is produced primarily in adipose tissue, and its major role is to regulate appetite by signaling to the brain that one has had enough to eat (Feve and Bastard, 2012). Because *ob/ob* mice lack this hormone, their food intake is uncontrolled and result in obesity. At birth, the mutant mice look similar compared to their littermates, but they gain weight quickly, reaching weights three times that of unaffected mice. In addition to extreme obesity, the mice develop hyperglycemia, increased insulin production (Garthwaite et al., 1980; Mayer and Barrnett, 1953), and suffer from infertility. Interestingly, the *ob/ob* syndrome can be reversed by exogenous leptin or transfection with the leptin gene (Halaas et al., 1995; Larcher et al., 2001; Pelleymounter et al., 1995). Because they have large pancreatic islets and a higher number of insulin-producing β-cells, they are often used in studies of β-cell function (Lindstrom, 2007) and have greatly advanced our understanding of diabetes, obesity, and metabolism. Furthermore, this model has been demonstrated to suffer impaired wound healing with defective immune functions, decreased collagen deposition, and reduced reepithelialization (Frank et al., 2000; Goodson and Hunt, 1986; Goren et al., 2003; Kampfer et al., 2005; Stallmeyer et al., 2001a; Stallmeyer et al., 2001b) making it a useful model for diabetic wound repair.

Whereas *ob/ob* animals lack the hormone leptin, *db/db* animals lack functioning receptors for leptin due to a homozygous point mutation in the gene encoding the receptor. The leptin receptor is highly expressed in the hypothalamus, and animals with a defect in the receptor are unable to regulate their energy stores. These animals become obese by 3-4 weeks of age. The mice are insulin resistant, hypertriglyceridemic (high blood levels of triglycerides, the most abundant fatty molecule), and have impaired glucose tolerance (Lindstrom, 2007). This model is a popular animal model that has been used to demonstrate wound healing defects. These mice display lower levels of growth factors and receptors that result in a reduced wound healing rate (Tsuboi et al., 1992; Werner et al., 1994), decreased epidermal nerves, and an inability to heal standard skin wounds (Olerud, 2008). Lastly, slow wound healing in these mice may be due mainly to impaired wound contraction (Chan et al., 2006; Sullivan et al., 2004), a major method of wound closure in mice, adding to the benefits of this model.

### 5.4.3 Chemically-induced models of diabetes

In contrast to genetic models of obesity, chemically-induced diabetes can be performed using mice that are normally not diabetic. They are cheaper to use than genetically-modified models, and diabetes can be induced as simply as by high-fat diets or by chemical injection (Rakieten et al., 1963). They also develop most of the pathological symptoms associated with diabetes, making the chemical induction of diabetes a popular method to use in research. However, no single model exists that manifests all aspects of diabetes, which include neural, retinal, renal, and cardiac complications.

The Streptozotocin (STZ)-induced model is a chemically-induced model derived from STZ, which is produced by *Streptomyces achromogenes* (Rakieten et al., 1963). STZ-induced diabetes functions by destroying pancreatic β-cells through oxidative stress, leading to insulin deficiency, hyperglycemia, and ketosis (Ozawa et al., 2011; Rerup, 1970; Yamamoto et al., 1981). Depending on the dose of STZ used, this model can mimic both type 1 and type 2 diabetes (Rakieten et al., 1963). It is cytotoxic to pancreatic β-cells after being transported through glucose transporter 2 (GLUT2), allowing generation of a type 1 diabetes model (Schnedl et al., 1994). However, STZ does not provide a state of insulin resistance, and can be given in combination with a high-fat diet to create a model of insulin resistance, making a model of type 2 diabetes. Blood glucose levels can reach over 250 mg/dL just days after the first STZ injection (Graham et al., 2011; Kurihara et al., 2008).

This method is simple, cost effective, and can be used over a broad range of animals. These mice display decreased granulation tissue accumulation (Cianfarani et al., 2006; Goodson and Hung, 1977; Seifter et al., 1981), altered T-cell function, and decreased macrophage phagocytosis (Seifter et al., 1981), characteristic of the diabetic condition. However, induction of diabetes may take weeks, and there is high variability in blood glucose levels (Rerup, 1970),

The exploration of diabetes and a better understanding of its causes and effects are ongoing, and the use of animal models allows researchers to mimic diabetic environments. Depending on what knowledge is desired, some models are more appropriate than others, and the availability of various options will hopefully assist in efficient and accurate studies of diabetes. With the availability of diabetic animals for

research, we can investigate the use of pharmacological inducers of Snai2 to promote wound healing.

## 5.5 Significance

In conclusion, the data presented throughout this dissertation advances the current knowledge regarding the contributions of Snai2 in wound healing. More importantly, it implicates Snai2 as having a crucial role in diabetes-impaired wound repair in that this protein known to be required for successful reepithelialization is covalently modified in the diabetic environment. Thus, these studies identify Snai2 as an attractive therapeutic target to promote wound closure in diabetes.

## REFERENCES


Accili, D., J. Drago, E.J. Lee, M.D. Johnson, M.H. Cool, P. Salvatore, L.D. Asico, P.A. Jose, S.I. Taylor, and H. Westphal. 1996. Early neonatal death in mice homozygous for a null allele of the insulin receptor gene. *Nat Genet*. 12:106-109.

Accili, D., J. Nakae, J.J. Kim, B.C. Park, and K.I. Rother. 1999. Targeted gene mutations define the roles of insulin and IGF-I receptors in mouse embryonic development. *J Pediatr Endocrinol Metab*. 12:475-485.

Acosta, J.B., W. Savigne, C. Valdez, N. Franco, J.S. Alba, A. del Rio, P. Lopez-Saura, G. Guillen, E. Lopez, L. Herrera, and J. Fernandez-Montequin. 2006. Epidermal growth factor intralesional infiltrations can prevent amputation in patients with advanced diabetic foot wounds. *Int Wound J*. 3:232-239.

Adams, R.H., and K. Alitalo. 2007. Molecular regulation of angiogenesis and lymphangiogenesis. *Nat Rev Mol Cell Biol*. 8:464-478.

Adamson, R. 2009. Role of macrophages in normal wound healing: an overview. *J Wound Care*. 18:349-351.

Ahmed, M.U., S.R. Thorpe, and J.W. Baynes. 1986. Identification of N epsilon-carboxymethyllysine as a degradation product of fructoselysine in glycated protein. *J Biol Chem*. 261:4889-4894.

Ahmed, N. 2005. Advanced glycation endproducts--role in pathology of diabetic complications. *Diabetes Res Clin Pract*. 67:3-21.

Al-Mashat, H.A., S. Kandru, R. Liu, Y. Behl, T. Desta, and D.T. Graves. 2006. Diabetes enhances mRNA levels of proapoptotic genes and caspase activity, which contribute to impaired healing. *Diabetes*. 55:487-495.

Aomatsu, K., T. Arao, K. Sugioka, K. Matsumoto, D. Tamura, K. Kudo, H. Kaneda, K. Tanaka, Y. Fujita, Y. Shimomura, and K. Nishio. 2011. TGF-beta induces sustained upregulation of SNAI1 and SNAI2 through Smad and non-Smad pathways in a human corneal epithelial cell line. *Invest Ophthalmol Vis Sci*. 52:2437-2443.

Arnoux, V., M. Nassour, A. L'Helgoualc'h, R.A. Hipskind, and P. Savagner. 2008. Erk5 controls Slug expression and keratinocyte activation during wound healing. *Mol Biol Cell*. 19:4738-4749.

Bailey, A.J., R.G. Paul, and L. Knott. 1998. Mechanisms of maturation and ageing of collagen. *Mech Ageing Dev*. 106:1-56.

Barrallo-Gimeno, A., and M.A. Nieto. 2005. The Snail genes as inducers of cell movement and survival: implications in development and cancer. *Development*. 132:3151-3161.

Bartkova, J., B. Gron, E. Dabelsteen, and J. Bartek. 2003. Cell-cycle regulatory proteins in human wound healing. *Arch Oral Biol*. 48:125-132.

Bazley, L.A., and W.J. Gullick. 2005. The epidermal growth factor receptor family. *Endocr Relat Cancer*. 12 Suppl 1:S17-27.

Berge, U., J. Behrens, and S.I. Rattan. 2007. Sugar-induced premature aging and altered differentiation in human epidermal keratinocytes. *Ann N Y Acad Sci*. 1100:524-529.

Berlanga-Acosta, J. 2011. Diabetic lower extremity wounds: the rationale for growth factors-based infiltration treatment. *Int Wound J*. 8:612-620.

Berlanga, J., D. Cibrian, I. Guillen, F. Freyre, J.S. Alba, P. Lopez-Saura, N. Merino, A. Aldama, A.M. Quintela, M.E. Triana, J.F. Montequin, H. Ajamieh, D. Urquiza, N. Ahmed, and P.J. Thornalley. 2005. Methylglyoxal administration induces diabetes-like microvascular changes and perturbs the healing process of cutaneous wounds. *Clin Sci (Lond)*. 109:83-95.

Bierhaus, A., M.A. Hofmann, R. Ziegler, and P.P. Nawroth. 1998. AGEs and their interaction with AGE-receptors in vascular disease and diabetes mellitus. I. The AGE concept. *Cardiovasc Res*. 37:586-600.

Bitar, M.S. 1997. Insulin-like growth factor-1 reverses diabetes-induced wound healing impairment in rats. *Horm Metab Res*. 29:383-386.

Blakytny, R., and E.B. Jude. 2009. Altered molecular mechanisms of diabetic foot ulcers. *Int J Low Extrem Wounds*. 8:95-104.

Boukamp, P., R.T. Petrussevska, D. Breitkreutz, J. Hornung, A. Markham, and N.E. Fusenig. 1988. Normal keratinization in a spontaneously immortalized aneuploid human keratinocyte cell line. *J Cell Biol*. 106:761-771.

Brem, H., O. Stojadinovic, R.F. Diegelmann, H. Entero, B. Lee, I. Pastar, M. Golinko, H. Rosenberg, and M. Tomic-Canic. 2007. Molecular markers in patients with chronic wounds to guide surgical debridement. *Mol Med*. 13:30-39.

Brown, N.S., and R. Bicknell. 2001. Cell migration and the boyden chamber. *Methods Mol Med*. 58:47-54.

Brownlee, M., H. Vlassara, A. Kooney, P. Ulrich, and A. Cerami. 1986. Aminoguanidine prevents Diabetes-Induced Arterial Wall Protein Cross-Linking. *Science*. 232:1629-1632.

Bucala, R. 1997. Lipid and lipoprotein modification by advanced glycosylation end-products: role in atherosclerosis. *Exp Physiol*. 82:327-337.

Bulteau, A.L., P. Verbeke, I. Petropoulos, A.F. Chaffotte, and B. Friguet. 2001. Proteasome inhibition in glyoxal-treated fibroblasts and resistance of glycated glucose-6-phosphate dehydrogenase to 20 S proteasome degradation in vitro. *J Biol Chem*. 276:45662-45668.

Cai, W., J.C. He, L. Zhu, C. Lu, and H. Vlassara. 2006. Advanced glycation end product (AGE) receptor 1 suppresses cell oxidant stress and activation signaling via EGF receptor. *Proc Natl Acad Sci U S A*. 103:13801-13806.

Casanova, M.L., F. Larcher, B. Casanova, R. Murillas, M.J. Fernandez-Acenero, C. Villanueva, J. Martinez-Palacio, A. Ullrich, C.J. Conti, and J.L. Jorcano. 2002. A critical role for ras-mediated, epidermal growth factor receptor-dependent angiogenesis in mouse skin carcinogenesis. *Cancer Res*. 62:3402-3407.

Cervantes-Laurean, D., M.J. Roberts, E.L. Jacobson, and M.K. Jacobson. 2005. Nuclear proteasome activation and degradation of carboxymethylated histones in human keratinocytes following glyoxal treatment. *Free Radic Biol Med*. 38:786-795.

Chan, R.K., P.H. Liu, G. Pietramaggiori, S.I. Ibrahim, H.B. Hechtman, and D.P. Orgill. 2006. Effect of recombinant platelet-derived growth factor (Regranex) on wound closure in genetically diabetic mice. *J Burn Care Res*. 27:202-205.

Chandler, H.L., C.M. Colitz, P. Lu, W.J. Saville, and D.F. Kusewitt. 2007. The role of the slug transcription factor in cell migration during corneal re-epithelialization in the dog. *Exp Eye Res*. 84:400-411.

Chandler, H.L., A.J. Gemensky-Metzler, I.D. Bras, T.E. Robbin-Webb, W.J. Saville, and C.M. Colitz. 2010. In vivo effects of adjunctive tetracycline treatment on refractory corneal ulcers in dogs. *J Am Vet Med Assoc*. 237:378-386.

Chang, H., S. Wind, and M.D. Kerstein. 1996. Moist wound healing. *Dermatol Nurs*. 8:174-176, 204.

Chen, S.C., J.Y. Guh, C.C. Hwang, S.J. Chiou, T.D. Lin, Y.M. Ko, J.S. Huang, Y.L. Yang, and L.Y. Chuang. 2010. Advanced glycation end-products activate extracellular signal-regulated kinase via the oxidative stress-EGF receptor pathway in renal fibroblasts. *J Cell Biochem*. 109:38-48.

Choi, J.S., K.W. Leong, and H.S. Yoo. 2008. In vivo wound healing of diabetic ulcers using electrospun nanofibers immobilized with human epidermal growth factor (EGF). *Biomaterials*. 29:587-596.

Cianfarani, F., G. Zambruno, L. Brogelli, F. Sera, P.M. Lacal, M. Pesce, M.C. Capogrossi, C.M. Failla, M. Napolitano, and T. Odorisio. 2006. Placenta growth factor in diabetic wound healing: altered expression and therapeutic potential. *Am J Pathol*. 169:1167-1182.

Cobaleda, C., M. Perez-Caro, C. Vicente-Duenas, and I. Sanchez-Garcia. 2007. Function of the zinc-finger transcription factor SNAI2 in cancer and development. *Annu Rev Genet*. 41:41-61.

Cohen, M.E., M. Yin, W.A. Paznekas, M. Schertzer, S. Wood, and E.W. Jabs. 1998. Human SLUG gene organization, expression, and chromosome map location on 8q. *Genomics*. 51:468-471.

Cooper, K.L., K.J. Liu, and L.G. Hudson. 2007. Contributions of reactive oxygen species and mitogen-activated protein kinase signaling in arsenite-stimulated hemeoxygenase-1 production. *Toxicol Appl Pharmacol*. 218:119-127.

Danielsen, A.J., and N.J. Maihle. 2002. The EGF/ErbB receptor family and apoptosis. *Growth Factors*. 20:1-15.

Darby, I.A., and T.D. Hewitson. 2007. Fibroblast differentiation in wound healing and fibrosis. *Int Rev Cytol*. 257:143-179.

DeFronzo, R.A. 1997. Insulin resistance: a multifaceted syndrome responsible for NIDDM, obesity, hypertension, dyslipidaemia and atherosclerosis. *Neth J Med*. 50:191-197.

Deonarine, K., M.C. Panelli, M.E. Stashower, P. Jin, K. Smith, H.B. Slade, C. Norwood, E. Wang, F.M. Marincola, and D.F. Stroncek. 2007. Gene expression profiling of cutaneous wound healing. *J Transl Med*. 5:11.

Desmouliere, A., C. Chaponnier, and G. Gabbiani. 2005. Tissue repair, contraction, and the myofibroblast. *Wound Repair Regen*. 13:7-12.

Dogan, S., S. Demirer, I. Kepenekci, B. Erkek, A. Kiziltay, N. Hasirci, S. Muftuoglu, A. Nazikoglu, N. Renda, U.D. Dincer, A. Elhan, and E. Kuterdem. 2009. Epidermal growth factor-containing wound closure enhances wound healing in non-diabetic and diabetic rats. *Int Wound J*. 6:107-115.

Eming, S.A., T. Krieg, and J.M. Davidson. 2007. Inflammation in wound repair: molecular and cellular mechanisms. *The Journal of Investigative Dermatology*. 127:514-525.

Falasca, M., C. Raimondi, and T. Maffucci. 2011. Boyden chamber. *Methods Mol Biol*. 769:87-95.

Fernandez-Montequin, J.I., E. Infante-Cristia, C. Valenzuela-Silva, N. Franco-Perez, W. Savigne-Gutierrez, H. Artaza-Sanz, L. Morejon-Vega, C. Gonzalez-Benavides, O. Eliseo-Musenden, E. Garcia-Iglesias, J. Berlanga-Acosta, R. Silva-Rodriguez, B.Y. Betancourt, and P.A. Lopez-Saura. 2007. Intralesional injections of Citoprot-P (recombinant human epidermal growth factor) in advanced diabetic foot ulcers with risk of amputation. *Int Wound J*. 4:333-343.

Fernandez-Montequin, J.I., C.M. Valenzuela-Silva, O.G. Diaz, W. Savigne, N. Sancho-Soutelo, F. Rivero-Fernandez, P. Sanchez-Penton, L. Morejon-Vega, H. Artaza-Sanz, A. Garcia-Herrera, C. Gonzalez-Benavides, C.M. Hernandez-Canete, A. Vazquez-Proenza, J. Berlanga-Acosta, and P.A. Lopez-Saura. 2009. Intra-lesional injections of recombinant human epidermal growth factor promote granulation and healing in advanced diabetic foot ulcers: multicenter, randomised, placebo-controlled, double-blind study. *Int Wound J*. 6:432-443.

Feve, B., and J.P. Bastard. 2012. From the conceptual basis to the discovery of leptin. *Biochimie*. 94:2065-2068.

Flatt, J.P. 1997. How NOT to approach the obesity problem. *Obes Res*. 5:632-633.

Frank, S., B. Stallmeyer, H. Kampfer, N. Kolb, and J. Pfeilschifter. 2000. Leptin enhances wound re-epithelialization and constitutes a direct function of leptin in skin repair. *J Clin Invest*. 106:501-509.

Fuchs, E., and S. Raghavan. 2002. Getting under the skin of epidermal morphogenesis. *Nat Rev Genet*. 3:199-209.

Galtier, F. 2010. Definition, epidemiology, risk factors. *Diabetes Metab*. 36:628-651.

Game, F.L., R.J. Hinchliffe, J. Apelqvist, D.G. Armstrong, K. Bakker, A. Hartemann, M. Londahl, P.E. Price, and W.J. Jeffcoate. 2012. A systematic review of interventions to enhance the healing of chronic ulcers of the foot in diabetes. *Diabetes Metab Res Rev*. 28 Suppl 1:119-141.

Garrett, T.P., N.M. McKern, M. Lou, T.C. Elleman, T.E. Adams, G.O. Lovrecz, H.J. Zhu, F. Walker, M.J. Frenkel, P.A. Hoyne, R.N. Jorissen, E.C. Nice, A.W. Burgess, and C.W. Ward. 2002. Crystal structure of a truncated epidermal growth factor receptor extracellular domain bound to transforming growth factor alpha. *Cell*. 110:763-773.

Garthwaite, T.L., D.R. Martinson, L.F. Tseng, T.C. Hagen, and L.A. Menahan. 1980. A longitudinal hormonal profile of the genetically obese mouse. *Endocrinology*. 107:671-676.

Giebel, L.B., and R.A. Spritz. 1991. Mutation of the KIT (mast/stem cell growth factor receptor) protooncogene in human piebaldism. *Proc Natl Acad Sci U S A*. 88:8696-8699.

Goh, S.Y., and M.E. Cooper. 2008. Clinical review: The role of advanced glycation end products in progression and complications of diabetes. *J Clin Endocrinol Metab*. 93:1143-1152.

Goldberg, T., W. Cai, M. Peppa, V. Dardaine, B.S. Baliga, J. Uribarri, and H. Vlassara. 2004. Advanced glycoxidation end products in commonly consumed foods. *J Am Diet Assoc*. 104:1287-1291.

Goldfine, I.D. 1987. The insulin receptor: molecular biology and transmembrane signaling. *Endocr Rev*. 8:235-255.

Goodson, W.H., 3rd, and T.K. Hung. 1977. Studies of wound healing in experimental diabetes mellitus. *J Surg Res*. 22:221-227.

Goodson, W.H., 3rd, and T.K. Hunt. 1986. Wound collagen accumulation in obese hyperglycemic mice. *Diabetes*. 35:491-495.

Goren, I., H. Kampfer, M. Podda, J. Pfeilschifter, and S. Frank. 2003. Leptin and wound inflammation in diabetic ob/ob mice: differential regulation of neutrophil and macrophage influx and a potential role for the scab as a sink for inflammatory cells and mediators. *Diabetes*. 52:2821-2832.

Graham, M.L., J.L. Janecek, J.A. Kittredge, B.J. Hering, and H.J. Schuurman. 2011. The streptozotocin-induced diabetic nude mouse model: differences between animals from different sources. *Comp Med*. 61:356-360.

Grinstein, G., R. Muzumdar, L. Aponte, P. Vuguin, P. Saenger, and J. DiMartino-Nardi. 2003. Presentation and 5-year follow-up of type 2 diabetes mellitus in African-American and Caribbean-Hispanic adolescents. *Horm Res*. 60:121-126.

Grotendorst, G.R., Y. Soma, K. Takehara, and M. Charette. 1989. EGF and TGF-alpha are potent chemoattractants for endothelial cells and EGF-like peptides are present at sites of tissue regeneration. *J Cell Physiol*. 139:617-623.

Gurtner, G.C., S. Werner, Y. Barrandon, and M.T. Longaker. 2008. Wound repair and regeneration. *Nature*. 453:314-321.

Halaas, J.L., K.S. Gajiwala, M. Maffei, S.L. Cohen, B.T. Chait, D. Rabinowitz, R.L. Lallone, S.K. Burley, and J.M. Friedman. 1995. Weight-reducing effects of the plasma protein encoded by the obese gene. *Science*. 269:543-546.

Han, L., Q. Ma, J. Li, H. Liu, W. Li, G. Ma, Q. Xu, S. Zhou, and E. Wu. 2011. High glucose promotes pancreatic cancer cell proliferation via the induction of EGF expression and transactivation of EGFR. *PLoS One*. 6:e27074.

Hande, K.R. 1998. Etoposide: four decades of development of a topoisomerase II inhibitor. *Eur J Cancer*. 34:1514-1521.

Hanft, J.R., and M.S. Surprenant. 2002. Healing of chronic foot ulcers in diabetic patients treated with a human fibroblast-derived dermis. *J Foot Ankle Surg*. 41:291-299.

Hansen, L.A., N. Alexander, M.E. Hogan, J.P. Sundberg, A. Dlugosz, D.W. Threadgill, T. Magnuson, and S.H. Yuspa. 1997. Genetically null mice reveal a central role for epidermal growth factor receptor in the differentiation of the hair follicle and normal hair development. *Am J Pathol*. 150:1959-1975.

Hayashida, T., M. Decaestecker, and H.W. Schnaper. 2003. Cross-talk between ERK MAP kinase and Smad signaling pathways enhances TGF-beta-dependent responses in human mesangial cells. *Faseb J*. 17:1576-1578.

Hemavathy, K., S.I. Ashraf, and Y.T. Ip. 2000a. Snail/slug family of repressors: slowly going into the fast lane of development and cancer. *Gene*. 257:1-12.

Hemavathy, K., S.C. Guru, J. Harris, J.D. Chen, and Y.T. Ip. 2000b. Human Slug is a repressor that localizes to sites of active transcription. *Molecular and Cellular Biology*. 20:5087-5095.

Hirahara, I., Y. Ishibashi, S. Kaname, E. Kusano, and T. Fujita. 2009. Methylglyoxal induces peritoneal thickening by mesenchymal-like mesothelial cells in rats. *Nephrol Dial Transplant*. 24:437-447.

Hong, J.P., H.D. Jung, and Y.W. Kim. 2006. Recombinant human epidermal growth factor (EGF) to enhance healing for diabetic foot ulcers. *Ann Plast Surg*. 56:394-398; discussion 399-400.

Hosgood, G. 2006. Stages of wound healing and their clinical relevance. *Vet Clin North Am Small Anim Pract*. 36:667-685.

Hotamisligil, G.S. 2006. Inflammation and metabolic disorders. *Nature*. 444:860-867.

Hotu, S., B. Carter, P.D. Watson, W.S. Cutfield, and T. Cundy. 2004. Increasing prevalence of type 2 diabetes in adolescents. *J Paediatr Child Health*. 40:201-204.

Hudson, L.G., and L.J. McCawley. 1998. Contributions of the Epidermal Growth Factor Receptor to Keratinocyte Motility. *Microscopy Research and Technique*. 43:444-455.

Hudson, L.G., K.M. Newkirk, H.L. Chandler, C. Choi, S.L. Fossey, A.E. Parent, and D.F. Kusewitt. 2009. Cutaneous wound reepithelialization is compromised in mice lacking functional Slug (Snai2). *Journal of Dermatological Science*. 56:19-26.

Huijberts, M.S., N.C. Schaper, and C.G. Schalkwijk. 2008. Advanced glycation end products and diabetic foot disease. *Diabetes Metab Res Rev*. 24 Suppl 1:S19-24.

Ingalls, A.M., M.M. Dickie, and G.D. Snell. 1950. Obese, a new mutation in the house mouse. *J Hered*. 41:317-318.

Islam, M.S., and T. Loots du. 2009. Experimental rodent models of type 2 diabetes: a review. *Methods Find Exp Clin Pharmacol*. 31:249-261.

Janis, J.E., R.K. Kwon, and D.H. Lalonde. 2010. A practical guide to wound healing. *Plast Reconstr Surg*. 125:230e-244e.

Jiang, R., Y. Lan, C.R. Norton, J.P. Sundberg, and T. Gridley. 1998. The Slug gene is not essential for mesoderm or neural crest development in mice. *Dev Biol*. 198:277-285.

John, W.G., and E.J. Lamb. 1993. The Maillard or browning reaction in diabetes. *Eye (Lond)*. 7 ( Pt 2):230-237.

Joshi, R.L., B. Lamothe, N. Cordonnier, K. Mesbah, E. Monthioux, J. Jami, and D. Bucchini. 1996. Targeted disruption of the insulin receptor gene in the mouse results in neonatal lethality. *Embo J*. 15:1542-1547.

Kampfer, H., R. Schmidt, G. Geisslinger, J. Pfeilschifter, and S. Frank. 2005. Wound inflammation in diabetic ob/ob mice: functional coupling of prostaglandin biosynthesis to cyclooxygenase-1 activity in diabetes-impaired wound healing. *Diabetes*. 54:1543-1551.

Karashima, T., P. Sweeney, J.W. Slaton, S.J. Kim, D. Kedar, J.I. Izawa, Z. Fan, C. Pettaway, D.J. Hicklin, T. Shuin, and C.P. Dinney. 2002. Inhibition of angiogenesis by the antiepidermal growth factor receptor antibody ImClone C225 in androgen-independent prostate cancer growing orthotopically in nude mice. *Clin Cancer Res*. 8:1253-1264.

Katafiasz, D., L.M. Smith, and J.K. Wahl, 3rd. 2011. Slug (SNAI2) expression in oral SCC cells results in altered cell-cell adhesion and increased motility. *Cell Adh Migr*. 5.

Khanna, S., S. Biswas, Y. Shang, E. Collard, A. Azad, C. Kauh, V. Bhasker, G.M. Gordillo, C.K. Sen, and S. Roy. 2010. Macrophage dysfunction impairs resolution of inflammation in the wounds of diabetic mice. *PLoS One*. 5:e9539.

Kim, J.H., P.M. Nishina, and J.K. Naggert. 1998. Genetic models for non insulin dependent diabetes mellitus in rodents. *J Basic Clin Physiol Pharmacol*. 9:325-345.

Kim, M.H., W. Liu, D.L. Borjesson, F.R. Curry, L.S. Miller, A.L. Cheung, F.T. Liu, R.R. Isseroff, and S.I. Simon. 2008. Dynamics of neutrophil infiltration during cutaneous wound healing and infection using fluorescence imaging. *The Journal of Investigative Dermatology*. 128:1812-1820.

Klip, A. 2009. The many ways to regulate glucose transporter 4. *Appl Physiol Nutr Metab*. 34:481-487.

Kragstrup, T.W., M. Kjaer, and A.L. Mackey. 2011. Structural, biochemical, cellular, and functional changes in skeletal muscle extracellular matrix with aging. *Scand J Med Sci Sports*. 21:749-757.

Krook, A., H. Wallberg-Henriksson, and J.R. Zierath. 2004. Sending the signal: molecular mechanisms regulating glucose uptake. *Med Sci Sports Exerc*. 36:1212-1217.

Krosnick, A. 2000. The diabetes and obesity epidemic among the Pima Indians. *N J Med*. 97:31-37.

Kueper, T., T. Grune, S. Prahl, H. Lenz, V. Welge, T. Biernoth, Y. Vogt, G.M. Muhr, A. Gaemlich, T. Jung, G. Boemke, H.P. Elsasser, K.P. Wittern, H. Wenck, F. Stab, and T. Blatt. 2007. Vimentin is the specific target in skin glycation. Structural

prerequisites, functional consequences, and role in skin aging. *J Biol Chem*. 282:23427-23436.

Kurihara, T., Y. Ozawa, N. Nagai, K. Shinoda, K. Noda, Y. Imamura, K. Tsubota, H. Okano, Y. Oike, and S. Ishida. 2008. Angiotensin II type 1 receptor signaling contributes to synaptophysin degradation and neuronal dysfunction in the diabetic retina. *Diabetes*. 57:2191-2198.

Kusewitt, D.F., C. Choi, K.M. Newkirk, P. Leroy, Y. Li, M.G. Chavez, and L.G. Hudson. 2009. Slug/Snai2 is a downstream mediator of epidermal growth factor receptor-stimulated reepithelialization. *The Journal of Investigative Dermatology*. 129:491-495.

Lan, C.C., I.H. Liu, A.H. Fang, C.H. Wen, and C.S. Wu. 2008. Hyperglycaemic conditions decrease cultured keratinocyte mobility: implications for impaired wound healing in patients with diabetes. *Br J Dermatol*. 159:1103-1115.

Lan, C.C., C.S. Wu, H.Y. Kuo, S.M. Huang, and G.S. Chen. 2009. Hyperglycaemic conditions hamper keratinocyte locomotion via sequential inhibition of distinct pathways: new insights on poor wound closure in patients with diabetes. *Br J Dermatol*. 160:1206-1214.

Lao, G., L. Yan, C. Yang, L. Zhang, S. Zhang, and Y. Zhou. 2012. Controlled release of epidermal growth factor from hydrogels accelerates wound healing in diabetic rats. *J Am Podiatr Med Assoc*. 102:89-98.

Lapolla, A., R. Flamini, T. Tonus, D. Fedele, A. Senesi, R. Reitano, E. Marotta, G. Pace, R. Seraglia, and P. Traldi. 2003. An effective derivatization method for quantitative determination of glyoxal and methylglyoxal in plasma samples by gas chromatography/mass spectrometry. *Rapid Commun Mass Spectrom*. 17:876-878.

Larcher, F., M. Del Rio, F. Serrano, J.C. Segovia, A. Ramirez, A. Meana, A. Page, J.L. Abad, M.A. Gonzalez, J. Bueren, A. Bernad, and J.L. Jorcano. 2001. A cutaneous gene therapy approach to human leptin deficiencies: correction of the murine ob/ob phenotype using leptin-targeted keratinocyte grafts. *FASEB journal : official publication of the Federation of American Societies for Experimental Biology*. 15:1529-1538.

Leney, S.E., and J.M. Tavare. 2009. The molecular basis of insulin-stimulated glucose uptake: signalling, trafficking and potential drug targets. *J Endocrinol*. 203:1-18.

Leto, D., and A.R. Saltiel. 2012. Regulation of glucose transport by insulin: traffic control of GLUT4. *Nat Rev Mol Cell Biol*. 13:383-396.

Lin, R.Y., R.P. Choudhury, W. Cai, M. Lu, J.T. Fallon, E.A. Fisher, and H. Vlassara. 2003. Dietary glycotoxins promote diabetic atherosclerosis in apolipoprotein E-deficient mice. *Atherosclerosis*. 168:213-220.

Lindstrom, P. 2007. The physiology of obese-hyperglycemic mice [ob/ob mice]. *ScientificWorldJournal*. 7:666-685.

Liu, B.F., S. Miyata, H. Kojima, A. Uriuhara, H. Kusunoki, K. Suzuki, and M. Kasuga. 1999. Low phagocytic activity of resident peritoneal macrophages in diabetic mice: relevance to the formation of advanced glycation end products. *Diabetes*. 48:2074-2082.

Livak, K.J., and T.D. Schmittgen. 2001. Analysis of relative gene expression data using real-time quantitative PCR and the 2(-Delta Delta C(T)) Method. *Methods*. 25:402-408.

Loomans, C.J., E.J. de Koning, F.J. Staal, M.B. Rookmaaker, C. Verseyden, H.C. de Boer, M.C. Verhaar, B. Braam, T.J. Rabelink, and A.J. van Zonneveld. 2004. Endothelial progenitor cell dysfunction: a novel concept in the pathogenesis of vascular complications of type 1 diabetes. *Diabetes*. 53:195-199.

Loughlin, D.T., and C.M. Artlett. 2009. 3-Deoxyglucosone-collagen alters human dermal fibroblast migration and adhesion: implications for impaired wound healing in patients with diabetes. *Wound Repair Regen*. 17:739-749.

Luevano-Contreras, C., and K. Chapman-Novakofski. 2010. Dietary advanced glycation end products and aging. *Nutrients*. 2:1247-1265.

Luevano-Contreras, C., M.E. Garay-Sevilla, K. Wrobel, and J.M. Malacara. 2013. Dietary advanced glycation end products restriction diminishes inflammation markers and oxidative stress in patients with type 2 diabetes mellitus. *J Clin Biochem Nutr*. 52:22-26.

Maillard, L.C. 1912. Action des acides amines sur les sucres: formation des melanoidines par voie methodique. *C. R. Academy of Sciences*. 154:66-68.

Maklad, A., J.R. Nicolai, K.J. Bichsel, J.E. Evenson, T.C. Lee, D.W. Threadgill, and L.A. Hansen. 2009. The EGFR is required for proper innervation to the skin. *J Invest Dermatol*. 129:690-698.

Marston, W.A., J. Hanft, P. Norwood, and R. Pollak. 2003. The efficacy and safety of Dermagraft in improving the healing of chronic diabetic foot ulcers: results of a prospective randomized trial. *Diabetes Care*. 26:1701-1705.

Mayer, J., and R.J. Barrnett. 1953. Sensitivity to cold in the hereditary obese-hyperglycemic syndrome of mice. *Yale J Biol Med*. 26:38-45.

Mazzalupo, S., M.J. Wawersik, and P.A. Coulombe. 2002. An ex vivo assay to assess the potential of skin keratinocytes for wound epithelialization. *The Journal of Investigative Dermatology*. 118:866-870.

McLafferty, E., C. Hendry, and F. Alistair. 2012. The integumentary system: anatomy, physiology and function of skin. *Nurs Stand*. 27:35-42.

Miller, A.G., S.J. Meade, and J.A. Gerrard. 2003. New insights into protein crosslinking via the Maillard reaction: structural requirements, the effect on enzyme function, and predicted efficacy of crosslinking inhibitors as anti-ageing therapeutics. *Bioorg Med Chem*. 11:843-852.

Moreo, K. 2005. Understanding and overcoming the challenges of effective case management for patients with chronic wounds. *Case Manager*. 16:62-63, 67.

Morita, K., K. Urabe, Y. Moroi, T. Koga, R. Nagai, S. Horiuchi, and M. Furue. 2005. Migration of keratinocytes is impaired on glycated collagen I. *Wound Repair Regen*. 13:93-101.

Mostafa, A.A., E.W. Randell, S.C. Vasdev, V.D. Gill, Y. Han, V. Gadag, A.A. Raouf, and H. El Said. 2007. Plasma protein advanced glycation end products, carboxymethyl cysteine, and carboxyethyl cysteine, are elevated and related to nephropathy in patients with diabetes. *Mol Cell Biochem*. 302:35-42.

Mustoe, T. 2004. Understanding chronic wounds: a unifying hypothesis on their pathogenesis and implications for therapy. *Am J Surg*. 187:65S-70S.

Nakamura, Y., C. Sotozono, and S. Kinoshita. 2001. The epidermal growth factor receptor (EGFR): role in corneal wound healing and homeostasis. *Exp Eye Res*. 72:511-517.

Nass, N., K. Vogel, B. Hofmann, P. Presek, R.E. Silber, and A. Simm. 2010. Glycation of PDGF results in decreased biological activity. *Int J Biochem Cell Biol*. 42:749-754.

Nather, A. 2011. Role of negative pressure wound therapy in healing of diabetic foot ulcers. *J Surg Tech Case Rep*. 3:10-11.

Nieto, M.A. 2002. The snail superfamily of zinc-finger transcription factors. *Nat Rev Mol Cell Biol*. 3:155-166.

Nieto, M.A., M.G. Sargent, D.G. Wilkinson, and J. Cooke. 1994. Control of cell behavior during vertebrate development by Slug, a zinc finger gene. *Science*. 264:835-839.

Obata, T., H. Maegawa, A. Kashiwagi, T.S. Pillay, and R. Kikkawa. 1998. High glucose-induced abnormal epidermal growth factor signaling. *J Biochem*. 123:813-820.

Olerud, J.E. 2008. Models for diabetic wound healing and healing into percutaneous devices. *J Biomater Sci Polym Ed*. 19:1007-1020.

Oliveira, D., J. Pereira, and R. Fernandes. 2012. Metabolic alterations in pregnant women: gestational diabetes. *J Pediatr Endocrinol Metab*. 25:835-842.

Ozawa, Y., T. Kurihara, M. Sasaki, N. Ban, K. Yuki, S. Kubota, and K. Tsubota. 2011. Neural degeneration in the retina of the streptozotocin-induced type 1 diabetes model. *Exp Diabetes Res*. 2011:108328.

Parent, A.E., C. Choi, K. Caudy, T. Gridley, and D.F. Kusewitt. 2004. The developmental transcription factor slug is widely expressed in tissues of adult mice. *J Histochem Cytochem*. 52:959-965.

Parent, A.E., K.M. Newkirk, and D.F. Kusewitt. 2010. Slug (Snai2) expression during skin and hair follicle development. *The Journal of Investigative Dermatology*. 130:1737-1739.

Pastore, S., F. Mascia, V. Mariani, and G. Girolomoni. 2008. The Epidermal Growth Factor Receptor System in Skin Repair and Inflammation. *Journal of Investigative Dermatology*. 128:1365-1374.

Paul, R.G., N.C. Avery, D.A. Slatter, T.J. Sims, and A.J. Bailey. 1998. Isolation and characterization of advanced glycation end products derived from the in vitro reaction of ribose and collagen. *Biochem J*. 330 ( Pt 3):1241-1248.

Pelleymounter, M.A., M.J. Cullen, M.B. Baker, R. Hecht, D. Winters, T. Boone, and F. Collins. 1995. Effects of the obese gene product on body weight regulation in ob/ob mice. *Science*. 269:540-543.

Peppa, M., H. Brem, P. Ehrlich, J.G. Zhang, W. Cai, Z. Li, A. Croitoru, S. Thung, and H. Vlassara. 2003. Adverse effects of dietary glycotoxins on wound healing in genetically diabetic mice. *Diabetes*. 52:2805-2813.

Peppa, M., and S.A. Raptis. 2011. Glycoxidation and wound healing in diabetes: an interesting relationship. *Curr Diabetes Rev*. 7:416-425.

Peppa, M., P. Stavroulakis, and S.A. Raptis. 2009. Advanced glycoxidation products and impaired diabetic wound healing. *Wound Repair Regen*. 17:461-472.

Perez-Losada, J., M. Sanchez-Martin, A. Rodriguez-Garcia, M.L. Sanchez, A. Orfao, T. Flores, and I. Sanchez-Garcia. 2002. Zinc-finger transcription factor Slug contributes to the function of the stem cell factor c-kit signaling pathway. *Blood*. 100:1274-1286.

Peters, V., and C.P. Schmitt. 2012. Murine models of diabetic nephropathy. *Exp Clin Endocrinol Diabetes*. 120:191-193.

Pinhas-Hamiel, O., and P. Zeitler. 2005. The global spread of type 2 diabetes mellitus in children and adolescents. *J Pediatr*. 146:693-700.

Portero-Otin, M., R. Pamplona, M.J. Bellmunt, M.C. Ruiz, J. Prat, R. Salvayre, and A. Negre-Salvayre. 2002. Advanced Glycation End Product Precursors Impair Epidermal Growth Factor Receptor Signaling. *Diabetes*. 51:1535-1542.

Rafehi, H., A. El-Osta, and T.C. Karagiannis. 2011. Genetic and epigenetic events in diabetic wound healing. *Int Wound J*. 8:12-21.

Rakieten, N., M.L. Rakieten, and M.R. Nadkarni. 1963. Studies on the diabetogenic action of streptozotocin (NSC-37917). *Cancer Chemother Rep*. 29:91-98.

Rattan, S.I., H. Sejersen, R.A. Fernandes, and W. Luo. 2007. Stress-mediated hormetic modulation of aging, wound healing, and angiogenesis in human cells. *Ann N Y Acad Sci*. 1119:112-121.

Repertinger, S.K., E. Campagnaro, J. Fuhrman, T. El-Abaseri, S.H. Yuspa, and L.A. Hansen. 2004. EGFR enhances early healing after cutaneous incisional wounding. *J Invest Dermatol*. 123:982-989.

Rerup, C.C. 1970. Drugs producing diabetes through damage of the insulin secreting cells. *Pharmacol Rev*. 22:485-518.

Saad, S., V.A. Stevens, L. Wassef, P. Poronnik, D.J. Kelly, R.E. Gilbert, and C.A. Pollock. 2005. High glucose transactivates the EGF receptor and up-regulates serum glucocorticoid kinase in the proximal tubule. *Kidney Int*. 68:985-997.

Saltiel, A.R., and C.R. Kahn. 2001. Insulin signalling and the regulation of glucose and lipid metabolism. *Nature*. 414:799-806.

Sanchez-Martin, M., J. Perez-Losada, A. Rodriguez-Garcia, B. Gonzalez-Sanchez, B.R. Korf, W. Kuster, C. Moss, R.A. Spritz, and I. Sanchez-Garcia. 2003. Deletion of the SLUG (SNAI2) gene results in human piebaldism. *Am J Med Genet A*. 122A:125-132.

Sanchez-Martin, M., A. Rodriguez-Garcia, J. Perez-Losada, A. Sagrera, A.P. Read, and I. Sanchez-Garcia. 2002. SLUG (SNAI2) deletions in patients with Waardenburg disease. *Hum Mol Genet*. 11:3231-3236.

Santoro, M.M., and G. Gaudino. 2005. Cellular and molecular facets of keratinocyte reepithelization during wound healing. *Exp Cell Res*. 304:274-286.

Savagner, P., D.F. Kusewitt, E.A. Carver, F. Magnino, C. Choi, T. Gridley, and L.G. Hudson. 2005. Developmental Transcription Factor Slug Is Required for Effective Re-epithelialization by Adult Keratinocytes. *Journal of Cellular Physiology*. 202:858-866.

Schaffer, C.J., and L.B. Nanney. 1996. Cell biology of wound healing. *Int Rev Cytol*. 169:151-181.

Schindelin, J., I. Arganda-Carreras, E. Frise, V. Kaynig, M. Longair, T. Pietzsch, S. Preibisch, C. Rueden, S. Saalfeld, B. Schmid, J.Y. Tinevez, D.J. White, V. Hartenstein, K. Eliceiri, P. Tomancak, and A. Cardona. 2012. Fiji: an open-source platform for biological-image analysis. *Nat Methods*. 9:676-682.

Schnedl, W.J., S. Ferber, J.H. Johnson, and C.B. Newgard. 1994. STZ transport and cytotoxicity. Specific enhancement in GLUT2-expressing cells. *Diabetes*. 43:1326-1333.

Schneider, M.R., S. Werner, R. Paus, and E. Wolf. 2008. Beyond wavy hairs: the epidermal growth factor receptor and its ligands in skin biology and pathology. *Am J Pathol*. 173:14-24.

Schwarzenbolz, U., S. Mende, and T. Henle. 2008. Model studies on protein glycation: influence of cysteine on the reactivity of arginine and lysine residues toward glyoxal. *Ann N Y Acad Sci*. 1126:248-252.

Sefton, M., S. Sanchez, and M.A. Nieto. 1998. Conserved and divergent roles for members of the Snail family of transcription factors in the chick and mouse embryo. *Development*. 125:3111-3121.

Seifter, E., G. Rettura, J. Padawer, F. Stratford, D. Kambosos, and S.M. Levenson. 1981. Impaired wound healing in streptozotocin diabetes. Prevention by supplemental vitamin A. *Ann Surg*. 194:42-50.

Sell, D.R., and V.M. Monnier. 1990. End-stage renal disease and diabetes catalyze the formation of a pentose-derived crosslink from aging human collagen. *J Clin Invest*. 85:380-384.

Setacci, C., G. de Donato, F. Setacci, and E. Chisci. 2009. Diabetic patients: epidemiology and global impact. *J Cardiovasc Surg (Torino)*. 50:263-273.

Shirley, S.H., L.G. Hudson, J. He, and D.F. Kusewitt. 2010. The skinny on Slug. *Molecular Carcinogensis*. 49:851-861.

Shlopov, B.V., J.M. Stuart, M.L. Gumanovskaya, and K.A. Hasty. 2001. Regulation of cartilage collagenase by doxycycline. *J Rheumatol*. 28:835-842.

Shook, D., and R. Keller. 2003. Mechanisms, mechanics and function of epithelial-mesenchymal transitions in early development. *Mech Dev*. 120:1351-1383.

Singer, A.J., and R.A. Clark. 1999. Cutaneous wound healing. *N Engl J Med*. 341:738-746.

Singh, R., A. Barden, T. Mori, and L. Beilin. 2001. Advanced glycation end-products: a review. *Diabetologia*. 44:129-146.

Sliman, S.M., T.D. Eubank, S.R. Kotha, M.L. Kuppusamy, S.I. Sherwani, E.S. Butler, P. Kuppusamy, S. Roy, C.B. Marsh, D.M. Stern, and N.L. Parinandi. 2010. Hyperglycemic oxoaldehyde, glyoxal, causes barrier dysfunction, cytoskeletal alterations, and inhibition of angiogenesis in vascular endothelial cells: aminoguanidine protection. *Mol Cell Biochem*. 333:9-26.

Spravchikov, N., G. Sizyakov, M. Gartsbein, D. Accili, T. Tennenbaum, and E. Wertheimer. 2001. Glucose effects on skin keratinocytes: implications for diabetes skin complications. *Diabetes*. 50:1627-1635.

Stallmeyer, B., H. Kampfer, M. Podda, R. Kaufmann, J. Pfeilschifter, and S. Frank. 2001a. A novel keratinocyte mitogen: regulation of leptin and its functional receptor in skin repair. *The Journal of Investigative Dermatology*. 117:98-105.

Stallmeyer, B., J. Pfeilschifter, and S. Frank. 2001b. Systemically and topically supplemented leptin fails to reconstitute a normal angiogenic response during skin repair in diabetic ob/ob mice. *Diabetologia*. 44:471-479.

Stockli, J., D.J. Fazakerley, and D.E. James. 2011. GLUT4 exocytosis. *J Cell Sci*. 124:4147-4159.

Stoll, S.W., S. Kansra, S. Peshick, D.W. Fry, W.R. Leopold, J.F. Wiesen, M. Sibilia, T. Zhang, Z. Werb, R. Derynck, E.F. Wagner, and J.T. Elder. 2001. Differential utilization and localization of ErbB receptor tyrosine kinases in skin compared to normal and malignant keratinocytes. *Neoplasia*. 3:339-350.

Stoscheck, C.M., L.B. Nanney, and J. Lloyd E. King. 1992. Quantitative Determination of EGF-R During Epidermal Wound Healing. *The Journal of Investigative Dermatology*. 99:645-649.

Sullivan, S.R., R.A. Underwood, N.S. Gibran, R.O. Sigle, M.L. Usui, W.G. Carter, and J.E. Olerud. 2004. Validation of a model for the study of multiple wounds in the diabetic mouse (db/db). *Plast Reconstr Surg*. 113:953-960.

Takahashi, M., K. Kushida, T. Ohishi, K. Kawana, H. Hoshino, A. Uchiyama, and T. Inoue. 1994. Quantitative analysis of crosslinks pyridinoline and pentosidine in articular cartilage of patients with bone and joint disorders. *Arthritis Rheum*. 37:724-728.

Takeuchi, M., and S. Yamagishi. 2008. Possible involvement of advanced glycation end-products (AGEs) in the pathogenesis of Alzheimer's disease. *Curr Pharm Des*. 14:973-978.

Taylor, S.I., A. Cama, D. Accili, F. Barbetti, M.J. Quon, M. de la Luz Sierra, Y. Suzuki, E. Koller, R. Levy-Toledano, E. Wertheimer, and et al. 1992. Mutations in the insulin receptor gene. *Endocr Rev*. 13:566-595.

Tepper, O.M., R.D. Galiano, J.M. Capla, C. Kalka, P.J. Gagne, G.R. Jacobowitz, J.P. Levine, and G.C. Gurtner. 2002. Human endothelial progenitor cells from type II diabetics exhibit impaired proliferation, adhesion, and incorporation into vascular structures. *Circulation*. 106:2781-2786.

Tessier, F.J. 2010. The Maillard reaction in the human body. The main discoveries and factors that affect glycation. *Pathol Biol (Paris)*. 58:214-219.

Thomas, M.C. 2011. Advanced glycation end products. *Contrib Nephrol*. 170:66-74.

Thorpe, S.R., and J.W. Baynes. 2002. CML: a brief history. *International Congress Series*. 1245:91-99.

Tiaka, E.K., N. Papanas, A.C. Manolakis, and G.S. Georgiadis. 2012. Epidermal growth factor in the treatment of diabetic foot ulcers: an update. *Perspect Vasc Surg Endovasc Ther*. 24:37-44.

Tokumaru, S., S. Higashiyama, T. Endo, T. Nakagawa, J.I. Miyagawa, K. Yamamori, Y. Hanakawa, H. Ohmoto, K. Yoshino, Y. Shirakata, Y. Matsuzawa, K. Hashimoto, and N. Taniguchi. 2000. Ectodomain shedding of epidermal growth factor receptor ligands is required for keratinocyte migration in cutaneous wound healing. *J Cell Biol*. 151:209-220.

Tonnesen, M.G., X. Feng, and R.A. Clark. 2000. Angiogenesis in wound healing. *J Investig Dermatol Symp Proc*. 5:40-46.

Tsang, M.W., W.K. Wong, C.S. Hung, K.M. Lai, W. Tang, E.Y. Cheung, G. Kam, L. Leung, C.W. Chan, C.M. Chu, and E.K. Lam. 2003. Human epidermal growth factor enhances healing of diabetic foot ulcers. *Diabetes Care*. 26:1856-1861.

Tsuboi, R., C.M. Shi, D.B. Rifkin, and H. Ogawa. 1992. A wound healing model using healing-impaired diabetic mice. *J Dermatol*. 19:673-675.

Tsuboi, R., C.M. Shi, C. Sato, G.N. Cox, and H. Ogawa. 1995. Co-administration of insulin-like growth factor (IGF)-I and IGF-binding protein-1 stimulates wound healing in animal models. *The Journal of Investigative Dermatology*. 104:199-203.

Tuyet, H.L., T.T. Nguyen Quynh, H. Vo Hoang Minh, D.N. Thi Bich, T. Do Dinh, D. Le Tan, H.L. Van, T. Le Huy, H. Doan Huu, and T.N. Tran Trong. 2009. The efficacy and safety of epidermal growth factor in treatment of diabetic foot ulcers: the preliminary results. *Int Wound J*. 6:159-166.

Uribarri, J., S. Woodruff, S. Goodman, W. Cai, X. Chen, R. Pyzik, A. Yong, G.E. Striker, and H. Vlassara. 2010. Advanced glycation end products in foods and a practical guide to their reduction in the diet. *J Am Diet Assoc*. 110:911-916 e912.

Usui, M.L., J.N. Mansbridge, W.G. Carter, M. Fujita, and J.E. Olerud. 2008. Keratinocyte migration, proliferation, and differentiation in chronic ulcers from patients with diabetes and normal wounds. *J Histochem Cytochem*. 56:687-696.

Uttamsingh, S., X. Bao, K.T. Nguyen, M. Bhanot, J. Gong, J.L. Chan, F. Liu, T.T. Chu, and L.H. Wang. 2008. Synergistic effect between EGF and TGF-beta1 in inducing oncogenic properties of intestinal epithelial cells. *Oncogene*. 27:2626-2634.

Velander, P., C. Theopold, T. Hirsch, O. Bleiziffer, B. Zuhaili, M. Fossum, D. Hoeller, R. Gheerardyn, M. Chen, S. Visovatti, H. Svensson, F. Yao, and E. Eriksson. 2008. Impaired wound healing in an acute diabetic pig model and the effects of local hyperglycemia. *Wound Repair Regen*. 16:288-293.

Venkatraman, J., K. Aggarwal, and P. Balaram. 2001. Helical peptide models for protein glycation: proximity effects in catalysis of the Amadori rearrangement. *Chem Biol*. 8:611-625.

Veves, A., V. Falanga, D.G. Armstrong, and M.L. Sabolinski. 2001. Graftskin, a human skin equivalent, is effective in the management of noninfected neuropathic diabetic foot ulcers: a prospective randomized multicenter clinical trial. *Diabetes Care*. 24:290-295.

Vytasek, R., L. Sedova, and V. Vilim. 2010. Increased concentration of two different advanced glycation end-products detected by enzyme immunoassays with new monoclonal antibodies in sera of patients with rheumatoid arthritis. *BMC Musculoskelet Disord*. 11:83.

Ward, C.W., M.C. Lawrence, V.A. Streltsov, T.E. Adams, and N.M. McKern. 2007. The insulin and EGF receptor structures: new insights into ligand-induced receptor activation. *Trends Biochem Sci*. 32:129-137.

Wenczak, B.A., J.B. Lynch, and L.B. Nanney. 1992. Epidermal growth factor receptor distribution in burn wounds. Implications for growth factor-mediated repair. *J Clin Invest*. 90:2392-2401.

Werner, S., M. Breeden, G. Hubner, D.G. Greenhalgh, and M.T. Longaker. 1994. Induction of keratinocyte growth factor expression is reduced and delayed during wound healing in the genetically diabetic mouse. *The Journal of Investigative Dermatology*. 103:469-473.

Werner, S., and R. Grose. 2003. Regulation of wound healing by growth factors and cytokines. *Physiol Rev*. 83:835-870.

White, M.F., and C.R. Kahn. 1994. The insulin signaling system. *J Biol Chem*. 269:1-4.

Winter, G.D. 1962. Formation of the scab and the rate of epithelization of superficial wounds in the skin of the young domestic pig. *Nature*. 193:293-294.

Wu, S., and D.G. Armstrong. 2005. Risk assessment of the diabetic foot and wound. *Int Wound J*. 2:17-24.

Xiong, Y., S.C. Dowdy, K.C. Podratz, F. Jin, J.R. Attewell, N.L. Eberhardt, and S.W. Jiang. 2005. Histone deacetylase inhibitors decrease DNA methyltransferase-3B messenger RNA stability and down-regulate de novo DNA methyltransferase activity in human endometrial cells. *Cancer Res*. 65:2684-2689.

Xu, K.P., Y. Li, A.V. Ljubimov, and F.S. Yu. 2009. High glucose suppresses epidermal growth factor receptor/phosphatidylinositol 3-kinase/Akt signaling pathway and attenuates corneal epithelial wound healing. *Diabetes*. 58:1077-1085.

Yager, D.R., L.Y. Zhang, H.X. Liang, R.F. Diegelmann, and I.K. Cohen. 1996. Wound fluids from human pressure ulcers contain elevated matrix metalloproteinase levels and activity compared to surgical wound fluids. *The Journal of Investigative Dermatology*. 107:743-748.

Yamamoto, H., Y. Uchigata, and H. Okamoto. 1981. Streptozotocin and alloxan induce DNA strand breaks and poly(ADP-ribose) synthetase in pancreatic islets. *Nature*. 294:284-286.

Zhang, Y., R. Proenca, M. Maffei, M. Barone, L. Leopold, and J.M. Friedman. 1994. Positional cloning of the mouse obese gene and its human homologue. *Nature*. 372:425-432.

Zhu, P., C. Yang, L.-H. Chen, M. Ren, G.-j. Lao, and L. Yan. 2011. Impairment of human keratinocyte mobility and proliferation by advanced glycation end products-modified BSA. *Archives of Dermatological Research*. 303:339-350.

Zieman, S., and D. Kass. 2004. Advanced glycation end product cross-linking: pathophysiologic role and therapeutic target in cardiovascular disease. *Congest Heart Fail*. 10:144-149; quiz 150-141.